Published as Chapter 5 in "*Handbook of Surface and Colloid Chemistry*"
Second Expanded and Updated Edition; K. S. Birdi, Ed.; CRC Press, New York, 2002.

# 5. CHEMICAL PHYSICS OF COLLOID SYSTEMS AND INTERFACES

**Authors: Peter A. Kralchevsky, Krassimir D. Danov, and Nikolai D. Denkov**

***Laboratory of Chemical Physics and Engineering, Faculty of Chemistry, University of Sofia, Sofia 1164, Bulgaria***

## CONTENTS

## 5.7 MECHANISMS OF ANTIFOAMING

In Sections 5.4 to 5.6 we considered the main interparticle forces which govern the stability of colloidal systems and some of the mechanisms, which result in destabilization of suspensions and emulsions (coagulation, demulsification). In various technologies (such as pulp and paper production, drug manufacturing, textile dying, crude oil processing, and many others) very voluminous and stable foams can appear, which impede the normal technological process and are, therefore, rather undesired. In these cases, various oils and oil-solid mixtures are introduced as additives to the foaming media for an efficient foam control.[673] Such oils and oil-silica mixtures are commonly termed as antifoams or defoamers.[673-677] Antifoams are used in consumer products as well (e.g., in washing powders and anti-dyspepsia drugs). Sometimes, oils are introduced in surfactant solutions for other reasons and the observed foam destabilization effect is undesired - a typical example is the use of silicone oils as hair conditioners in shampoos.[678,679] The mechanisms responsible for the foam destruction effect of oil-based antifoams are still not entirely understood and are the subject of intensive studies.

A typical antifoam consists of an oil (polydimethylsiloxane or hydrocarbon), dispersed hydrophobic solid particles (e.g., hydrophobized silica), or a mixture of both.[674] The oil-solid mixtures are often called antifoam *compounds*. The weight concentration of the solid particles in compounds is around several percent (typically between 2 to 8). A strong synergistic effect between the oil and the solid particles is observed in the compounds – in most cases, the latter

are much more efficient than either of their individual components, if taken separately.[674,675] The compounds are used at a concentration below 0.1 wt %, whereas the oils are used at higher concentrations (up to several percent) due to their lower antifoam efficiency. The antifoams are usually pre-emulsified in the form of oil drops or mixed oil-solid globules of micrometer size.

A detailed discussion on many aspects of the mechanisms of antifoaming can be found in review articles by Garrett,[674] Wasan and Christiano,[676] as well as in the books by Exerowa and Kruglyakov,[675] and Kralchevsky and Nagayama.[676] In the present section, we compare the mechanisms of foam destruction by oils and oil-silica compounds. The discussion is based on results obtained during the last several years (some of them are still unpublished), so that the section is aimed to complement the aforementioned reviews.

### 5.7.1 Location of Antifoam Action – Fast and Slow Antifoams

An important question about the mechanism of foam destruction is which is the structural element (foam film or Plateau border) actually destroyed by the antifoam globules. This question has a practical importance, because the diameter of the globules in the commercial antifoams should fit the typical size of the structural element to be destroyed - the film thickness or the cross-section of the Plateau border (PB), respectively.[678] Most of the researchers consider that the antifoam globules rupture the foam films,[674,675] whereas Koczo et al.[676,680] suggest that the antifoam globules first escape from the foam films into the neighboring Plateau borders (PB) and get trapped there; only afterwards, the globules are assumed to destroy the PB and the neighboring foam films.

Direct microscopic observations by a high-speed video camera showed that the foam destruction by typical antifoam compounds (comprising silicone oil and silica) occurred through rupture of the foam lamellae.[681,682] Experiments with small (millimeter sized) and large (centimeter sized) foam films showed that the compounds induced the formation of a hole in the foam films at the early stages of the film thinning process, Figure 57. This is possible, because the foam films stabilized by low molecular mass surfactants thin rapidly, within several seconds, down to a thickness of one to several micrometers which is comparable to the diameter of the antifoam globules.[681] As a result, the foam films rupture within several seconds after their formation. Accordingly, the foam produced from such solutions disappear completely for less than 10 sec in a standard shake test.[681]

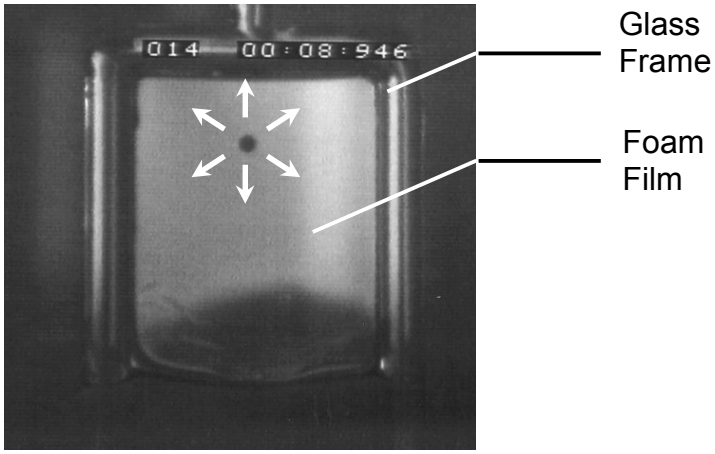


**FIGURE 57**. Image of a large foam film in the moment of its rupture by pre-emulsified globules of an antifoam compound (4.2 wt % of hydrophobic silica dispersed in silicone oil). The film is formed on a rectangular glass frame which is rapidly withdrawn from 10 mM solution of the anionic surfactant dioctyl sulfosuccinate (hereafter denoted for brevity as AOT). One sees a hole (the black circle in the upper part of the film) which, in reality, rapidly expands with time. The film ruptures 0.5 sec after its formation at a thickness about several micrometers. The image is taken by a high-speed video camera as explained in Reference 681.

For this reason, the antifoams that are able to break the foam films are termed “the fast antifoams”.[683] Experiments with several ionic and nonionic surfactants have confirmed that the observed foam film destruction is rather typical for mixed oil-silica antifoams.[681-685]

On the other hand, similar experimental methods showed[678,679,686,687] that the foam destruction occured in a different manner when pure oils (without silica particles) were used as antifoams. The oil drops were seen to leave the foam films (without rupture) during the film thinning process. The antifoam drops were accumulated in the PBs and remained trapped there for a certain period of time,[678,679] as presumed by Koczo et al.[680] The slow process of water drainage from the foam led to a gradual narrowing of the PBs and the oil drops became strongly compressed with time. When the compressing capillary pressure exceeded some critical value, the oil drops entered the walls of the Plateau border, inducing its destruction and the rupture of the neighboring foam films, Figure 58.[678] Much longer time was needed for foam destruction in this case - typically, more than several minutes. That is why, these antifoams were termed the "slow antifoams".[683] Furthermore, a residual foam of well defined height, which remained stable for many hours, was observed in such systems.

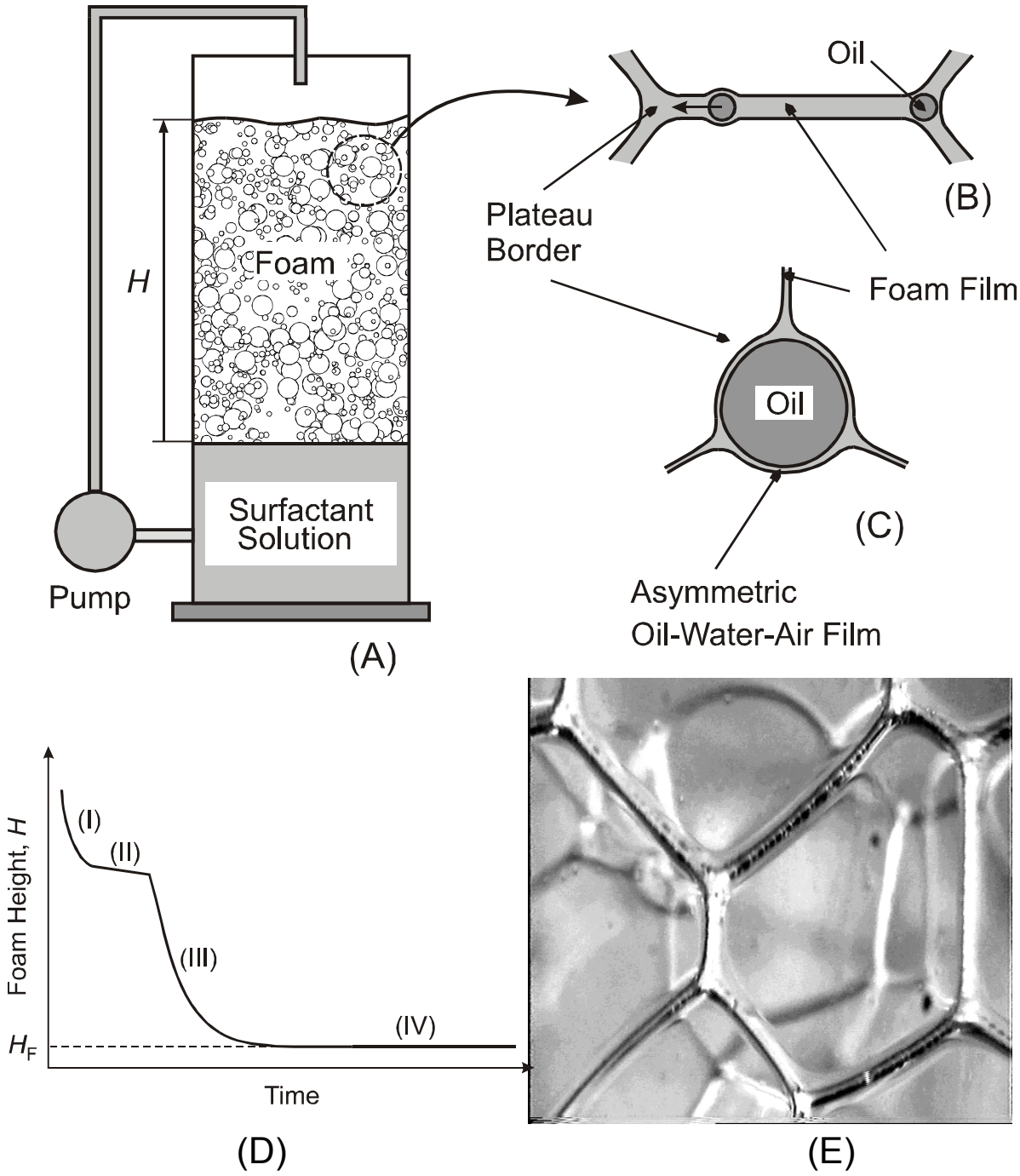


**FIGURE 58.** Foam destruction by oil drops (slow antifoams):[678,679,698] (A, B) The oil drops are rapidly expelled from the foam films into the neighboring Plateau borders (PBs) soon after the foam is formed; (C) The drops are strongly compressed in the narrowing PBs and asymmetric oil-water-air films are formed. The drop entry and foam destruction occur when the compressing pressure exceeds a certain critical value, which depends on the particular system; (D) Schematic presentation of the main stages of foam evolution in the presence of oil drops - (I) drainage of liquid from the foam without bubble coalescence; (II) stable foam due to the insufficient compression of the oil drops; (III) foam destruction as a result of drop entry in the PBs; (IV) long-living residual foam with final height $H_F$; (E) Photograph of real foam cells with many oil drops trapped in the PBs (the drops are visualized by the wavy profile of the PBs).

These studies show that the foam destruction may occur through rupture of either the foam films or the PBs, depending on the particular system. Further experiments have shown that the main factor determining the position of foam destruction, and whether a given antifoam behaves as fast or slow, is the magnitude of the so-called entry barrier (see Section 5.7.3 below).

### 5.7.2 BRIDGING-STRETCHING MECHANISM

As mentioned above, microscopic observations by a high-speed video camera were made[681] to clarify the detailed mechanism of foam film rupture by mixed antifoams. They showed that when an antifoam globule connected (bridged) the surfaces of a foam film, an unstable oil bridge was formed, which stretched with time due to uncompensated capillary pressures at the oil-air and oil-water interfaces, and eventually ruptured the entire foam film (Figure 59). The term "bridging-stretching" was suggested[681,688] to describe this mechanism. The bridging-stretching mechanism explains why the typical antifoam compounds contain a high excess of oil – the antifoam globules should be able to deform for effectuation of the bridge stretching and rupture.

The stability of oil bridges in foam films was theoretically studied by Garrett[674,689] on the basis of the theory of capillarity. The analysis showed that a necessary condition for having an unstable bridge is that the bridging coefficient:

$$B = \sigma_{AW}^2 + \sigma_{OW}^2 - \sigma_{OA}^2 \tag{337}$$

should be positive. Here, $\sigma$ is interfacial tension and the subscripts AW, OW, and OA denote the air-water, oil-water, and oil-air interfaces, respectively. A more refined capillary model[688] showed that oil bridges, formed from oil drops of diameter comparable to, or smaller than the film thickness, might be metastable even at positive values of $B$. Therefore, the size of the oil bridges should be above a certain critical value (which depends on the film thickness and the interfacial tensions) for having an unstable oil bridge. This theoretical result was invoked to explain the reduced stability of the foam films in the presence of a spread oil layer (for details see Reference 688).

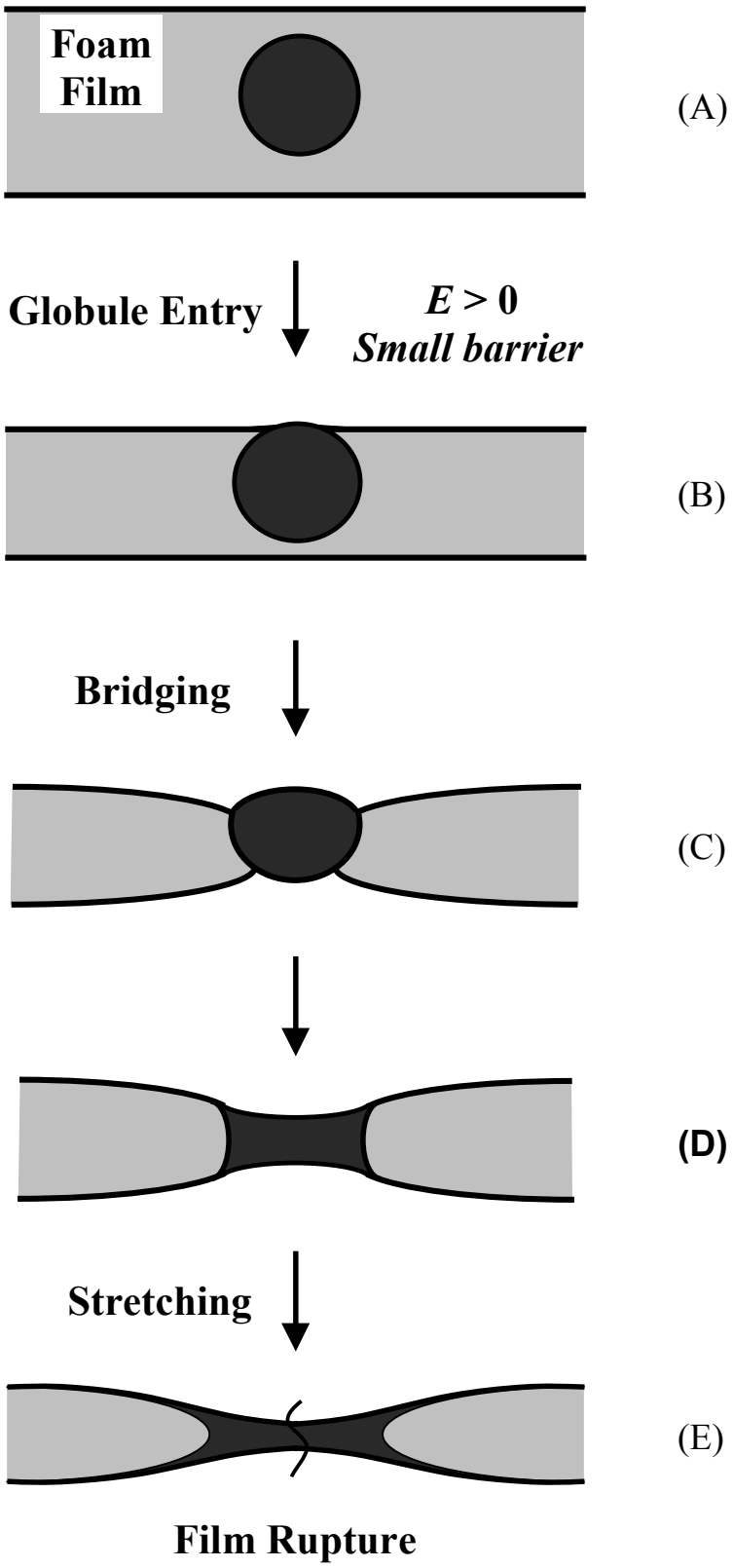


**FIGURE 59.** Schematic presentation of the bridging-stretching mechanism of foam film rupture by antifoam globules:[681,688] After an oil bridge is formed (A-C), it stretches due to uncompensated capillary pressures at the oil-water and oil-air interfaces (C-E). Finally, the bridge ruptures in its thinnest central region (the vertical wavy line in E). The globule entry is possible only if the entry coefficient, $E > 0$, and the entry barrier is low (see section 5.7.3)

### 5.7.3 ROLE OF THE ENTRY BARRIER

Any mechanism of foam destruction by pre-emulsified antifoam globules requires an entry of these globules at the surface of the foam film or the Plateau border (e.g., Figures 58 and 59). The entry event depends on two major factors: (1) The equilibrium position of an oil drop (lens) on the air-water interface, which is determined by the values of the interfacial tensions $\sigma_{AW}$, $\sigma_{OW}$, and $\sigma_{OA}$, see Figure 7; and (2) The repulsive forces (e.g., of electrostatic origin), which stabilize the asymmetric oil-water-air film, formed when an antifoam globule approaches the foam film surface; the barrier created by these forces should be overcome for the globule entry to occur.[674,676,680,690-694]

A theoretical analysis shows (see, e.g., Reference 674) that if the so-called entry coefficient:

$$E = \sigma_{AW} + \sigma_{OW} + \sigma_{OA} \tag{338}$$

is negative (as it is the case with some oils and surfactant solutions), the oil drops do not have a stable equilibrium position at the surface and spontaneously submerge into the surfactant solution. Such oils are inactive as antifoams because no oil bridges can be formed (factor 1 is decisive). One of the main reasons to use silicone oils in various antifoam formulations is that these oils usually have positive values of $B$ and $E$ coefficients in the solutions of most conventional (hydrocarbon-based) surfactants.[674,695] Besides, it was theoretically shown that a positive value of $B$ necessarily corresponds to a positive value of $E$ (the reverse is not always true).[677,696]

The experiments show, however, that many oils with positive $B$ and $E$ coefficients might have low antifoam efficiency.[678,679,686,687] In these cases, the stability of the asymmetric oil-water-air films is very high, and the formation of unstable oil bridges becomes impossible for kinetic reasons (factor 2 is decisive). The repulsive interaction that should be overcome for effectuation of the antifoam globules entry on the solution surface is usually termed “the entry barrier”. A recently developed film trapping technique (FTT)[687,697,698] allowed one to quantify precisely the entry barrier with actual micrometer-sized antifoam globules, and a number of important results have been obtained. The principle of the FTT and some of the main conclusions, drawn from the results obtained by this technique, are briefly discussed below.

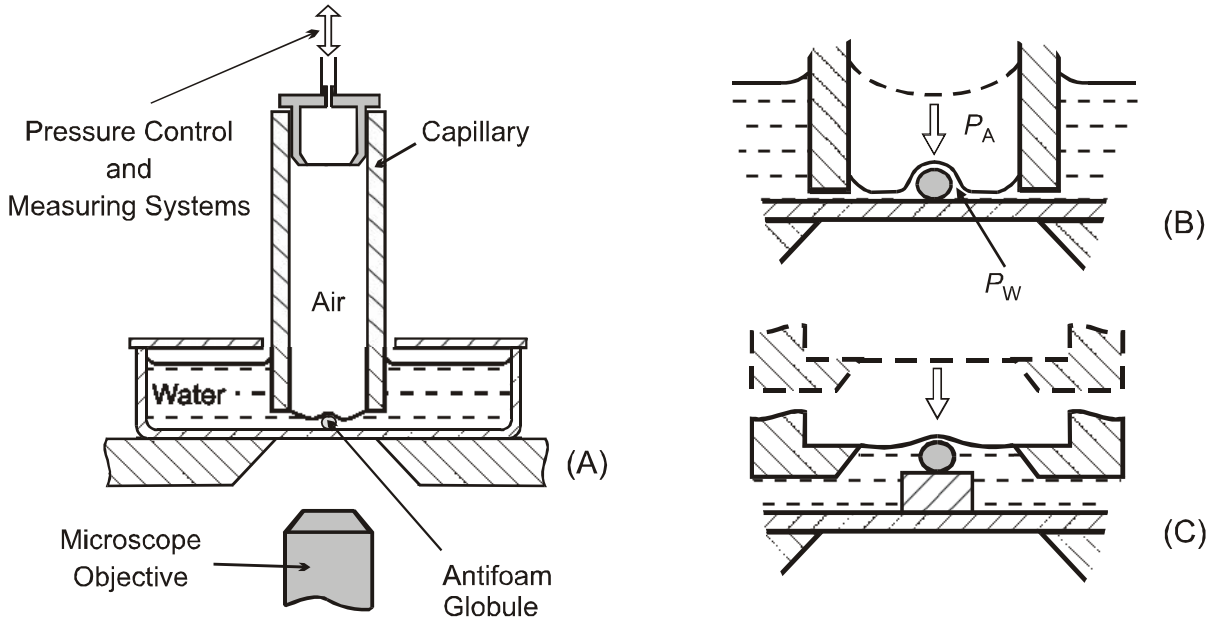


**FIGURE 60.** Scheme of the experimental setup and the basic principle of the Film trapping technique, FTT:[697] (A) Vertical capillary, partially immersed in surfactant solution containing antifoam globules, is held close to the bottom of the experimental vessel. (B) The air pressure inside the capillary, $P_A$, is increased and the convex air-water meniscus in the capillary is pressed against the glass substrate. Some of the antifoam globules remain trapped in the formed glass-water-air film and are compressed by the meniscus. At a given critical capillary pressure, $P_C^{CR} = P_A - P_W$, the asymmetric film formed between the antifoam globule and the solution surface ruptures and an event of globule entry is observed by an optical microscope. (C) Another modification called "gentle FTT" is used for measuring entry barriers lower than 20 Pa - an initially flat meniscus is formed, which allows the trapping of antifoam globules at a virtually zero capillary pressure.

### 5.7.3.1 Film Trapping Technique

The principle and the experimental setup of the FTT are illustrated in Figure 60.[687,697,698] Briefly, a vertical glass capillary is positioned at a small distance above the flat bottom of a glass vessel. The lower end of the capillary is immersed in the working surfactant solution which contains dispersed antifoam globules. The capillary is connected to a pressure control system which allows one to vary and to measure the air pressure in the capillary, $P_A$. When $P_A$ increases, the air-water meniscus in the capillary is pushed against the glass substrate and a wetting film (glass-water-air) is formed which traps some of the antifoam globules. The setup allows one to determine the capillary pressure of the air-water meniscus around the trapped drops, $P_C = P_A - P_W$, where $P_W$ is the pressure in the aqueous film (for details, see References 697 and 698). The experiments show that the trapped antifoam globules enter

(pierce) the surface of the wetting film at a given, critical capillary pressure, $P_C^{CR}$. Therefore, the equipment allows one to measure $P_C^{CR}$ as a function of various parameters, such as the types of oil and surfactant, concentration of solid particles in the compound, size of the antifoam globules, etc. A larger value of $P_C^{CR}$ corresponds to a higher entry barrier (more difficult drop entry) and vice versa. For compounds having very low entry barriers, a special version of the FTT was developed[697] (gentle FTT), see Figure 60C. Experiments in the presence and absence of a pre-spread oil layer can be performed, which allows one to evaluate the effect of oil spreading on the entry barrier.

#### 5.7.3.2 Critical Entry Pressure for Foam Film Rupture

Experiments with a large set of systems (various oils, compounds, and surfactants) showed[683,698] that there is a well defined threshold value, $P_{TR} \approx 15$ Pa, which separates the fast (foam film breaking) from the slow (Plateau border breaking) antifoams. Some of the results from these experiments are summarized in Figure 61, where the relationship between the foam lifetime and the entry barrier, $P_C^{CR}$, is shown. One sees from this figure that all experimental points fall into two distinct regions: (1) Systems in which the foam is destroyed for less than 10 sec, i.e. these correspond to fast antifoams; for them $P_C^{CR} < 15$ Pa; (2) Systems for which the defoaming time is longer than 5 min (slow antifoams); for them $P_C^{CR} > 20$ Pa. Therefore, the magnitude of the entry barrier is of crucial importance for the time scale of foam destruction by oil-based antifoams. Another relation of $P_C^{CR}$ with the antifoam activity (more precisely, with the height of the residual foam, $H_F$, in the presence of oil drops; see Figure 58D) was discussed in References 678 and 698.

One should note that at high surfactant concentrations, only oil-solid compounds have been observed to behave as fast antifoams, whereas both oils and compounds could behave as slow antifoams depending on the magnitude of the entry barrier (at low surfactant concentrations, the pure oils could also act as fast antifoams). In all experiments it was found that the hydrophobic solid particles reduce the entry barrier by one to two orders of magnitude, but sometimes $P_C^{CR}$ remains higher than the threshold value, $P_{TR}$, and the compound is unable to break the foam films. In the latter cases, the compound globules are expelled into the neighboring Plateau borders during the process of foam film drainage. These results confirm the idea of Garrett[674] that the main role of the solid particles in the antifoam compounds is to reduce the entry barrier of the globules.

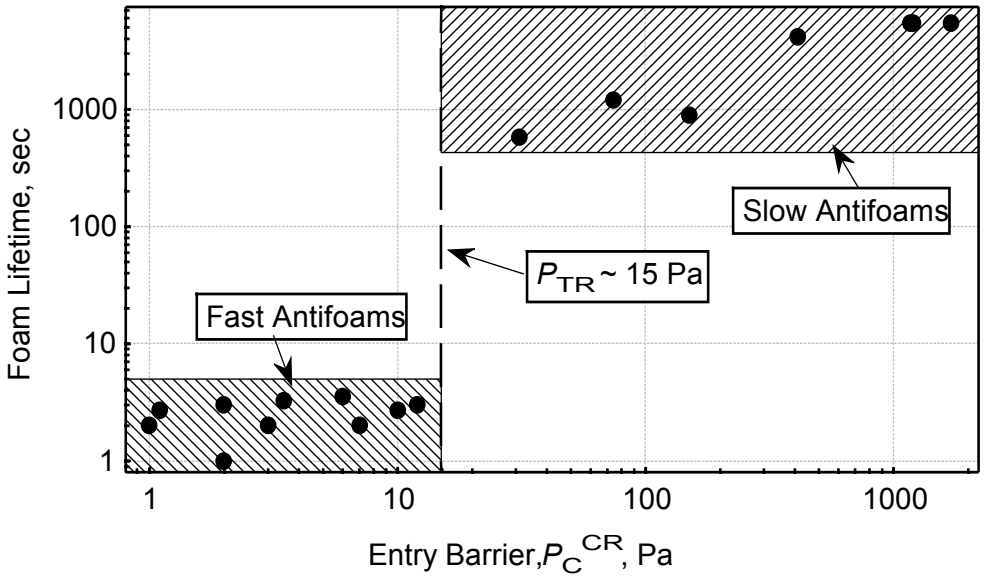


**FIGURE 61.** Correlation between the entry barrier, $P_C^{CR}$, and the foam lifetime measured for various surfactant-antifoam systems: The experimental data (solid circles) fall into two distinct regions: systems in which the foam is destroyed in less than 5 s (fast antifoams) and $P_C^{CR} < 15$ Pa; and systems for which the defoaming time is longer than 8 min (slow antifoams) and $P_C^{CR} > 20$ Pa. The composition of the various systems is given in Reference 698.

### 5.7.3.3 Optimal Hydrophobicity of Solid Particles

Some authors accept[695,699] that the use of more hydrophobic solid particles results in more active antifoam compounds. In a recent study,[685] this idea was experimentally tested by applying the following procedure for a gradual increase of silica hydrophobicity: initially hydrophilic silica particles were mixed with silicone oil at a room temperature, and this mixture was stored under mild stirring for a long period of time. Under these conditions, the adsorption of silicone oil on the silica surface is a slow process which takes weeks before the final, most hydrophobic state of the particles is reached. The antifoam efficiency of the compound was tested every day, and the results obtained with various systems unambiguously showed the presence of a well pronounced, optimal silica hydrophobicity corresponding to highest antifoam efficiency.

The antifoam efficiency in these experiments was evaluated[685] by an automatic shake test. Briefly, 100 mL of the foaming solution was placed in a standard 250 mL glass bottle and 0.01 % of the compound was introduced into this sample. The bottle was then mechanically agitated in a series of consecutive shake cycles. After each cycle of agitation for 10 s, the solution remained quiescent for another 60 s and the defoaming time was measured (defined as the time for appearance of a clean water-air interface without bubbles).

Afterwards, a new shaking cycle was performed and this procedure was repeated until the defoaming time exceeded 60 s in three consecutive cycles - this was considered as the moment of compound exhaustion (see section 5.7.4 and Figure 64 below for further explanations). Larger number of cycles before the compound exhaustion corresponds to better antifoam durability (efficiency) and vice versa.

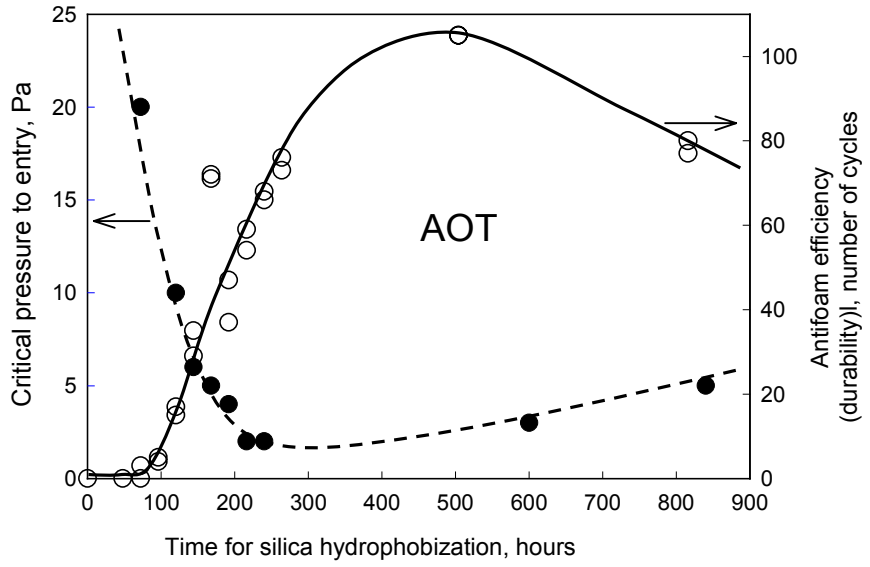


(A)

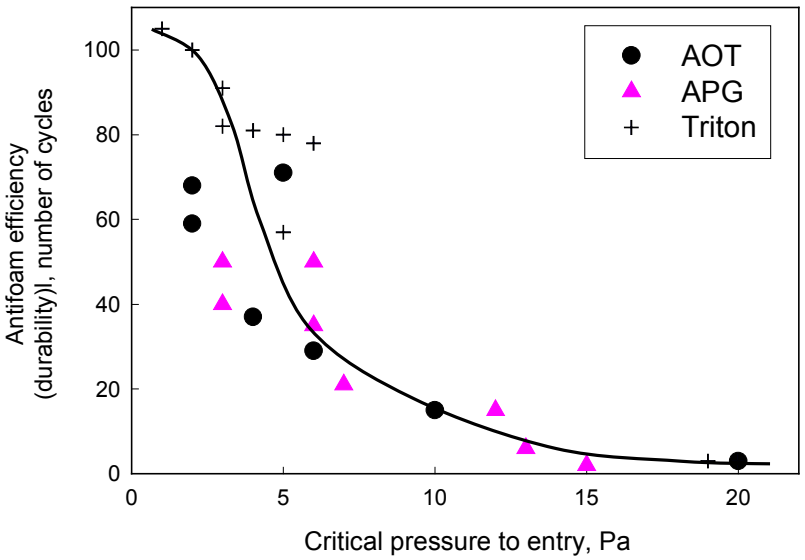


(B)

**FIGURE 62.** (A) Critical pressure for globule entry, $P_C^{CR}$ (full circles), and efficiency (empty circles) of a silicone oil-silica compound in 10 mM AOT solution, as functions of the time of silica hydrophobization; (B) The dependence of the compound efficiency on $P_C^{CR}$ for solutions of three different surfactants: 10 mM anionic AOT, 0.6 mM nonionic APG; and 1 mM nonionic Triton X-100 (adapted from Reference 685).

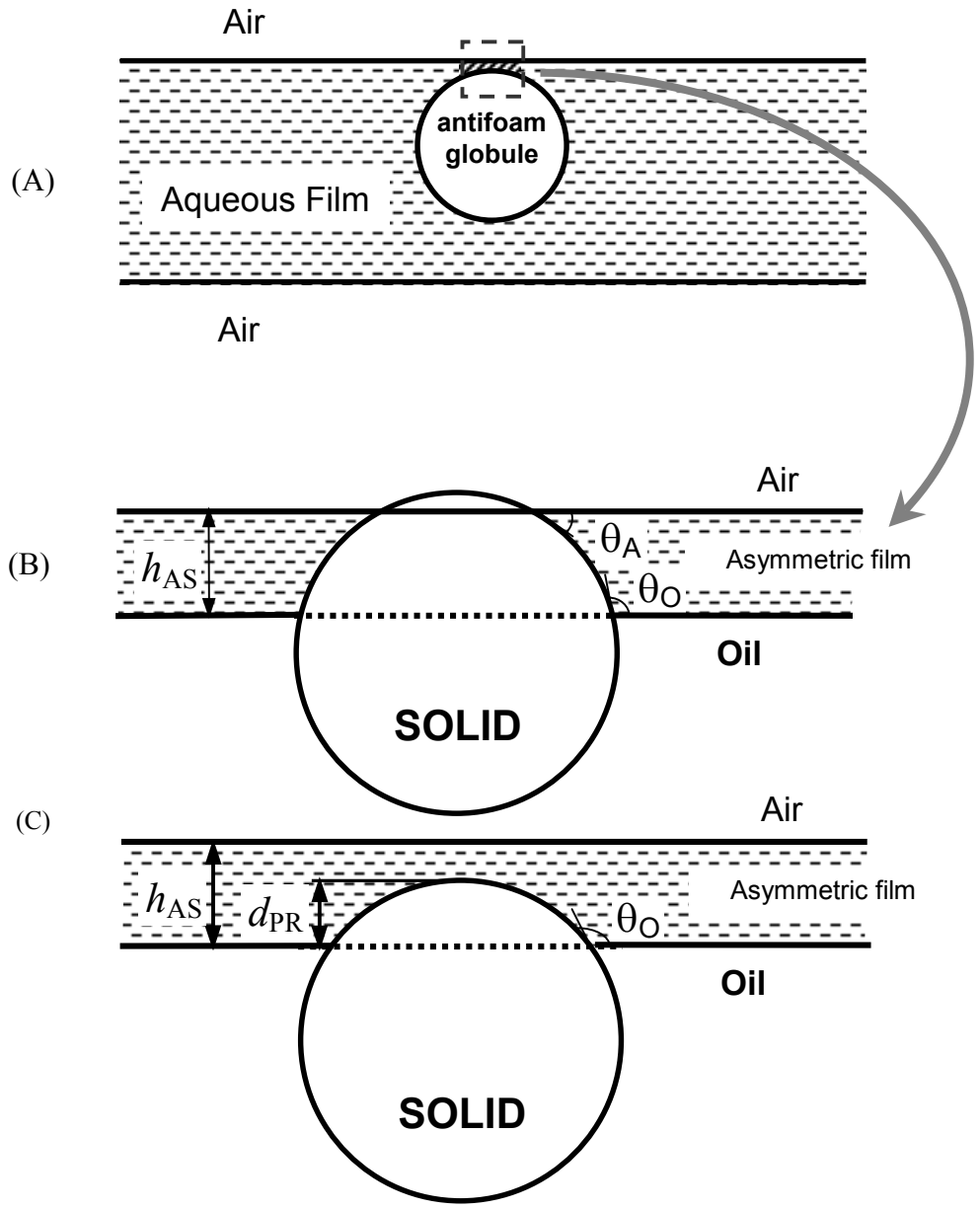


**FIGURE 63**. Schematic explanation of the optimal hydrophobicity of the solid particles in oil-solid antifoam compounds: (A) When an antifoam globule approaches the foam film surface, an asymmetric oil-water-air film of thickness $h_{AS}$ forms. (B) The zone of contact in an enlarged scale. If the protrusion depth, $d_{PR}$, of the solid particle is larger than $h_{AS}$, the particle should be sufficiently hydrophobic ($\theta_A + \theta_O > 180°$) in order to pierce the air/water interface and induce a film rupture; however, if the particle is insufficiently hydrophobic ($\theta_A + \theta_O < 180°$), it would stabilize the film.[674] (C) On the other side, if the solid particles is over-hydrophobized, then $d_{PR} < h_{AS}$ and the particle is again unable to pierce the asymmetric film.[685]

The observed maximum (see the illustrative result presented in Figure 62A) was explained[685] as a result of two requirements which stem from the main role of the silica particles, namely, to assist the globule entry by rupturing the asymmetric oil-water-air films,

see Figure 63. The first requirement, formulated by Garrett,[674] is that the particles should be sufficiently hydrophobic to be dewetted by the oil-water and air-water interfaces (otherwise, the solid particles would stabilize, rather than destabilize the asymmetric film). The other requirement[685] is that the particles should protrude sufficiently deep into the aqueous phase in order to bridge the surfaces of the asymmetric oil-water-air film, and it is better satisfied by more hydrophilic particles. Therefore, an optimal hydrophobicity is expected, at which both requirements are balanced, the entry barrier is low, and the antifoam is most active. Indeed, a straightforward correlation between the antifoam efficiency and the magnitude of the entry barrier, $P_C^{CR}$, was observed in the studied systems, Figure 62B. For spherical particles, the optimal hydrophobicity was expressed as a most favorable three-phase contact angle solid-water-oil:[685]

$$\cos\theta_O \approx h_{AS} / R_P - 1 \tag{339}$$

where $h_{AS}$ is the thickness of the asymmetric oil-water-air film, and $R_P$ is the particle radius, see Figure 63. This angle corresponds to the condition $h_{AS} = d_{PR}$, where $d_{PR} = R_P(1+\cos\theta_O)$ is the equilibrium protrusion depth of the solid particle into the aqueous phase.

#### 5.7.3.4 Role of the Pre-spread Oil Layer

It has been known for many years[674,700,701] that some correlation exists between the spreading behavior of the oils and their antifoam activity. The value of the spreading coefficient:

$$S = \sigma_{AW} - \sigma_{OW} - \sigma_{OA} \tag{340}$$

which characterizes the mode of spreading of the oil on the surface of the solution, and the rate of oil spreading have been often considered as important factors for the antifoam activity. However, as shown by Garrett et al.,[702] the oil spreading is not a necessary condition for having an active antifoam, and many studies[678,679,686] have confirmed that the correlation is not always present.

The effect of the spread oil on the entry barriers of various oils and oil-silica compounds was studied by the FTT.[683,684,687] The experimental results showed that the presence of a pre-spread oil layer on the surface of the solution reduces by several times the entry barrier for mixed oil-silica compounds, see Table 8. Furthermore, it was found[684] that the entry barrier in many systems is below the threshold value $P_{TR} \approx 15$ Pa (which separates the fast from slow antifoams, see Figure 61), only in the presence of a pre-spread layer of oil.

In other words, these antifoams behave as fast ones only because the oil spreads rapidly on the solution surface during foaming, reducing in this way the entry barrier below $P_{TR}$. The results for the entry barrier of oil drops (without silica) also showed a moderate reduction of the entry barrier by a pre-spread oil in most systems.[684,687] However, at least in one of the studied systems (hexadecane drops in solutions of the anionic surfactant sodium dodecyl-benzenesulfonate; see Table 8) a significant increase of the entry barrier upon oil spreading was observed.[687] The entry barrier of the oils in surfactant solutions above their critical micelle concentration (CMC) is higher than $P_{TR}$ both in the presence and absence of spread oil, which explains why the pure oils behave as slow antifoams at typical surfactant concentrations.

**Table 8.** Entry barriers, $P_C^{CR}$, of different antifoams in surfactant solutions in the presence and absence of a pre-spread layer of oil, from which the antifoam is prepared. SDDBS and AOT denote the anionic surfactants sodium dodecyl-benzenesulfonate and sodium dioctyl-sulfosuccinate, respectively. Triton X-100 is the nonionic surfactant nonylphenol deca(ethyleneglycolether). Compound 1 is a mixture of silicone oil and hydrophobized silica; Compound 2 is an emulsion of Compound 1, which contains also solid particles of Span 60 (data from References 684 and 687).

| Antifoam | Surfactant | Spread Layer | $P_C^{CR}$, Pa |
|---|---|---|---|
| Dodecane | 2.6 mM SDDBS | No | 96 ± 5 |
| | | Yes | 48 ± 5 |
| Hexadecane | 2.6 mM SDDBS | No | 80 ± 5 |
| | | Yes | 400 ± 10 |
| Silicone oil | 10 mM AOT | No | 28 ± 1 |
| | | Yes | 19 ± 2 |
| Compound 1 | 10 mM AOT | No | 8 ± 1 |
| | | Yes | 3 ± 2 |
| Compound 2 | 10 mM AOT | No | 20 ± 5 |
| | | Yes | 4 ± 1 |
| Compound 1 | 1 mM Triton X-100 | No | 30 ± 1 |
| | | Yes | 5 ± 2 |
| Compound 2 | 1 mM Triton X-100 | No | 22 ± 1 |
| | | Yes | 7 ± 1 |

One can conclude from the results shown in Table 8, that there is a well pronounced synergistic effect between the solid particles present in compounds and the spread oil. Most of the studied fast antifoams have sufficiently low entry barriers exclusively as a result of the combined action of the solid particles and the spread oil layer.[684]

As mentioned in section 5.7.2, the spread layer of oil has another important role as well. The spread oil is able to feed the oil bridges, formed in foam films, by a mechanism explained in Reference 688 – as a result, larger and less stable oil bridges are formed.

### 5.7.4 MECHANISMS OF COMPOUND EXHAUSTION AND REACTIVATION

The process of antifoam exhaustion (deactivation) is illustrated in Figure 64 - the time for foam destruction in a standard shake test is shown as a function of the number of the shaking cycle (see section 5.7.3.3 for the used shake test).[703] Shorter defoaming time means more active antifoam and vice versa. As seen from Figure 64, the initial high activity of the antifoam deteriorates with the foaming cycles and the defoaming time becomes longer than 60 s after 45 cycles – the antifoam has been exhausted. This process is very undesired from practical viewpoint, and more durable antifoams (able to sustain a larger number of foam destruction cycles) are searched by the manufacturers.

Interestingly, the addition of a new portion of oil (without silica particles) leads to a complete restoration of the antifoam activity (Figure 64). Note that the oil itself has a very weak antifoam activity in the absence of silica. Therefore, the antifoam reactivation certainly involves the solid particles that have been introduced with the first portion of mixed antifoam. The subsequent foaming cycles lead to a second exhaustion series, and such consecutive periods of exhaustion/reactivation can be repeated several times.

Systematic experiments[703] with solutions of the anionic surfactant sodium dioctyl-sulfosuccinate (AOT) showed that the exhaustion of mixed silica-silicone oil antifoams is due to two closely interrelated processes: (1) partial segregation of the oil and silica into two distinct, inactive populations of antifoam globules, silica-free and silica-enriched; (2) disappearance of the spread oil layer from the solution surface, Figure 65. The oil drops deprived of silica, which appear in process 1, are unable to enter the air-water interface and to destroy the foam lamellae, because the entry barrier is too high for them. On the other hand, the antifoam globules enriched in silica trap some oil, which is not available for spreading on the solution surface. As a result, the spread oil layer gradually disappears from the solution

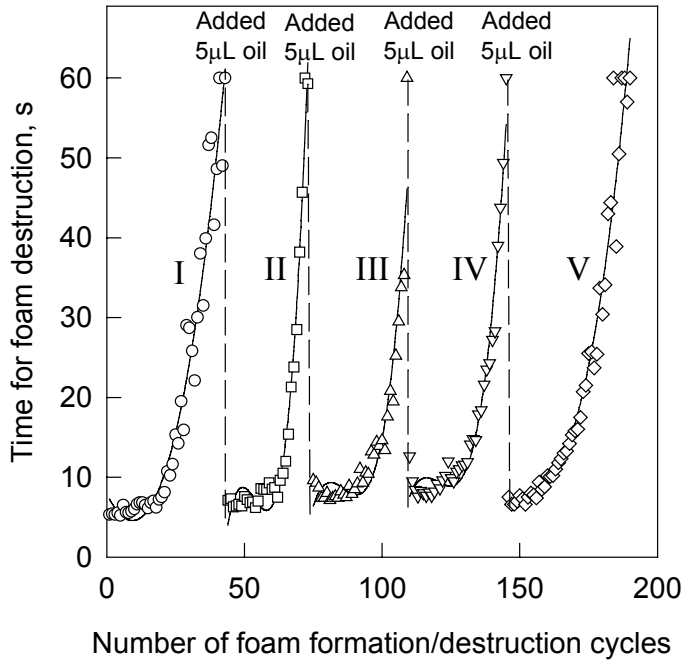


**FIGURE 64**. Consecutive cycles of exhaustion and reactivation of mixed oil-silica compound in 10 mM solution of the anionic surfactant sodium dioctyl-sulfosuccinate (AOT). An initially active antifoam (defoaming time ≈ 5 s) gradually looses its activity with the number of foam formation/destruction cycles in a standard shake test.[703] The introduction of silicone oil results in a perfect restoration of the antifoam activity. Five exhaustion curves (indicated by roman numbers; the symbols indicate the experimentally measured defoaming time) and the corresponding four reactivation events (the vertical dashed lines) are shown; adapted from Reference 703.

surface (process 2) due to oil emulsification in the moment of foam film rupture. Ultimately, both types of globules, silica-enriched and silica-free, become unable to destroy the foam films, and the antifoam transforms into an exhausted state. Accordingly, the reactivation process is due to: (1) restoration of the spread oil layer, and (2) rearrangement of the solid particles from the exhausted antifoam with the fresh oil into new antifoam globules having optimal silica concentration. No correlation between the size of the antifoam globules and their activity was established in these experiments, which showed that the reduction of the globule size (which is often considered as the main factor in the antifoam exhaustion) was a second-order effect in the studied systems. Similar conclusions were drawn from experiments with nonionic surfactants as well.[682]

In conclusion, a progress has been achieved during the last several years in revealing the mechanisms of foam destruction by oil-based antifoams. This progress has been greatly facilitated by the various methods for direct microscopic observations of the foams and foam films (including some of the foam destruction events), and by the implementation of the Film trapping technique for a direct measurement of the entry barriers of the antifoam globules.

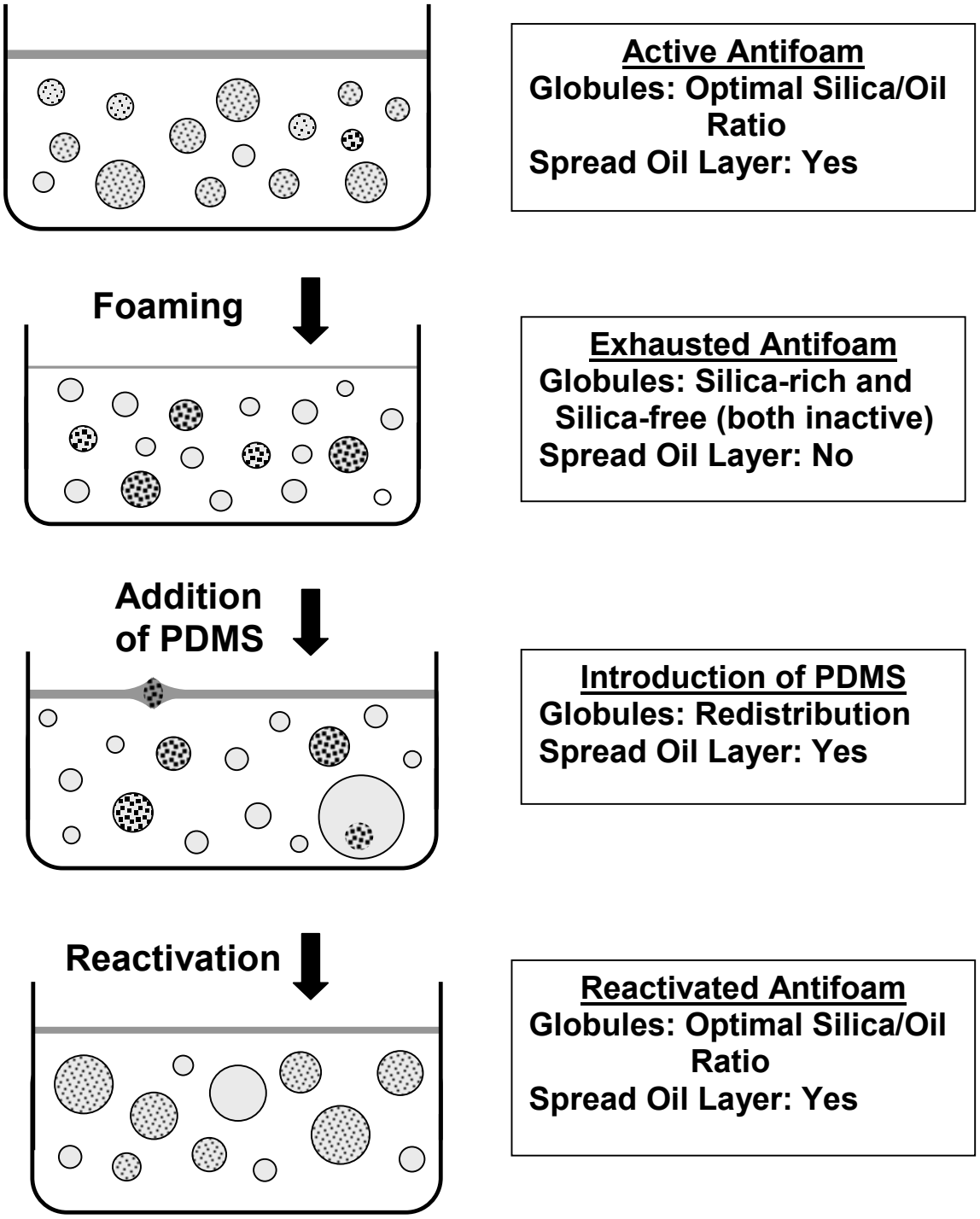


**FIGURE 65.** Schematic presentation of the processes of antifoam exhaustion and reactivation of emulsified oil-silica antifoam compound.

## 5.8 ELECTROKINETIC PHENOMENA IN COLLOIDS

The term "electrokinetic phenomena" refers to several processes which appear when a charged surface (or colloidal particle) is set in a relative motion with respect to the adjacent liquid phase. Classically, four types of electrokinetic phenomena are distinguished: electroosmosis, streaming potential, electrophoresis and sedimentation potential (Figure 66). These will be discussed in Sections 5.8.2 to 5.8.6. Nowadays, the electrical conductivity (at constant electrical field) and the dielectric response (at alternating electrical field) of the disperse systems are often considered together with the electrokinetic phenomena, because the theoretical approaches and the governing equations are similar (Section 5.8.7). Experimental methods based on all these phenomena are widely used for characterization of the electrical surface potential in dispersions. A comprehensive presentation of the topic until the end of 1980s can be found in review articles[704-714] and monographs.[715-717] The recent development of the area is reviewed in the collective monograph, Reference 718. The major experimental techniques are described in Chapter 4 of Ref. 716 and Chapters 8 to 14 in Reference 718. Recently, a substantial interest has been raised by the apparent discrepancy between the results obtained by different electrokinetic methods for one and the same system. This problem is discussed in Section 5.8.8. Finally, the electrokinetic properties of air-water and oil-water interfaces are briefly described in Section 5.8.9.

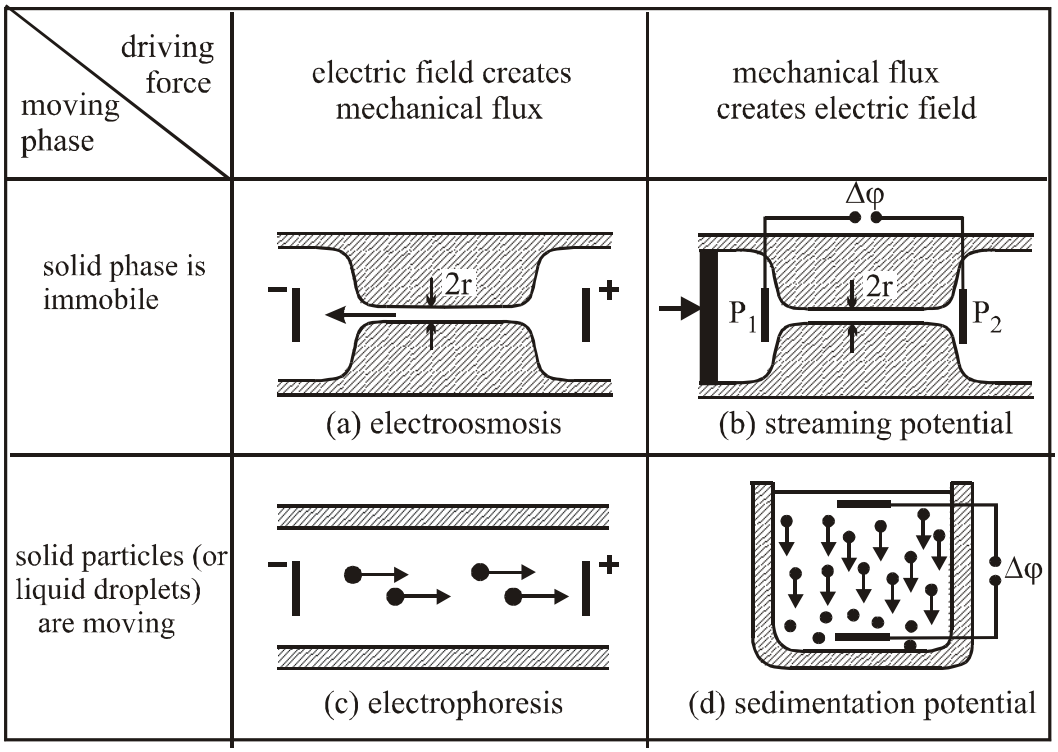


**FIGURE 66.** The four basic electrokinetic phenomena: (a) Electroosmotic liquid flow through a capillary (of charged walls) appears when an electric potential difference is applied; (b) Streaming electric potential appears when a pressure drop drives the liquid to flow through the capillary; (c) Electrophoretic motion of charged particles is observed in an external electric field; (d) Sedimentation potential is established when charged particles are moving under the action of gravity.

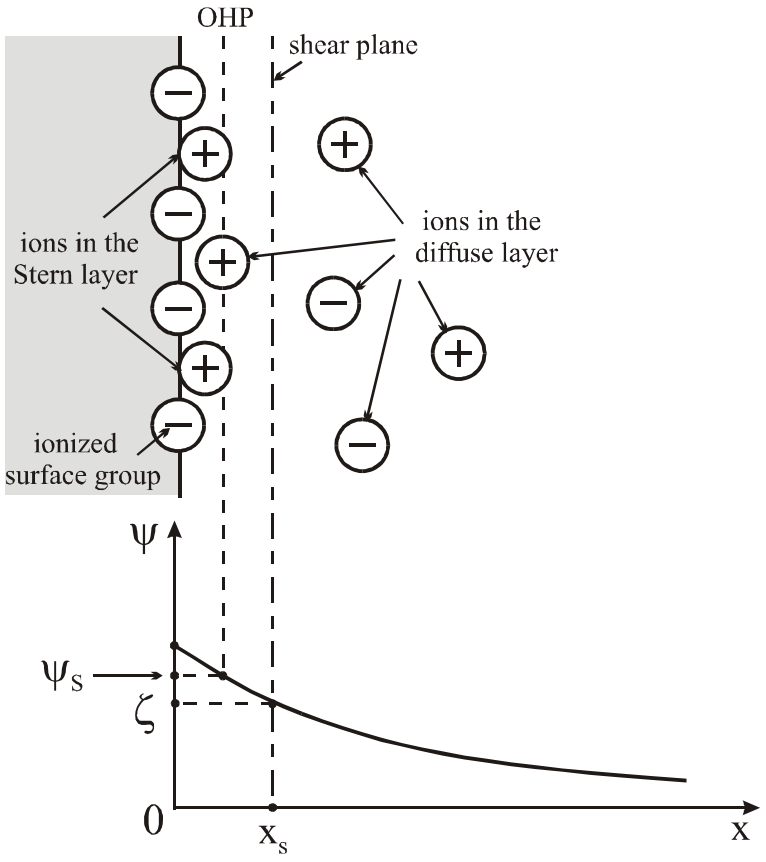


**FIGURE 67.** Schematic presentation of the structure of the electrical double layer (EDL). The surface charge is created by ionized surface groups and/or by ions tightly adsorbed in the Stern layer. The plane of closest approach of the ions from the diffuse part of the electrical double layer is called the outer Helmholtz plane (OHP). The electric potential in the OHP plane is referred to as the surface potential, $\psi_s$, in the text. The shear plane, $x=x_s$, separates the hydrodynamically immobile liquid that moves together with the surface, $x<x_s$, from the mobile liquid, $x>x_s$, which has non-zero relative velocity with respect to the surface. Note that the ions in the immobile part of the EDL can move with respect to the surface under an applied electric field, which gives rise to the anomalous surface conductivity (section 5.6.8).

### 5.8.1 POTENTIAL DISTRIBUTION AT A PLANAR INTERFACE AND AROUND A SPHERE

When a dielectric phase (solid or fluid) is placed in contact with polar liquid, such as water, the interface gets charged due to either specific adsorption of ions initially dissolved in the polar liquid, or dissociation of surface ionizable groups.[14,34,717] The final result of these two processes is the formation of an electrical double layer (see Figure 67), which may contain three types of ions:

1. Ions attached to the surface by chemical bond are those parts of the ionized groups which remain bound after the dissociation process.

2. Ions bound by very strong Coulomb attraction (after partial loss of molecules from the ion solvating shell) or by some other noncovalent specific, short-range attraction build up the so-called Stern layer.

3. Ions that are involved in more or less free Brownian motion present the diffuse part of the electrical double layer.

The ions from groups (1) and (2), considered together, determine the effective surface charge density, $\sigma_s$, which must be balanced by an excess of counterions in the diffuse layer (equal in magnitude and opposite in sign). The distribution of electrical potential in the diffuse layer is usually rather accurately described by the Poisson-Boltzmann (PB) equation:

$$\nabla^2\psi = -\frac{e}{\varepsilon\varepsilon_0}\sum_j Z_j n_{b,j} \exp\left[-\frac{eZ_j\psi}{kT}\right] \tag{341}$$

where $\psi$ is the local (average) value of the electrical potential; $e$ is the elementary charge; $\varepsilon$ is the relative dielectric permittivity of the liquid; $\varepsilon_0$ is the electrical permittivity *in vacuo*; and $Z_j$ and $n_{b,j}$ are the number of charges and the bulk number concentration, respectively, of ion $j$. The model of the electrical double layer based on Equation 341 is called in the literature Gouy-Chapmen or Gouy-Stern model. For symmetrical ($Z$:$Z$) electrolyte, the PB equation can be written in the form:

$$\nabla^2\psi = \frac{2eZn_0}{\varepsilon\varepsilon_0}\sinh\left(\frac{eZ\psi}{kT}\right) \tag{342}$$

where $n_0$ is the bulk electrolyte number concentration. For a flat interface (see Figure 67), Equation 342 has an exact analytical solution:[34,278,717]

$$\psi(x) = \frac{2kT}{eZ}\ln\left[\frac{1+\gamma_s\exp(-\kappa x)}{1-\gamma_s\exp(-\kappa x)}\right] \tag{343}$$

where

$$\gamma_s \equiv \tanh\left(\frac{ze\psi_s}{4kT}\right), \qquad \kappa \equiv \left(\frac{2e^2Z^2n_0}{\varepsilon\varepsilon_0 kT}\right)^{1/2}$$

and $\psi_s$ is the electrical potential at the surface of closest approach of the ions from the diffuse layer to the interface. This surface is called the *outer Helmholtz plane* and $\psi_s$ is called the *surface potential*. The surface charge and potential are interrelated by the expression:

$$\sigma_s = -\varepsilon\varepsilon_0\left(\frac{d\psi}{dx}\right)_{x=0} = (8\varepsilon\varepsilon_0 kTn_0)^{1/2}\sinh\left(\frac{eZ\psi_s}{2kT}\right) \tag{344}$$

which is a direct corollary[14,34] from Equation 342 and the condition for overall electroneutrality of the interface.

If the surface potential is small, one can expand in series the logarithm in the right-hand-side of Equation 343 and derive the Debye-Hückel equation:

$$\psi(x) = \psi_s \exp(-\kappa x), \qquad \frac{Ze\psi_s}{kT} < 1 \tag{345}$$

On the other hand, the potential always decays exponentially far from the interface ($\kappa x \gg 1$) at an arbitrary magnitude of $\psi_s$ (see Equation 343):

$$\psi(x) = \frac{4kT}{eZ}\gamma_s \exp(-\kappa x), \qquad \kappa x >> 1 \tag{345a}$$

The potential distribution around a spherical particle can be found from the PB equation (Equation 341), which in this case reads:

$$\frac{1}{r^2}\frac{d}{dr}\left(r^2 \frac{d\psi}{dr}\right) = -\frac{e}{\varepsilon\varepsilon_0}\sum_j Z_j n_{b,j} \exp\left[-\frac{eZ_j\psi(r)}{kT}\right] \tag{346}$$

The respective boundary conditions are

$$\psi(r = R) = \psi_s, \qquad \psi(r \to \infty) = 0$$

Equation 346 has an analytical solution only in the case of small surface potential:

$$\psi(r) = \psi_s \frac{R\exp[-\kappa(r-R)]}{r}, \quad \frac{Ze\psi_s}{kT} < 1 \tag{347}$$

In this case, the surface charge density is a linear function of $\psi_s$:

$$\sigma_s = \frac{\varepsilon\varepsilon_0(1+\kappa R)}{R}\psi_s, \qquad \frac{Ze\psi_s}{kT} < 1 \tag{348}$$

For a large surface potential, $\psi_s$, the potential distribution can be found by numerical integration of the PB equation. Far from the sphere surface, the potential always obeys the law:

$$\psi(r) = \psi_s^* \frac{R\exp[-\kappa(r-R)]}{r}, \qquad \kappa(r-R) >> 1 \tag{349}$$

where $\psi_s^*(\kappa R, \psi_s)$ is an effective potential, which can be found by numerical solution of the PB equation. By using the method of matched asymptotic expansions, Chew and Sen[719] obtained for a thin electrical double layer ($\kappa R > 1$):

$$\psi_s^* = \frac{4kT}{Ze}\left(\gamma_s + \frac{\gamma_s^3}{2\kappa R}\right) \tag{350}$$

A useful relationship between $\psi_s$ and $\sigma_s$ for a sphere was proposed by Loeb et al.:[720]

$$\sigma_s = \frac{\varepsilon\varepsilon_0\kappa kT}{Ze}\left[2\sinh\left(\frac{Ze\psi_s}{2kT}\right) + \frac{4}{\kappa R}\tanh\left(\frac{Ze\psi_s}{4kT}\right)\right] \tag{351}$$

and was theoretically justified by other authors.[718,721-724] Equation 351 coincides with the exact numerical results within an accuracy of a few percent for $\kappa R>0.5$ and arbitrary surface potential.[716,720] A general approach for derivation of approximate (but accurate) expressions relating $\psi_s$ and $\sigma_s$, including for systems containing non-symmetric electrolytes, has been proposed by Ohshima.[724,725]

### 5.8.2 ELECTROOSMOSIS

When an electrical field of intensity $E$ is applied in parallel to a charged flat interface, the excess of counterions in the diffuse layer gives rise to a body force exerted on the liquid. The liquid starts moving with local velocity varying from zero in the plane of shear ($x=x_s$) to some maximal value, $V_{EO}$, at a large distance from the wall (see Figure 67). The magnitude of this electroosmotic velocity was calculated by Smoluchowski[726] under the assumptions that: (1) the ion distribution in the diffuse layer obeys the PB equation, (2) at each point the electrical force is balanced by the viscous friction, and (3) the liquid viscosity in the diffuse layer is equal to that of the bulk liquid, $\eta$. The final result reads:[726]

$$V_{EO} = -\frac{\varepsilon\varepsilon_0\zeta}{\eta}E \tag{352}$$

where $\zeta$ is the electrical potential in the shear plane, i.e., $\zeta \equiv \psi(x=x_s)$. The quantity

$$\mu_{EO} = \frac{V_{EO}}{E} = -\frac{\varepsilon\varepsilon_0\zeta}{\eta} \tag{353}$$

is called *electroosmotic mobility*. The Smoluchowski consideration is also applicable to capillaries of a radius much larger than the Debye screening length, $\kappa^{-1}$. Therefore, by measuring the liquid flow through a capillary, like that shown in Figure 66, one can determine the $\zeta$ potential of the capillary surface. It is usually acceptable[716] to measure the liquid flux (volume displaced per unit time), $J_{EO}$, along with the electric current transported by the liquid, $I_{EO}$:

$$J_{EO} = \pi r^2 V_{EO} \quad \text{and} \quad I_{EO} = \pi r^2 \chi_b E \tag{354}$$

where $r$ is the capillary radius and $\chi_b$ is the bulk conductivity of the liquid. The ratio

$$\left|J_{\mathrm{EO}} / I_{\mathrm{EO}}\right| = \left|V_{\mathrm{EO}} / \chi_b E\right| = \frac{\varepsilon\varepsilon_0\zeta}{\eta\chi_b} \tag{355}$$

does not depend on the capillary radius and can be used to determine ζ. Quite often, however, the high concentration of ions in the double electric layer leads to a much higher conductivity in the surface region, compared to that in the bulk electrolyte solution. To account for this effect Bikerman[727] introduced the term "specific surface conductivity", $\chi_s$, which presents an excess quantity over the bulk conductivity. Then, Equation 354 is modified to read:

$$I_{\mathrm{EO}} = \left(\pi r^2 \chi_b + 2\pi r \chi_s\right) E \tag{356}$$

and Equation 355 acquires the form:

$$\left|J_{\mathrm{EO}} / I_{\mathrm{EO}}\right| = \frac{\varepsilon\varepsilon_0\zeta}{\eta\left(\chi_b + 2\chi_s / r\right)} \tag{357}$$

Alternatively, instead of measuring the electro-osmotic liquid flux at zero pressure difference across the capillary, one can determine[716] ζ by measuring the counterpressure, $\Delta P_{\mathrm{EO}}$, necessary to completely stop the net liquid transport through the capillary:

$$\Delta P_{\mathrm{EO}} = \frac{8\varepsilon\varepsilon_0\zeta}{\pi r^4\left(\chi_b + 2\chi_s / r\right)} I_{\mathrm{EO}} \tag{358}$$

Bikerman[727] obtained the following expression for $\chi_s$ in the case of a symmetrical (*Z*:*Z*) electrolyte, under the assumption that the surface conductivity is due only to the ions located in the movable part of the diffuse layer:

$$\chi_s = \frac{2Z^2 e^2 n_0}{kT\kappa}\left\{D^+\left[\exp\left(-\frac{Ze\zeta}{2kT}\right)-1\right]\left(1+\frac{3m^+}{Z^2}\right)+D^-\left[\exp\left(\frac{Ze\zeta}{2kT}\right)-1\right]\left(1+\frac{3m^-}{Z^2}\right)\right\} \tag{359}$$

where $D^{\pm}$ are ion diffusion coefficients, while $m^{\pm}$ are dimensionless ion mobilities, defined as

$$m^{\pm} = \frac{2}{3}\left(\frac{kT}{e}\right)^2 \frac{\varepsilon\varepsilon_0}{\eta}\frac{Z^2}{D^{\pm}} = \frac{2\varepsilon\varepsilon_0 N_A kT}{3\eta}\frac{Z^2}{\Lambda^0} = 12.84\times10^{-4}\left(\frac{Z^2}{\Lambda^0}\right) \quad \text{at } 25^{\circ}\mathrm{C} \text{ in water} \tag{360}$$

Λ° ($m^2$ $ohm^{-1}$ $mol^{-1}$) is the limiting molar conductivity of ions at infinite dilution. The typical values of $\chi_s$ are around $10^{-9}ohm^{-1}$. For comparison, the bulk conductivity, $\chi_b$, is given by:

$$\chi_b = \frac{e^2}{kT}\sum D_j Z_j^2 n_{b,j} \tag{361}$$

and can vary within a wide range (note that $\chi_s$ and $\chi_b$ have different dimensions).

Equation 357 shows that for determination of ζ and $\chi_s$, one needs measurements with several capillaries made of the same material, but having different radii. The effect of the surface conductivity can be neglected when the criterion:

$$\frac{2\chi_s}{\chi_b r} \sim \frac{\exp\left(\frac{Ze\psi_s}{2kT}\right)}{\kappa r} << 1 \tag{362}$$

is satisfied.[716,717,728] In other words, the surface conductivity is negligible at low surface potential and high ionic strength. Besides, Equation 355 can be applied[716,728,729] also to electroosmotic flow in porous plugs or membranes if: (1) the typical pore size is much larger than $\kappa^{-1}$, (2) the effects of the surface conductivity, $\chi_s$, are negligible, and (3) the flow is laminar.

This consideration can be extended to include capillaries of radii comparable to $\kappa^{-1}$ and the cases when the potential distribution cannot be approximated using the results for a planar wall.[707,716]

The so-called plane interface technique[730,731,732] is a modification of the electroosmotic method, in which submicrometer particles are used as probes to visualize the osmotic velocity profile close to an interface. The method allowed precise determination of the ζ potential at mica, quartz, sapphire, and fused-silica surfaces as a function of pH.[731,732] The attempt[730,732,733] to apply the plane interface technique to the air-water interface, however, gave ambiguous results, probably due to the interfacial fluidity.

### 5.8.3 STREAMING POTENTIAL

If a pressure drop, $\Delta P = P_1 - P_2$, is imposed at the ends of a capillary, like that shown in Figure 66, the liquid starts moving through the capillary.[716,723] The charges in the mobile part of the double layer at the capillary wall are thus forced to move toward the end of the capillary. As a result, a streaming current, $I_{ST}$, appears which leads to the accumulation of excess charge at the capillary end. This excess charge gives rise to an electric potential difference between the ends of the capillary, called *streaming potential*, $E_{ST}$. On its own, the streaming potential causes a current flow, $I_C$, in a direction opposite to $I_{ST}$. Finally, a steady state is established when $|I_C| = |I_{ST}|$ and the net electric current across the capillary becomes zero. One can directly measure $E_{ST}$ by probe electrodes, and the following relationship is used to determine the ζ potential of the capillary walls:[716]

$$\frac{E_{ST}}{\Delta P} = \frac{\varepsilon\varepsilon_0\zeta}{\eta\left(\chi_b + 2\chi_s / r\right)} \tag{363}$$

Alternatively, instead of measuring $E_{ST}$, one can measure the streaming current, $I_{ST}$, by using the appropriate electrical circuit:[716]

$$I_{ST} = -\frac{\varepsilon\varepsilon_0}{\eta}\frac{\pi r^2}{L}\Delta P\zeta \tag{364}$$

Here, $L$ denotes the length of the capillary. An important advantage of the streaming current measurement is that the surface conductivity does not matter for the calculation (see Equation 364), and experimental determination of $\chi_s$ is not necessary. Similar experiments were performed by Scales et al.[734] to determine the $\zeta$ potential of mica surface.

Equations 363 and 364 are valid only if the capillary radius is much larger than the thickness of the diffuse layer. A number of modifications were suggested in the literature to extend the theoretical consideration to narrower capillaries and porous plugs (see, for example, the review article by Dukhin and Derjaguin[707] and the book of Hunter[716]). Measurements of the streaming potential, streaming current and electrical conductance of plugs made of latex particles were performed and analyzed by van den Hoven and Bijsterbosch.[735]

### 5.8.4 ELECTROPHORESIS

The movement of a charged colloidal particle in an external electrical field is called *electrophoretic motion* and the respective phenomenon is electrophoresis. The electrophoretic velocity in the two limiting cases, of a thin and thick electrical double layer around a spherical particle, can be calculated by Smoluchowski[736] and Hückel[737] formulas:

$$V_{\mathrm{EL}} = \frac{\varepsilon\varepsilon_0\zeta}{\eta}E, \qquad \kappa R >> 1 \qquad \text{(Smoluchowski)} \tag{365}$$

$$V_{\mathrm{EL}} = \frac{2}{3}\frac{\varepsilon\varepsilon_0\zeta}{\eta}E, \qquad \kappa R << 1 \qquad \text{(Hückel)} \tag{366}$$

It is important to note that Equation 365 is valid for particles of arbitrary shape and size, if the following requirement is fulfilled: The dimensions of the particle and the local radii of curvature of the particle surface are much larger than the Debye screening length.

The problem for spherical particles at arbitrary $\kappa R$ was solved by Henry[738] who obtained:

$$\mu_{\mathrm{EL}} = \frac{V_{\mathrm{EL}}}{E} = \frac{2}{3}\frac{\varepsilon\varepsilon_0\zeta}{\eta}f_1(\kappa R) = \frac{Q}{6\pi\eta R(1+\kappa R)}f_1(\kappa R) \qquad \text{(Henry)} \tag{367}$$

where $\mu_{\mathrm{EL}}$ is the particle electrophoretic mobility, $Q$ is the particle charge, and $f_1(\kappa R)$ is a correction factor given by:

$$f_1(\kappa R)=\frac{3}{2}-\frac{9}{2}(\kappa R)^{-1}+\frac{75}{2}(\kappa R)^{-2}-330(\kappa R)^{-3}, \qquad \kappa R>1$$

$$f_1(\kappa R)=1+\frac{1}{16}(\kappa R)^2-\frac{5}{48}(\kappa R)^3-\frac{1}{96}\left[(\kappa R)^4-(\kappa R)^5\right] \qquad (368)$$

$$+\left[\frac{1}{8}(\kappa R)^4-\frac{1}{96}(\kappa R)^6\right]\exp(\kappa R)\mathrm{E}_1(\kappa R), \qquad \kappa R<1$$

and $\mathrm{E}_1(x)\equiv\int_1^\infty e^{-sx}\frac{ds}{s}$ is an integral exponent of the first order. The limiting values, $f_1(\kappa R\to\infty)=3/2$ and $f_1(\kappa R\to 0)=1$, reduce Henry's equation to the equations of Smoluchowski and Hückel, respectively. The effect of the surface conductivity, $\chi_s$, can be phenomenologically included in this approach, as shown by Henry.[739] Also, if the material of the particle has finite electrical conductivity, $\chi_p$, its electrophoretic mobility is given by:[738]

$$\mu_{\mathrm{EL}}=\frac{2}{3}\frac{\varepsilon\varepsilon_0\zeta}{\eta}f_2\left(\kappa R,\chi_p/\chi_b\right) \qquad (369)$$

where

$$f_2\left(\kappa R,\chi_p/\chi_b\right)=1+2\frac{\left(\chi_b-\chi_p\right)}{\left(2\chi_b+\chi_p\right)}\left[f_1(\kappa R)-1\right] \qquad (370)$$

It was shown,[707,708,715] however, that the approach of Henry is strictly valid only for small values of the ζ potential, $\frac{Ze\zeta}{kT}<1$, because it neglects the relaxation and the retardation effects, connected with distortion of the counterion atmosphere around the moving particle. Solutions of the problem for not-too-high ζ potentials were suggested by Overbeek[740] and Booth.[741] The mobility of a spherical, non-conducting particle of arbitrary ζ potential and arbitrary $\kappa R$ was rigorously calculated by Wiersema et al.[742] and by O'Brien and White.[743] In Figure 68, the results of O'Brien and White[743] for the particle mobility as a function of the ζ potential at different values of $\kappa R$ are represented. One interesting conclusion from these calculations is that the mobility has a maximum for $\kappa R>3$, i.e., a given value of $\mu_{\mathrm{EL}}$ may result from two different values of ζ. The maximum in these curves appears at $\zeta\sim 150$ mV. The numerical algorithm of O'Brien and White[743] is sufficiently rapid to allow application to individual sets of experimental data.

Explicit approximate expressions were suggested by several authors. For a thin electrical double layer, Dukhin and Derjaguin[707] derived a formula, which was additionally simplified (without loss of accuracy) by O'Brien and Hunter:[744]

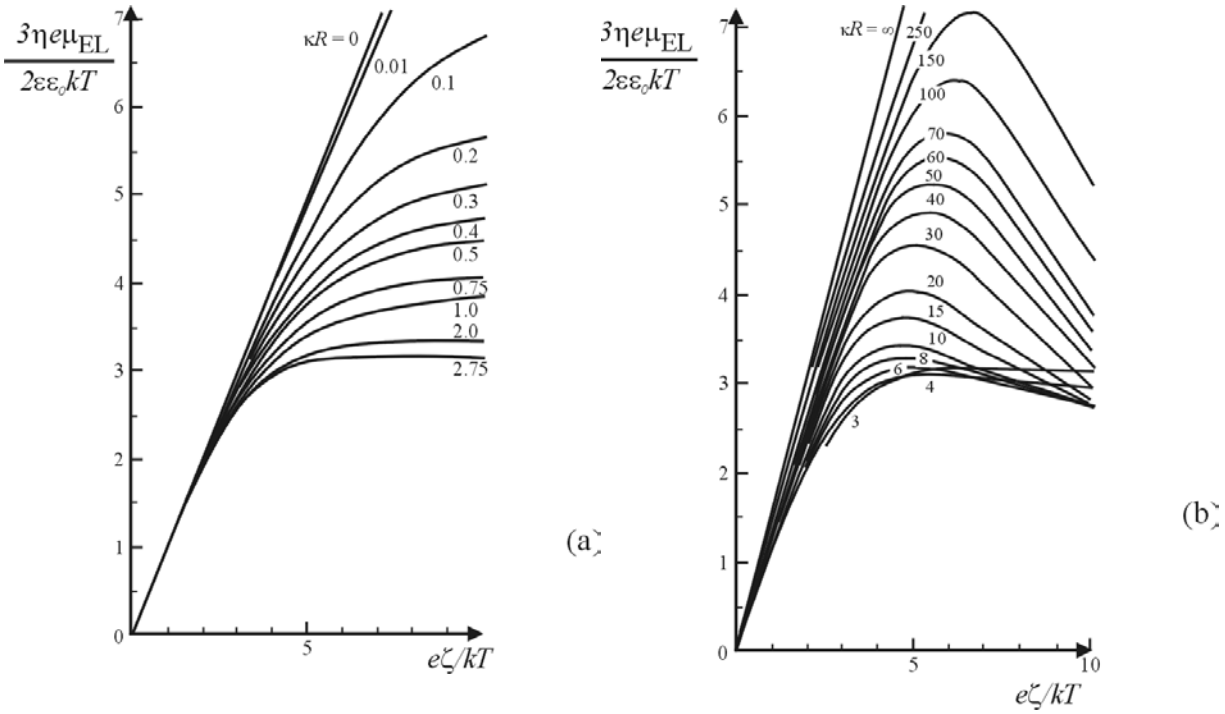


**FIGURE 68.** The dimensionless electrophoretic mobility of spherical particles vs. the dimensionless ζ potential for various values of κ*R*: (a) κ*R* varies between 0 and 2.75; (b) κ*R* varies between 3 and infinity. (From O'Brien R.W. and White L.R., *J. Chem. Soc. Faraday Trans. 2*, 74, 1607, 1978. With permission).

$$\mu_{EL} = \frac{\varepsilon\varepsilon_0}{\eta}\zeta - 4\frac{\varepsilon\varepsilon_0 kT}{e}\left\{\frac{\frac{\tilde{\zeta}}{2} - \frac{\ln 2}{Z}\left[1 - \exp\left(-Z\tilde{\zeta}\right)\right]}{2 + \frac{\kappa R}{\tilde{M}}\exp\left(-Z\tilde{\zeta}/2\right)}\right\}, \qquad \kappa R >> 1 \tag{371}$$

where $\tilde{\zeta} \equiv \frac{e\zeta}{kT}$ is the dimensionless $\zeta$ potential, $\tilde{M} = (1+3m/Z^2)$, and $m$ is the dimensionless mobility of the ions (see Equation 360). Equation 371 was derived assuming equal valency and mobility of the counter- and coions. The comparison with the exact numerical calculations showed that Equation 371 is rather accurate for κ*R*>30 and arbitrary ζ potential. Another explicit formula of high accuracy (less than 1% for arbitrary ζ potential) and wider range of application (κ*R*>10) was suggested by Ohshima et al.[745]

For low values of the ζ potential, Ohshima[746] suggested an approximate expression for the Henry's function (Equations 367 and 368), which has a relative error of less than 1 % for arbitrary values of κ*R*:

$$\mu_{EL} = \frac{2}{3}\frac{\varepsilon\varepsilon_0\zeta}{\eta}\left(1 + \frac{1}{2\left\{1 + 2.5/\left[\kappa R(1 + 2e^{-\kappa R})\right]\right\}^3}\right) \tag{372}$$

Recently, Ohshima[747] derived an extension of Equation 372, which is accurate for $\tilde{\zeta} < 3$ at arbitrary values of $\kappa R$.

The electrophoretic mobility of particles having a cylindrical or ellipsoidal shape was studied theoretically by Stigter,[748] van der Drift et al.,[749] and Ohshima.[750] The polyelectrolytes[751-753] and the spherical particles covered by a layer of polymer[754,755] (or of polyelectrolyte) are two other types of systems that have been matters of great interest. In a recent series of papers Ohshima and Kondo[756-758] derived a general analytic formula for the case of a hard particle, covered by a layer of polyelectrolyte. In the corresponding limiting cases, the general expression reduces to the known expressions for a hard spherical particle, a plate-like particle covered by a polyelectrolyte layer, or a charged porous sphere. [756,757]

Churaev and Nikologorskaja[759] performed measurements of the electrophoretic mobility and the diffusion coefficient of silica particles before and after adsorption of polyethylenoxides. They found that the experimental data can be explained only by assuming that the adsorbed polymer layer not only shifts the shear plane apart from the particle surface (thus increasing the hydrodynamic radius of the particles) but also substantially reduces the particle surface potential. According to the authors[759] the decrease in the surface charge could be due to the lower dielectric permittivity in the adsorption layer compared to that of water. It is rather possible that a similar effect played a role in the experiments of Furusawa et al.,[760] who showed that the adsorption of hydroxylpropylcellulose on latex particles may completely shield their charge (the particle $\zeta$ potential becomes zero). Since the adsorption layer was shown to be very stable in a wide range of pH and electrolyte concentrations, such particles can be used as a reference sample for electrophoretic measurements. These particles exactly follow the electroosmotic liquid flow in the cell and, hence, represent a convenient probe sample for the plane interface technique mentioned in Section 5.8.2.

The effect of the interparticle interactions on the electrophoretic mobility in concentrated dispersions was theoretically studied by Levine and Neale.[761] They used a cell model with two alternative boundary conditions at the cell boundary to describe the hydrodynamic flow: the free surface model of Happel[762] and the zero vorticity model of Kuwabara.[763] The results[761] suggested that the zero vorticity model is more appropriate, because it represents in a more correct way the limit to low particle concentration. Experiments at very low electrolyte concentrations, when the electrostatic interactions between the particles are very strong, were performed by Deggelmann et al.[764] They observed a strong increase in the electrophoretic mobility at lower ionic strength (when the electrostatic interaction is stronger and the particles form a liquid-like structure) which was in apparent

contradiction with the predictions of the Levine and Neale's theory.[761] One possible explanation of this surprising result could be that the decrease of the ionic strength leads to a simultaneous increase in the surface potential,[34] and this effect prevails over the increased interparticle interactions. Further development of the electrokinetic theory for concentrated dispersions was presented by Kozak and Davis,[765] and by Ohshima.[757,766]

Another interesting experimental study of concentrated suspensions of human erythrocytes was performed by Zukoski and Saville.[767] Although volume fractions as high as 75% were employed, the electrophoretic mobility changed by the factor $(1-\phi)$ in the whole concentration range, which was simply explained by the backflow of liquid necessary to conserve the suspension volume. The electrostatic and hydrodynamic particle-particle interactions apparently cancelled each other in these experiments. One should note that the electrolyte concentration was relatively high and, contrary to the experiments of Deggelmann et al.,[764] the electrical double layers were thin in comparison with the particle size.

A recent progress was achieved in the theoretical description of the electrophoretic mobility of spherical particles in oscillating electrical field[768] (so-called dynamic mobility); see also section 5.8.7.2. General equations at an arbitrary frequency, $\zeta$ potential, and $\kappa R$, as well as analytical formulas for low $\zeta$ potentials, were derived by Mangelsdorf and White.[768] Theory and experiment[769] demonstrated rather strong frequency dependence of the electrophoretic response of the particles in the hertz and kilohertz regions. A general theoretical expressions, along with explicit approximate formulas, for the dynamic electrophoretic mobility of spheres and cylinders were derived by Ohshima.[757,770,771] The electrophoretic measurements in oscillating fields are stimulated also by the fact that the undesirable effect of the electroosmotic flow in the experimental cell, created by the charge at the cell walls, is strongly suppressed in this type of equipment.[769,772]

Another important recent development is the construction of equipment capable of measuring the mobility of nanometer-sized particles, such as micelles and protein molecules. The different mobility of proteins in polymer gels is widely used for their separation and identification,[773] but this method is not suitable for the physico-chemical study of proteins, because the interactions of the protein molecules with the polymer gel matrix could be rather specific. For a long time the electrophoretic mobility of proteins in a free solution was studied by the "moving boundary method" of Tiselius,[774] since electrophoretic equipment based on dynamic light scattering (Section 5.7.2.1) is limited to particles of a size between approximately 50 nm and 10 μm. The method of Tiselius is not so easy and, in principle, it is not very suitable for micellar solutions, because a boundary between solutions of different concentrations must be formed. Imae et al.[775-780] described an improved version of electrophoretic light scattering equipment applicable to particles of a diameter as small as several nanometers. The feasibility of this equipment was demonstrated[776] by measuring the

electrophoretic mobility of micelles of sodium dodecylsulfate (SDS) and of mixed micelles of SDS with nonionic surfactants. The electrokinetic properties of micelles are discussed in the recent review by Imae.[780] This experimental advance is accompanied by progress in the theoretical analysis of the electrophoretic mobility of non-spherical and non-uniformly charged particles (such as proteins) with some spatial charge distribution on the particle surface.[781-784] One quite interesting conclusion from the work of Yoon[784] was that Henry's formula, Equations 367-368, is correct for spherical particles of arbitrary charge distribution (with $Q$ being the net particle charge in this case), provided that the electrical potential is low and can be described by the linearized PB equation.

More details about the method of electrophoretic mobility measurement by means of dynamic light scattering are given in Section 5.9.2.1.

### 5.8.5 SEDIMANTATION POTENTIAL

When a charged particle is sedimenting under the action of gravity (Figure 66(d)) the ions in the electrical double layer are not obliged to follow the particle motion. Instead, a continuous flow of ions enters the lower half of the particle diffuse layer and leaves its upper half. The net effect is a spatial separation of the negative and positive charges which creates the sedimentation potential of intensity, $E_{\mathrm{SED}}$. At a steady state, the electrical current caused by the particle motion must be counterbalanced by an equal-in-magnitude (but opposite-in-direction) current created by $E_{\mathrm{SED}}$. The intensity, $E_{\mathrm{SED}}$, can be directly measured by means of electrode probes placed at two different levels in the suspension of settling particles. Smoluchowski[785] derived the following equation connecting $E_{\mathrm{SED}}$ and the $\zeta$ potential of spherical non conducting particles:

$$E_{\mathrm{SED}} = \frac{\varepsilon\varepsilon_0}{\eta}\frac{F_g \rho_p}{\chi_b} \qquad \text{at } \kappa R >> 1 \tag{373}$$

where $F_g = gV_p(d_p - d_0)$ is the gravity force (with subtracted Archimedes' force) acting on a particle; $\rho_p$ is the particle number concentration; $g$ is gravity acceleration; $V_p$ is the particle volume; $d_p$ is the particle mass density; and $d_0$ is the mass density of the disperse medium. Generalization of the theoretical consideration to arbitrary values of $\kappa R$ was given by Booth.[786] The theory was later refined by Ohshima et al.,[787] who performed exact numerical calculations and proposed explicit formulas for the cases of not-too-high surface potential and for thin electrical double layers. The effect of particle concentration was considered by Levine et al.,[788] who used a cell model to account for the hydrodynamic interaction between the particles. The theory of Levine et al.,[788] is restricted to thin double layers ($\kappa R$>10) and low surface potentials.

### 5.8.6 ELECTROKINETIC PHENOMENA AND ONZAGER RECIPROCAL RELATIONS

All electrokinetic phenomena include the coupled action of an electrical force (with the respective electrical current) and a hydrodynamic force (with the respective hydrodynamic flux). Therefore, one can apply the general approach of the linear thermodynamics of irreversible processes to write:[789,790]

$$\begin{aligned} J_1 &= \alpha_{11} F_1 + \alpha_{12} F_2 \\ J_2 &= \alpha_{21} F_1 + \alpha_{22} F_2 \end{aligned} \tag{374}$$

where $F_j$ ($j$=1,2) are the forces, $J_j$ are coupled fluxes, and $\alpha_{ij}$ are phenomenological coefficients. According to the Onsager reciprocal relations, $\alpha_{12}$ must be equal to $\alpha_{21}$, i.e., the following relationships must be satisfied (see Equation 374):

$$\left(\frac{J_1}{F_2}\right)_{F_1=0} = \left(\frac{J_2}{F_1}\right)_{F_2=0} \tag{375}$$

Other relations, which directly follow from the assumption $\alpha_{12}=\alpha_{21}$ are

$$\left(\frac{J_1}{F_2}\right)_{J_2=0} = \left(\frac{J_2}{F_1}\right)_{J_1=0}; \quad \left(\frac{J_1}{J_2}\right)_{F_1=0} = -\left(\frac{F_2}{F_1}\right)_{J_2=0}; \quad \left(\frac{J_1}{J_2}\right)_{F_2=0} = -\left(\frac{F_2}{F_1}\right)_{J_1=0} \tag{376}$$

In the cases of the immobile solid phase (electroosmosis and streaming potential; see Figures 66(a) and (b)), one can identify:[789,790]

$$\begin{aligned} J_1 &\equiv J_w; & F_1 &\equiv \Delta P \\ J_2 &\equiv I; & F_2 &\equiv E \end{aligned} \tag{377}$$

where $J_w$ is the water flux and $I$ is the current. Then, the counterpart of Equation 375 reads

$$\left(\frac{J_w}{E}\right)_{\Delta P=0} = \left(\frac{I}{\Delta P}\right)_{E=0} \tag{378}$$

Equation 378 connects the phenomenological coefficients appearing in electroosmosis (the left-hand side) with those in streaming potential experiments (the right-hand side). One must note that Equation 378 is valid even if the surface conductivity is important or when the double layers are not thin with respect to the capillary diameter. Furthermore, this type of relationship is valid even for electrokinetic experiments with porous plugs and membranes having pores of nonuniform size and shape. The respective counterparts of the other relations (Equation 376) are

$$\left(\frac{I}{\Delta P}\right)_{J_w=0} = \left(\frac{J_w}{E}\right)_{I=0}; \quad \left(\frac{I}{J_w}\right)_{E=0} = -\left(\frac{\Delta P}{E}\right)_{J_w=0}; \quad \left(\frac{I}{J_w}\right)_{\Delta P=0} = -\left(\frac{\Delta P}{E}\right)_{I=0} \tag{379}$$

In the case of mobile charged particles (electrophoresis and sedimentation potential; Figures 66(c) and (d)), one should identify $J_1$ as the flux of particles, $J_p$, and $F_1$ as the gravity force, $F_g$. Then, the Onsager relations read:

$$\left(\frac{J_p}{E}\right)_{F_g=0} = \left(\frac{I}{F_g}\right)_{E=0}; \qquad \left(\frac{I}{F_g}\right)_{J_p=0} = \left(\frac{J_p}{E}\right)_{I=0} \tag{380a}$$

$$\left(\frac{I}{J_p}\right)_{E=0} = -\left(\frac{F_g}{E}\right)_{J_p=0}; \qquad \left(\frac{I}{J_p}\right)_{F_g=0} = -\left(\frac{F_g}{E}\right)_{I=0} \tag{380b}$$

Again, Equations 379 and 380 are valid even for concentrated dispersions when strong electrostatic and hydrodynamic interactions between the particles may take place.

One can verify that all explicit expressions given in Sections 5.8.2-5.8.5 satisfy the Onsager relations.

### 5.8.7 Electric Conductivity and Dielectric Response of Dispersions

#### 5.8.7.1 Electric Conductivity

Here we will consider briefly the conductivity, $\chi$, of dispersions subjected to a constant electric field of intensity, $E$. The behavior of dispersions in alternating fields is considered in Section 5.8.7.2.

Charged particles influence the net conductivity in several ways: (1) the presence of particles having dielectric constant and conductivity different from those of the medium affects the local electrical field and the conditions for ion transport (e.g., nonconducting particles act as obstacles to the electromigrating ions and polarize the incident electric field); (2) the increased ionic concentration in the diffuse ion cloud, surrounding the particles, leads to higher local conductivity; and (3) the migrating charged particles may also contribute to the total electric current.

Effect (1) was analyzed by Maxwell,[791] who derived the following expression for the conductivity of diluted suspension of uncharged particles:

$$\chi = \chi_b\left(\frac{1-2\Omega\phi}{1+\Omega\phi}\right), \qquad \Omega = \frac{\chi_b - \chi_p}{2\chi_b + \chi_p} \tag{381}$$

where $\chi_p$ is the conductivity of the particles, $\chi_b$ is the conductivity of the medium, and $\phi$ is the particle volume fraction. As shown by Maxwell, this result includes an important contribution from the polarization of the field by the particles. Fricke[792] modified the Maxwell approach to consider particles of oblate or prolate spheroidal shape and obtained the formula:

$$\chi = \chi_b \left( \frac{1 - X\Omega\phi}{1 + \Omega\phi} \right), \qquad \Omega = \frac{\chi_b - \chi_p}{X\chi_b + \chi_p} \tag{382}$$

where the $X$ factor depends on the particle conductivity and shape. Since the theory of Fricke[792] assumes random orientation of the particles, it is strictly valid only for diluted suspensions of non-interacting particles and a not-too-high intensity of the electrical field. These expressions were used by Zukoski and Saville[767] to interpret the conductivity data from human erythrocyte suspensions at high ionic strength and relatively low surface potential where the effect of the surface conductivity is negligible (see Equation 362).

The contribution of the particle surface conductivity (effect (2)) for a thin electrical double layer can be accounted for phenomenologically in a similar way, and the final result for non-conducting particles reads:[707,793]

$$\chi = \chi_b \left[ 1 - \frac{3}{2}\phi \left( 1 - \frac{3\chi_s}{\chi_b R + \chi_s} \right) \right], \qquad \kappa R >> 1 \tag{383}$$

Numerical procedures for calculating the conductivity of dispersions without restriction to double layer thickness were developed by O'Brien.[794,795] A formula for thin electrical double layers, explicitly accounting for the ion mobility, is given by Ohshima et al.[796]

As discussed by Dukhin and Derjaguin,[707] the electrophoretic migration of the particles (effect (3)) is negligible if the measurements are performed under conditions such that the particles cannot release their charges on the electrodes.

### 5.8.7.2 Dispersions in Alternating Electrical Field

As mentioned in Section 5.8.4, the electrical field, in general, polarizes the electrical double layer (EDL) around a charged particle. This means that the spherical symmetry of the ion cloud brakes down, and the additional force appearing between the charged particle and the distorted ion atmosphere must be taken into account for proper description of the particle dynamics. If the external field is suddenly switched off, some finite period of time is needed for restoration of the spherically symmetrical configuration. This time can be estimated[278,715,797] from the ion diffusivity and from the characteristic path length, $l$, the ions should travel:

$$\tau_{\mathrm{REL}} \sim \frac{l^2}{D_{\mathrm{SI}}} \approx \frac{\left(R + \kappa^{-1}\right)^2}{D_{\mathrm{SI}}} = \frac{\left(1 + \kappa R\right)^2}{\kappa^2 D_{\mathrm{SI}}} \tag{384}$$

where $D_{\mathrm{SI}} \approx 10^{-9} \mathrm{m}^2/\mathrm{s}$ is the ion diffusion coefficient. If the particles are subjected to an oscillatory field of frequency, $\omega$, much higher than $\tau_{\mathrm{REL}}^{-1}$, the ion clouds will have no time to respond, and the system will behave as though containing particles with nonpolarizable

double layers. On the other hand, at a low frequency, $\omega \ll \tau_{\mathrm{REL}}^{-1}$, the ion clouds will polarize, exactly following the temporal changes of the applied field. At intermediate frequencies, $\omega \sim \tau_{\mathrm{REL}}^{-1}$, the EDL will follow the field variations with some delay, and the dielectric constant of the colloidal dispersion, ε, will show a strong dependence on ω. The numerical estimate (see Equation 384) shows that $\tau_{\mathrm{REL}}$ is typically of the order of $10^{-3}$s and the characteristic frequency, $\omega_{\mathrm{REL}}$, falls in the kilohertz range. For thin electrical double layers, there is an additional relaxation time, $\tau_\kappa$, connected with the ion transport across the double layer[715,797,798] (i.e., in a radial direction with respect to the particle surface). Since the diffusion path in this case is $l \sim \kappa^{-1}$, the relaxation time is[798]

$$\tau_\kappa \sim \kappa^{-2} / D_{\mathrm{SI}} \tag{385}$$

Therefore, $\tau_\kappa$ is inversely proportional to the electrolyte concentration, and the corresponding characteristic frequency, $\omega_\kappa$, is typically in the megahertz range.

The polarizability of the individual molecules is also frequency dependent, but the characteristic values are of the order of $10^{11}$ $\mathrm{sec}^{-1}$ and $10^{15}$ $\mathrm{sec}^{-1}$ for the rotational and electronic polarization, respectively.[34] Therefore, in the typical frequency domain for investigation of dispersions ($1\ \mathrm{sec}^{-1} \le \omega \le 10^8\ \mathrm{sec}^{-1}$) the polarizability, $\varepsilon_p$, of the material building up the particles is frequency independent. On the other hand, the disperse medium (which is usually an electrolyte solution) has a dielectric permittivity, $\varepsilon_b$, for which the frequency dependence can be described by the Debye-Falkenhagen theory.[799] Besides, the characteristic relaxation time of the bulk electrolyte solutions is also given by Equation 385.[799]

The typical experiment for determination of the dielectric response of a suspension consists[278,715,797] of measuring the magnitude and phase-lag of the current, $I_c(t)$, passing through the suspension under an applied, oscillating electrical field, $E(t)=E_0\cos(\omega t)$. The current, in turn, contains two components - one connected with the free charges and another one connected with the polarization. It is widely accepted[278,715] to use the complex presentation of the applied field

$$E(t) = \mathrm{Re}\{E_0 \exp(i\omega t)\} \tag{386}$$

where $\mathrm{Re}\{f\}$ means that the real part of the complex function, $f$, is considered. Very often the $\mathrm{Re}\{x\}$ sign is not explicitly stated, but is understood. This formalism, using complex functions, is rather convenient because the magnitude and the phase-lag of the current both can be described by one quantity - the complex conductivity, $\chi^*$:

$$I_c(t) = \mathrm{Re}\{\chi^* E_0 \exp(i\omega t)\} \tag{387}$$

The physical meaning of the real and of the imaginary parts of $\chi^*$ is the following.[715] $\mathrm{Re}\{\chi^*\}$ is proportional to the dissipated energy in the system - the heat produced per one period of the field oscillation is equal to $\frac{1}{2}E_0^2\,\mathrm{Re}\{\chi^*\}$. On the other hand, the phase-lag of the current (with respect to the applied field) is characterized by the phase angle, $\varphi = \arctan\left[\frac{\mathrm{Im}\{\chi^*\}}{\mathrm{Re}\{\chi^*\}}\right]$.

The complex conductivity, $\chi^*$, of a dispersion is usually defined as:[278]

$$\chi^*(\omega,\phi) = \chi(\omega,\phi) - i\omega\varepsilon_0\varepsilon'(\omega,\phi) \tag{388}$$

where $\chi$ is the real part of $\chi^*$ and $\varepsilon'$ is the "loss-free" part of the dielectric response. Alternatively, one can define:[278]

$$\chi^*(\omega,\phi) = \chi(0,\phi) + \omega\varepsilon_0\varepsilon''(\omega,\phi) - i\omega\varepsilon_0\varepsilon'(\omega,\phi) \tag{389}$$

where the frequency dependence of the real part of $\chi^*$ was totally assigned to the imaginary part of the dielectric constant. Both conventions are used in the literature,[278] and one should note that in the first case the dielectric constant of the suspension is a real number ($\varepsilon=\varepsilon'$, $\varepsilon''=0$), while in the second case $\varepsilon$ is considered a complex number ($\varepsilon=\varepsilon'+i\varepsilon''$). Also, since the effect of the particles is of primary interest, one considers the changes of these quantities with respect to the properties of the disperse medium:[278]

$$\Delta\chi(\omega,\phi) \equiv \frac{\chi(\omega,\phi) - \chi(\omega,0)}{\chi(\omega,0)\phi}; \qquad \Delta\varepsilon'(\omega,\phi) \equiv \frac{\varepsilon'(\omega,\phi) - \varepsilon'(\omega,0)}{\phi}$$
$$\Delta\varepsilon'' \equiv \frac{\chi(\omega,\phi) - \chi(0,\phi)}{\omega\varepsilon_0\phi} \tag{390}$$

In Figure 69 the typical frequency dependencies of $\Delta\chi$, $\Delta\varepsilon'$, and $\Delta\varepsilon''$ in the kilohertz range are schematically represented (a number of real experimental plots are given in the books by Dukhin and Shilov[715] and Russel et al.[278]). As shown in the figure, the value of $\varepsilon''$ goes through a maximum, which corresponds to a maximal dissipation of energy in the suspension. The values of $\chi$ and $\varepsilon'$ are, respectively, monotonously decreasing and increasing with the frequency. In general, the experiments show that the magnitude of $\Delta\varepsilon'$ increases with the values of $\kappa R$ and the $\zeta$ potential. The magnitude of $\Delta\chi$ also increases with the $\zeta$ potential but decreases with $\kappa R$. The magnitude of $\Delta\varepsilon''$ increases with the $\zeta$ potential. In dilute dispersions, none of the three quantities depend on the particle concentration in the framework of the experimental accuracy, as would be expected. The theory of the dielectric response in this low-frequency range was mostly developed by Dukhin and his colleagues,[715] and analytical formulas are available for thin electrical double layers[715] or low surface potential.[710]

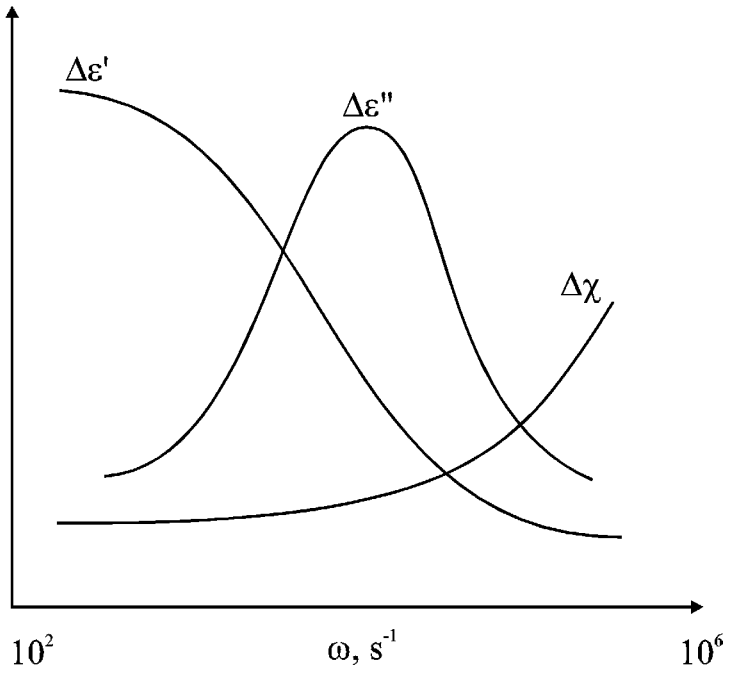


**FIGURE 69.** Schematic presentation of the electric conductivity, $\Delta\chi$, the real part, $\Delta\varepsilon'$, and the imaginary part, $\Delta\varepsilon''$, of the dielectric permittivity increments of dispersion as functions of the frequency of the electric field, $\omega$. For definitions of $\Delta\chi$, $\Delta\varepsilon'$, and $\Delta\varepsilon''$, see Equation 390.

During the last decade the dielectric response of dispersions in the megahertz range was extensively studied. O'Brien[798] presented the complex conductivity of a dilute dispersion in the form (see Equation 381):

$$\chi^* = (\chi_b + i\omega\varepsilon_0\varepsilon_b)\frac{(1-2\Omega\phi)}{(1+\Omega\phi)} \tag{391}$$

where the complex function $\Omega(\chi_b, \chi_s, \varepsilon_b, \varepsilon_p, \omega)$ is given by the expression:

$$\Omega \equiv \frac{\chi_b - 2\chi_s/R + i\omega\varepsilon_0(\varepsilon_b - \varepsilon_p)}{2(\chi_b + \chi_s/R) + i\omega\varepsilon_0(2\varepsilon_b + \varepsilon_p)} \tag{392}$$

Here, $\varepsilon_p$ is the relative dielectric permittivity of the particle substance. As shown by O'Brien,[798] at high frequency ($\omega \gg D\kappa^2 \sim \chi_b/\varepsilon_0\varepsilon_b$), Equation 392 reduces to the result for uncharged particles, $\Omega = (\varepsilon_b - \varepsilon_p)/(2\varepsilon_b + \varepsilon_p)$. At low frequency ($\omega \ll \chi_b/\varepsilon_0\varepsilon_b$), Equation 392 coincides with the high-frequency limit of the formula derived by Hinch et al.:[800]

$$\Omega = \frac{1}{2} - \frac{3}{2}\beta/[2 + \beta(1+\delta)] \tag{393}$$

where

$$\beta = \frac{2}{\kappa R}\left(1 + 3\frac{m}{Z^2}\right)\exp\left(\frac{eZ\zeta}{2kT}\right) \tag{394}$$

$$\delta=\left[1+\left(i\omega R^2/D_{\mathrm{SI}}\right)^{1/2}\right]/\left[1+\left(i\omega R^2/D_{\mathrm{SI}}\right)^{1/2}+\frac{1}{2}i\omega R^2/D_{\mathrm{SI}}\right] \tag{395}$$

The high-frequency limit of Equation 393 is $\Omega=(1-\beta)/(2+\beta)$ which, as stated above, is identical to the low-frequency limit of Equation 392 because $\chi_s/\chi_b R=\beta/2$.[798] One can conclude that the combination of Equations 391-393 covers the whole range of frequencies that are of interested.[798]

This approach was further extended by O'Brien[798] to include the cases of concentrated dispersion of randomly packed spheres and porous plugs. A comparison with experimental data on Pyrex plugs revealed very good agreement in the frequency range from $10^3$ to $10^7 sec^{-1}$. Midmore et al.[801] measured the dielectric response of concentrated latex suspensions ($\phi$ was varied between 0.1 and 0.5) in the range between 1 and 10 MHz and also found that the data can be well reproduced by the cell type of theoretical model. However, the estimated $\zeta$ potential from the conductivity measurements was considerably larger than the value determined by electrophoretic measurement (this issue will be discussed in the following section). Equipment and procedures for performing calibration and measurement of the dielectric response of dispersions are described in References 801-803. A large set of numerical results for various values of the particle $\zeta$ potential and the ionic strength of the disperse medium were presented by Grosse et al.[804]

We will now briefly describe the technique of colloid vibration potential (CVP) for determination of the particle $\zeta$ potential. In this type of experiment, an ultrasonic wave is introduced into the suspension, thus leading to oscillatory motion of the particles. Due to the difference in the mass densities of the particles and the surrounding fluid, the ion cloud does not follow the particle motion (similar to the case of particle sedimentation), and spatial separation of the positive and negative charges appears. The corresponding electrical potential is called the *colloid vibration potential* and can be measured by two probe electrodes separated by distance $\lambda/2$ in the direction of the ultrasound propagation ($\lambda$ is the sound wavelength). The theory for diluted suspensions was developed by Enderby[805] and Booth[806] and further extended to concentrated systems by Marlow et al.[807] The connection between the colloid vibration potential, $E_{\mathrm{CVP}}$, and the particle $\zeta$ potential is[807,808]

$$E_{\mathrm{CVP}}=\frac{2P_0\phi}{\chi_b}\frac{\left(d_p-d_b\right)}{d_b}\frac{\varepsilon_b\varepsilon_0}{\eta}\zeta f_2\left(\kappa R,\phi\right) \tag{396}$$

where $P_0$ is the amplitude of the sound pressure, while $d_p$ and $d_b$ are the mass densities of the particles and medium, respectively. The function $f_2(\kappa R,\phi)$ accounts for the particle-particle interactions; for diluted systems, $f_2(\kappa R,\phi\to 0)=1$, and for thin EDL $f_2(\kappa R\gg 1,\phi)=(1-\phi)$.

The experiments performed by several research groups[807-809] showed good agreement of theoretical predictions with the experimental data. This is rather encouraging and a little

surprising result, keeping in mind that the experiments with simple electrolytes (where a similar effect called "ionic vibration potential" is existing[810]) produced data which are often not well explained[809] by the corresponding theory.[810] The CVP technique can be applied to concentrated dispersions.

O'Brien[811] showed that the CVP is related through the Onzager relations to the so-called electrokinetic sonic amplitude (ESA). The latter appears when an alternating electric field is applied to a suspension of charged particles. The ensuing oscillatory motion of the particles creates a macroscopic acoustic wave, whose amplitude and phase lag can be experimentally measured and used for characterization of the dispersed particles. The method allows one to determine the size and $\zeta$ potential of the particles in a concentrated dispersion without need of dilution.[812-818] In general, the problem consists of two stages: first, the dynamic electrophoretic mobility is determined from the CVP or ESA data, and second, the particle $\zeta$ potential is calculated from the dynamic mobility by using various theoretical models. The effect of surface conductivity on the analysis of the ESA and CVP data was recently considered by Dukhin et al.[817] and by Löbbus et al.[818] The CVP and ESA are often termed electroacoustic phenomena in the literature.

### 5.8.8 ANOMALOUS SURFACE CONDUCTANCE AND DATA INTERPRETATION

Theoretical interpretation of the measured electrokinetic quantities is always based on a number of explicit and implicit assumptions. Since the meaning of the obtained data depends on the adequacy of the theory used for their interpretation, the underlying assumptions are often questioned and discussed in the literature.[705,707,716,819] In this section, we briefly discuss the current evaluation of the importance of some effects that are not taken into account in the conventional theory.

All the consideration up to now implies that the dielectric permittivity and the viscosity in the electrical double layer (at least for $x \geq x_s$; see Figure 67) are equal to those of the bulk disperse medium. A more refined approach[793,819] shows that for thin double layers the formulas, stemming from the Smoluchowski theory, may remain unaltered if the "real" $\zeta$ potential ($\zeta = \psi(x_s)$) is replaced by the quantity:[793]

$$\zeta_{\text{obs}} = \frac{\eta_b}{\varepsilon_b}\int_0^{\infty}\frac{\varepsilon(x)}{\eta(x)}\frac{d\psi}{dx}dx = \frac{\eta_b}{\varepsilon_b}\int_0^{\zeta}\frac{\varepsilon(\psi)}{\eta(\psi)}d\psi \tag{397}$$

where $\varepsilon(x)$ and $\eta(x)$ account for local variations of the dielectric constant and viscosity in the double layer, while $\varepsilon_b$ and $\eta_b$ are the respective values in the bulk medium. Hunter[819] analyzed a number of theoretical and experimental results and concluded that this effect is "small under most conditions". Recently, Chan and Horn[820] and Israelachvili[821] performed dynamic

experiments using the surface force apparatus and showed that the water viscosity is practically constant down to distances one to two molecular diameters from a smooth mica surface. Their experiments also demonstrated that the shear plane at a smooth surface is shifted no more than one to two molecular layers apart from the surface. Therefore, one may expect that for smooth surfaces the $\zeta$ potential should be very close to the surface potential, $\psi_s$, at least for not-too-high electrolyte concentrations and surface potentials.

The case of a rough solid surface is much more complicated,[707,793] because the surface roughness affects not only the position of the shear plane, but also the surface charge density distribution and the surface conductivity. Therefore, a general approach to rough surfaces is missing and one should choose between several simple models (see below) to mimic as close as possible the real surface.

Another very important issue in this respect is the way to account for the surface conductivity. The formula of Bickerman[727] (Equation 359), the correction factor to the electrophoretic mobility of Henry[738] (Equation 368), and the formula of O'Brien and Hunter[744] (Equation 371), quoted above are derived under the assumption that only the ions in the movable part ($x \geq x_s$; Figure 67) of the EDL contribute to the surface conductivity, $\chi_s$. Moreover, the ions in the EDL are taken to have the same mobility as that in the bulk electrolyte solution. A variety of experimental data[707,715,793,822-827] suggests, however, that the ions behind the shear plane ($x < x_s$) and even those adsorbed in the Stern layer may contribute to $\chi_s$. The term ″anomalous surface conductance″ was coined for this phenomenon. Such an effect can be taken into account theoretically, but new parameters (such as the ion mobility in the Stern layer) must be included in the consideration. Hence, the interpretation of data by these more complex models usually requires the application of two or more electrokinetic techniques which provide complementary information.[803,828] Dukhin and van de Ven[828] specify three major (and relatively simple) types of models as being most suitable for data interpretation. These models differ in the way they consider the surface conductivity and the connection between $\psi_s$ and $\zeta$:

- Model 1 ($\zeta=\psi_s$ and $\chi_s=\chi_s^{EDL}$): This is the simplest possible model accounting for the surface conductivity, because it assumes that an immobile part of the diffuse layer is absent. As a result, $x_s=0$, $\zeta=\psi_s$, and $\chi_s$ is due only to ions in the diffuse layer.

- Model 2 ($\zeta\neq\psi_s$, $\chi_s=\chi_s^{EDL}$): In this model two parts of the diffuse layer (hydrodynamically mobile and immobile, respectively) are distinguished. The surface conductivity is taken to include contributions from the ions in the whole diffuse layer, including the hydrodynamically immobile part. The mobility of the ions in the diffuse layer is considered to be the same as that in the bulk, while the mobility of the ions in the Stern layer is set equal to zero. The Gouy-Chapmen theory, e.g. Equation 343, is

used to connect the values of $\zeta$ and $\psi_s$. Therefore, the value of $x_s$ is an important parameter in this model. According to Dukhin and van de Ven,[828] this model is most suitable for particles with a rough surface or for a surface covered with a layer of nonionic surfactants or polymers.[822,823,825]

- Model 3 ($\zeta=\psi_s$, $\chi_s=\chi_s^{EDL}+\chi_s^{Stern}$): As in model 1, it is assumed that the whole diffuse part of the EDL is hydrodynamically mobile. In addition, the ions in the Stern layer are allowed to move in external electrical field and to contribute to $\chi_s$. This model seems to be appropriate for the description of electrophoresis of biological cells (if glycocalix on the cell surface is not present) and particles covered by ionic surfactants.[824]

Theoretical descriptions of the electrokinetic phenomena in the framework of these three models were developed in the literature and reviewed by Dukhin and van de Ven.[828] The effect of particle polydispersity on the data interpretation by the different models was analyzed in the same study.[828]

The interest in anomalous surface conductance has been high during the last several years[795,817,818,822-833] due to the finding that most of the studied latex samples have showed electrokinetic properties that cannot be described by conventional theory. In particular, the electric potential determined by electrophoresis was substantially lower than that measured in dielectric studies.[795,801,823-826] Also, the electrophoretic $\zeta$ potential, calculated from the conventional theory, showed a maximum as a function of the electrolyte concentration, while one should expect a gradual decrease.[803,829] Several hypotheses[825,826] were discussed in the literature to explain this discrepancy, most of them being connected with the anomalous surface conductance of the latex particles. According to the "hairy model",[826,827] the particle surface is covered by a layer of flexible polymer chains, which are extended into the solution at a distance, which depends on the electrolyte concentration. Since the position of the shear plane, $x_s$, is to be close to the outer boundary of this polymer layer, the thickness of the immobile hydrodynamic layer (and the corresponding anomalous surface conductance created by the ions in the immobile layer) appears to be strongly dependent on the ionic strength. This hypothesis found some experimental confirmation in experiments[827] with latex particles, preheated for a certain period of time at a temperature above the glass transition temperature of the polymer. As shown by Rosen and Saville,[827] the electrokinetic properties of the preheated latexes become much closer to those expected from the classical theory. On the other hand, Shubin et al.[803] made systematic measurements to distinguish which type of ions are responsible for the anomalous conductance of the latex particles, those in the diffuse part or those in the Stern layer. The authors[803] concluded that their data can be interpreted only by assuming ion transport in the Stern layer. Recent theoretical analysis of Saville[833] showed that the presence of a thin permeable (hairy) polymer layer on the surface of colloid particles

indeed has an important effect on their electrophoretic mobility, while the suspension conductivity might be very slightly affected.

Experiments[830-832] made in different laboratories suggest that the importance of the discussed effect depends strongly on the type of used particles. Gittings and Saville[831] and Russell et al.[830] found out latex samples (commercial and laboratory-made ones) for which the electrokinetic properties can be well described by the classical theory, without need to invoke the anomalous surface conductance. These observations were complemented by the results of Bastos-Gonzales et al.,[832] who performed heat treatment of polystyrene latexes with different surface groups. The experiments by several methods showed[832] that the surface of the sulfate and aldehyde latexes changed upon heating, while the sulfonate and carboxyl latexes did not show a detectable change of their properties. Better understanding of the electrokinetic properties of latex particles is of significant importance, because the latexes are widely used[278,717] as model systems for quantitative investigation of a variety of colloidal phenomena, and their reliable characterization is needed for these tasks.

### 5.8.9 Electrokinetic Prtoperties of Air-Water and Oil-Water Interfaces

The experimental methods based on electrokinetic phenomena (and especially electrophoresis) have found very widespread application for routine characterization of electrical surface properties of solid particles, liquid droplets, porous media, synthetic membranes, etc. A systematic presentation of the main results obtained on different types of systems is given in Chapters 6 to 8 of Reference 716, and in Chapters 8 to 33 of Reference 718. A glance at the books[278,715-718] and review articles[704-714] in the field, however, shows that the properties of air-water and oil-water interfaces are either not considered at all or only briefly mentioned. This fact is surprising, as a number of studies[834-843] (the first of them being performed more than seventy years ago) have convincingly demonstrated a substantial negative $\zeta$ potential at bare (without any surfactant) air-water and oil-water interfaces. This spontaneous charging cannot be explained in a trivial way - it requires the specific preferential adsorption of some kind of ion, because from a purely electrostatic viewpoint the approach of an ion to the interface of water and a nonpolar fluid is unfavorable because of the image forces.[34] Measurements of the electrophoretic mobility of air bubbles and oil droplets demonstrated a strong pH dependence of their $\zeta$ potential: it is almost zero at a pH of around 3 and goes down to –120 mV at a pH ~ 11. Therefore, two main hypotheses, connected with the dissociation-association equilibrium of water $\left( H_2O = H^+ + OH^- \right)$ were suggested in the literature to explain the phenomenon: (1) specific adsorption of $HO^-$ ions in the boundary water molecules, and (2) negative adsorption, i.e., depletion of $H^+$ ions in the boundary layer.

Marinova et al.[842] performed a series of systematic measurements of the electrophoretic mobility of oil-in-water emulsion droplets to check these (and some other) possible hypotheses. Analyzis of the obtained results leads to the conclusion that the charges originate from hydroxyl ions, which specifically adsorb at the oil-water interface. The pH-dependence of the surface charge was interpreted by using Stern's adsorption isotherm, yielding the value of ~ 25 $kT$ for the specific adsorption energy per $HO^-$ ion. Although some speculations about the underlying mechanism were presented[841,842] the molecular picture behind this value is rather obscured. One may expect that the computer methods for studying the molecular structuring and dynamics at interfaces (including hydrogen-bond effects) will be very helpful in revealing the physical origin of the surface charge. Dunstan and Saville[841] suggested the idea that the specific adsorption of ions, responsible for the charging of hydrophobic surfaces, may be connected with the anomalous electrokinetic behavior of latex particles, as discussed in the previous section.

The air-water and oil-water interfaces, covered with adsorption layers of nonionic surfactants, are also negatively charged at neutral pH, which has an important impact on the stability of foams and emulsions.[462,835,842,844-846] Again, a strong pH-dependence of the $\zeta$ potential is established: the higher the pH, the larger in magnitude the $\zeta$ potential. The effect of the adsorbing nonionic surfactants on the magnitudes of the surface potential of air-water interfaces was analyzed in detail in Reference 846. The electrokinetic properties of fluid interfaces in the presence of cationic or anionic surfactants are more understandable (at least qualitatively): the interfaces are positively or negatively charged, respectively. In the presence of an adsorbed protein layer, the interfacial electric potential is usually close to that of the protein molecules at the pH of the disperse medium. In this way, the surface charge may change from negative to positive around the isoelectric point of the protein.

## 5.9 OPTICAL PROPERTIES OF DISPERSIONS AND MICELLAR SOLUTIONS

The light scattering methods for studying colloidal systems can be classified in two wide groups: static light scattering (SLS) and dynamic light scattering (DLS). The latter is often called quasi-elastic light scattering (QELS) or photon correlation spectroscopy (PCS). In SLS methods, the averaged-over-time intensity of the scattered light is measured as a function of the particle concentration and/or scattering angle. In DLS methods, the time fluctuations of the scattered light are measured. The light scattering methods possess a number of advantages, which make them particularly suitable for investigation of colloid systems. In general, these methods are noninvasive; applicable to very small and unstable (when dried) particles, such as surfactant micelles and lipid vesicles; suitable for characterization of particle size and shape, as well as of interparticle interactions; and relatively fast, and not requiring

very expensive equipment. The theoretical basis of light scattering methods is outlined in Sections 5.9.1 and 5.9.2. The main applications of the methods to surfactant solutions and colloidal dispersions are summarized in Section 5.9.3.

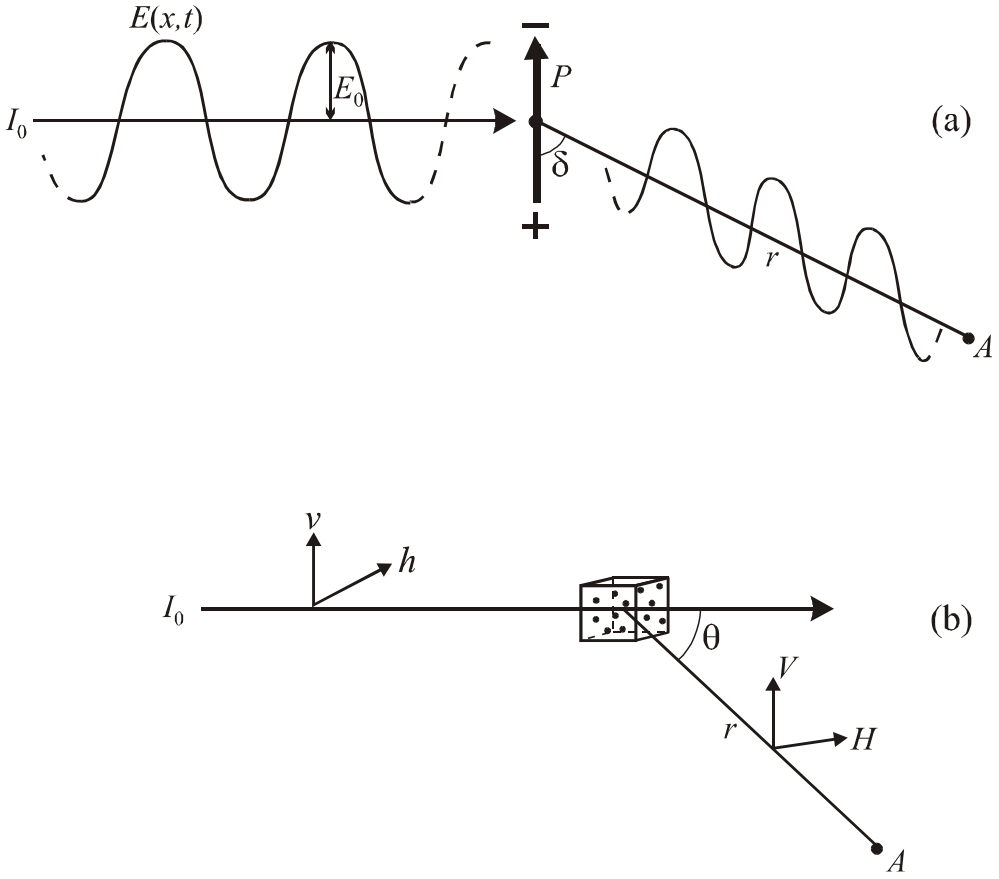


**FIGURE 70.** Geometry of the light scattering experiment. (a) Plane polarized monochromatic beam of intensity $I_0$ induces the variable dipole, $p$, which emits an electromagnetic wave (scattered light); the detector is at point $A$. (b) The incident beam can be vertically polarized, horizontally polarized or nonpolarized with respect to the scattering plane. Angle δ is formed between the directions of the dipole and the scattered beam, while the angle θ is between the directions of the incident and scattered beams. The axes ($v$,$h$) and ($V$,$H$) denote the vertical and horizontal directions for the incident and scattered beam, respectively.

### 5.9.1 STATIC LIGHT SCATTERING

A comprehensive presentation of the SLS theory can be found in the monographs by Van de Hulst[847] and Kerker.[848] The basic concepts are discussed in the textbooks by Hiemenz and Rajagopalan,[849] and Lyklema;[850] a collection of the classical papers on this topic is reprinted in Reference 851.

#### 5.9.1.1 Rayleigh Scattering

The scattering of light from colloidal particles of dimensions much smaller than the light wavelength (e.g., surfactant micelles) can be analyzed in the framework of the Rayleigh theory,[852] which was originally developed for light scattering from gases. A beam of monochromatic, polarized light can be described by the amplitude of its electrical vector (see Figure 70).

$$E = E_0 \cos 2\pi\left(\nu t - \frac{x}{\lambda}\right) \tag{398}$$

Here, $x$ is the coordinate in direction of the incident beam, $t$ is time, and $\nu$ and $\lambda$ are the frequency and the wavelength of the light, respectively. The light induces a variable dipole in the particle:

$$p = \alpha E = \alpha E_0 \cos 2\pi\left(\nu t - \frac{x}{\lambda}\right) \tag{399}$$

where $\alpha$ is the excess particle polarizability (i.e., the difference between the polarizability of the particle and the polarizability of the same volume of the medium). The induced dipole creates an electromagnetic field of the same frequency (scattered light) with an intensity (energy flux per unit area perpendicular to the scattered beam) averaged over time of:[849]

$$\langle I_s \rangle_t = \frac{16\pi^4}{\lambda_0^4 r^2}\left(\frac{\alpha}{4\pi\varepsilon_0}\right)^2 \langle I_0 \rangle_t \sin^2\delta, \qquad \langle I_0 \rangle_t = \frac{c\varepsilon_0}{2}E_0^2 \approx 1.328\times 10^{-3} E_0^2 \text{ W/m}^2 \tag{400}$$

where the brackets denote time averaging, $\delta$ is the angle between the direction of the induced dipole and the direction of the scattered beam, $\langle I_0 \rangle_t$ is the intensity of the incident beam, $\lambda_0$ is the light wavelength *in vacuo*, $r$ is the distance between the scattering dipole and the detector, $c$ is the speed of light, and $\varepsilon_0$ is the dielectric permittivity of the *vacuo*. For vertically polarized light, $\delta=\pi/2$, while for horizontally polarized light $\delta=(\pi/2-\theta)$; $\theta$ is the scattering angle (see Figure 70). Nonpolarized light can be formally considered as the superposition of one vertically polarized and one horizontally polarized beam of equal intensity. In the Rayleigh theory,[852] the scatterers are considered to be independent from each other, and the total intensity of the scattered light from a suspension of number concentration $\rho$ is proportional to the number of particles observed by the detector, $N$ ($N=\rho V_S$; $V_S$ is the scattering volume). To characterize the light scattering with a quantity independent from the geometry of the equipment, one usually considers the reduced intensity of the scattered light called Rayleigh ratio:

$$R(\theta) \equiv \frac{\langle I_s \rangle_t}{\langle I_0 \rangle_t} \frac{r^2}{V_S} = \frac{16\pi^4}{\lambda_0^4} \left( \frac{\alpha}{4\pi\varepsilon_0} \right)^2 \rho P(\theta) \tag{401}$$

where the factor $P(\theta)$ depends on the polarization of the incident beam. In the case of small particles (of dimensions much smaller than $\lambda$):

$$P_v(\theta) = 1, \qquad P_h(\theta) = \cos^2\theta, \qquad P_u(\theta) = \frac{1}{2}\left(1 + \cos^2\theta\right) \tag{402}$$

where the subscripts *v*, *h* and *u* denote vertically polarized, horizontally polarized or non-polarized incident beam, respectively. In the more general case, $P(\theta)$ also depends on the size and shape of the scattering particles (see bellow); hence, it is sometimes called scattering formfactor of the particles. By using the continuum theory of dielectric polarization, one can express the excess polarizability of a spherical particle of radius $R$ and refractive index $n_p$ which is immersed in a medium of refractive index, $n_m$, by means of the Lorenz-Lorentz equation:[34]

$$\left( \frac{\alpha}{4\pi\varepsilon_0} \right) = n_m^2 \left( \frac{n_p^2 - n_m^2}{n_p^2 + 2n_m^2} \right) R^3 \tag{403}$$

Since in many cases $n_p$ and $R$ are not known and the particles may have a non-spherical shape, another way for deducing the excess particle polarizability is used: $\alpha$ is expressed through the change of the refractive index of the suspension, $n$, with the particle concentration:[853]

$$\alpha = \frac{\varepsilon_0\left(n^2 - n_m^2\right)}{\rho} \approx 2\varepsilon_0 n_m \left( \frac{dn}{d\rho} \right) = 2\varepsilon_0 n_m \frac{M}{N_A} \left( \frac{dn}{dc} \right) \tag{404}$$

Here $M$ is the mass of a particle, $c$ is the particle mass concentration ($c=\rho M/N_A$ and $N_A$ is the Avogadro number). The quantity ($dn/dc$) presents the refractive index gradient of the suspension and is measured by refractometer of high sensitivity. Combining Equations 401 and 404, one can derive the following expression for the Rayleigh ratio of a suspension of independent scatterers:

$$R_j(\theta) \equiv cKMP_j(\theta), \qquad K \equiv \frac{4\pi^2 n_0^2}{\lambda_0^4 N_A} \left( \frac{dn}{dc} \right)^2 \quad \text{and} \quad j = v,h,u \tag{405}$$

which (in principle) allows one to determine the particle mass, $M$, from the intensity of the scattered light. Equation 405 has several important limitations: (1) the particle dimensions must be much smaller compared to the light wavelength, (2) the particle concentration must be very low to avoid the interparticle interactions and the interference of light beams scattered by different particles, and (3) the particles do not absorb light (the suspension is colorless).

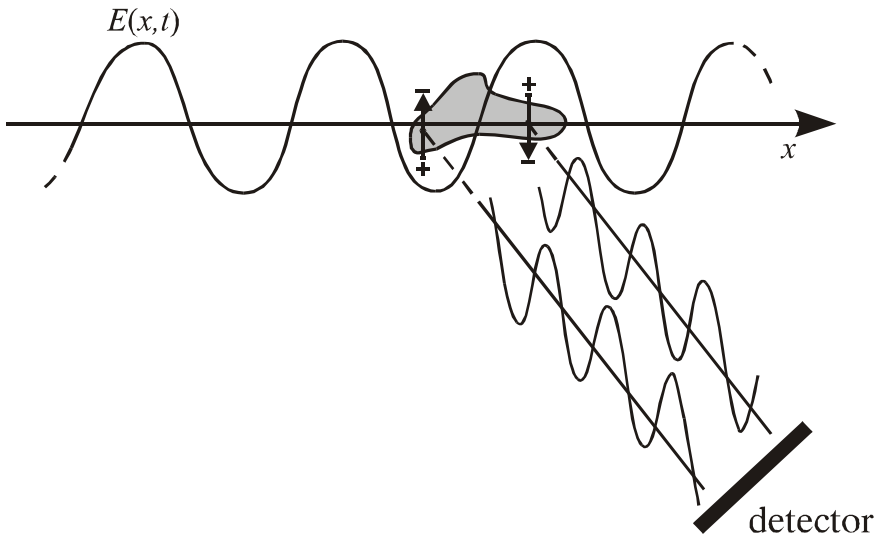


**FIGURE 71** The Rayleigh-Debye-Gans[857-859] theory is based on the assumptions that: (1) the incident beam propagates without being affected by the particles, and (2) the scattered light, received by the detector, is a superposition of the beams emitted from the induced dipoles in the different parts of the particle.

### 5.9.1.2 Rayleigh-Debye-Gans Theory

The radiation of a particle, comparable in size to the light wavelength, leads to induction of dipoles in different parts of the particle that are not in phase (Figure 71). The net scattered light, received by the detector, is a result of the interference of the beams scattered from the different points of the particle. In this case, the function $P(\theta)$ depends on the particle size and shape. If the particles have an anisodiametrical shape, $P(\theta)$ could depend on their orientation as well. Typical examples are rod-like particles that are preferentially oriented along a given direction by electric[854-856] or hydrodynamic field. In most systems, however, the particles are randomly oriented, and averaging over all possible orientations is performed to calculate $P(\theta)$.

A rather general approach for determination of the function $P(\theta)$ was proposed by Rayleigh[857] and further developed by Debye[858] and Gans.[859] The main assumption in the Rayleigh-Debye-Gans (RDG) theory is that the incident beam that excites the electrical dipoles in the particle is not influenced (in neither magnitude nor phase) by the presence of the particle. This requirement is better satisfied by smaller particles having a refractive index close to that of the disperse medium. The respective quantitative criterion reads:

$$\frac{4\pi l}{\lambda}\left|n_p - n_m\right| << 1 \tag{406}$$

where $l$ is a length of the order of the size of the particle ($l$ coincides with the radius for spheres). For such "soft" scatterers, the phase difference of the waves created by the induced

dipoles in different parts of the particle (considered to be independent in the RDG theory) can be calculated by geometrical consideration.

Since the scattered waves propagating in a forward direction, θ=0°, are all in phase (positive interference), the intensity of the scattered light is maximal in this direction and $P(0) = 1$. Comparison with Equation 405 shows that $R(0) = cKM$; hence, one can define:

$$P_j(\theta) \equiv R_j(\theta) / R(0), \qquad j = v,h,u \tag{407}$$

The general expression for the scattering form factor of randomly oriented particles and vertically polarized light reads:[858]

$$P_v(\theta) = \frac{1}{N^2} \sum_{i=1}^{N} \sum_{j=1}^{N} \frac{\sin(qr_{ij})}{qr_{ij}} \tag{408}$$

where $q = \frac{4\pi n}{\lambda_0} \sin(\theta/2)$ is the magnitude of the scattering vector, and $r_{ij}$ is the distance between the $i$-th and $j$-th scattering subunit. The double sum is taken over all subunits of total number $N$. The particle scattering factor was calculated for typical particle shapes (see Table 9 and Table 8.5 in Reference 848).

Once $P_v(\theta)$ is known, one can calculate $P_h(\theta)$ and $P_u(\theta)$ through the relationships (see Equation 402):

$$P_h(\theta) = P_v(\theta) \cos^2 \theta, \qquad P_u(\theta) = \frac{1}{2} P_v(\theta) (1 + \cos^2 \theta) \tag{409}$$

The expansion in series of $\sin(qr_{ij})$ in the right-hand side of Equation 408 leads to a fairly simple and general result:[860]

$$\lim_{\theta \to 0} P_v(\theta) \approx 1 - \left[ \frac{q^2}{3! N^2} \right] \sum_{i=1}^{N} \sum_{j=1}^{N} r_{ij}^2 = 1 - \frac{q^2 \left\langle R_g^2 \right\rangle}{3} \tag{410}$$

where $\left\langle R_g^2 \right\rangle^{1/2}$ is the radius of gyration for a particle that is arbitrary in shape and size. This result shows that the initial part of the function $P(\theta)$, corresponding to small scattering angles, enables one to determine the radius of gyration, no matter what the particle shape is. For that purpose, the experimentally measured intensity of the scattered light is represented in the form (see Equation 405):

$$\frac{Kc}{R_v(\theta)} = [MP_v(\theta)]^{-1} = \frac{1}{M} \left[ 1 + \frac{16}{3} \frac{\pi^2}{\lambda^2} \left\langle R_g^2 \right\rangle \sin^2(\theta/2) + O(q^4) \right] \tag{411}$$

**Table 9. Scattering function, $P_v(q)$, single particle translational diffusion coefficient, $D_0$, and single particle rotational diffusion coefficient, $\Theta$, for particles of different shape**

| Shape of particle | $P_v(q)$, $D_0$, $\Theta$ | Ref. |
|---|---|---|
| 1. Homogeneous sphere of radius $R$ | $P_v(q)=\left[\frac{3}{\widetilde{R}^3}\left(\sin\widetilde{R}-\widetilde{R}\cos\widetilde{R}\right)\right]$<br>$D_0=\frac{kT}{6\pi\eta R};\qquad \Theta=\frac{kT}{8\pi\eta R^3}$ | 857 |
| 2. Ellipsoid with semiaxes $(R, R, pR)$ | $P_v(q)=\int_0^{\frac{\pi}{2}}\left[\frac{3}{\widetilde{R}^3}\left(\sin\widetilde{R}-\widetilde{R}\cos\widetilde{R}\right)\right]^2\left(\widetilde{R}\sqrt{\cos^2\theta+p^2\sin^2\theta}\right)\cos\theta d\theta$<br>$D_0=\frac{kT}{6\pi\eta R}\left[\frac{3}{4}p\beta+\frac{1}{8}p\alpha_{\mathrm{II}}+\frac{1}{4}\frac{\alpha_{\mathrm{I}}}{\mathrm{p}}\right]$<br>$\Theta=\frac{3kT}{16\pi pR^3\eta}\frac{\left(p^2\alpha_{\mathrm{II}}+\alpha_{\mathrm{I}}\right)}{\left(p^2+1\right)}$<br>$\alpha_{\mathrm{II}}=\frac{2\left(p^2\beta-1\right)}{p^2-1};\quad \alpha_{\mathrm{I}}=\frac{p^2(1-\beta)}{p^2-1}$<br>$\beta=\frac{\cosh^{-1}p}{p\left(p^2-1\right)^{1/2}}\quad \text{for } p>1\,(\text{prolate ellipsoid})$<br>$\beta=\frac{\cos^{-1}p}{p\left(1-p^2\right)^{1/2}}\quad \text{for } p<1\,(\text{oblate ellipsoid})$ | 860<br>862<br>863<br>see also (864) |
| 3. Thin rod-like particle of length $L$ and diameter $d$ | $P_v(q)=\frac{2}{qL}\int_0^{qL}\frac{\sin u}{u}du-\left[\frac{2\sin(qL/2)}{qL}\right]^2$<br>$D_0=\frac{kT}{3\pi\eta L}\ln(L/d);$<br>$\Theta=\frac{3kT}{\pi\eta L^3}\left[\ln(2L/d)-0.5\right]$ | 865<br>see also (866, 867)<br>863<br>see also (864, 868, 869) |
| 4. Thin disc of radius $R$ | $P_v(q)=\frac{2}{\widetilde{R}^2}\left[1-\frac{\mathrm{J}_1\left(2\widetilde{R}\right)}{\widetilde{R}}\right]$<br>$D_0=\frac{kT}{12\eta R};\qquad \Theta=\frac{3kT}{32\eta R^3}$ | 870<br>871<br>863 |
| 5. Gaussian coil of contour length $L$ and persistent length, $l_p$. If the coil is considered to contain $N$ segments of length $l$, then $L=Nl$ and $l=2l_p$ | $P_v(q)=\frac{2}{z^2}\left[\exp(-z)+z-1\right];\quad z=q^2\left\langle R_g^2\right\rangle$<br>$\left\langle R_g^2\right\rangle=\frac{1}{3}Ll_p=\frac{1}{6}Nl^2$<br>$D=\frac{kT}{3\pi\eta L}\left[1.303\left(L/l_p\right)^{1/2}\right],\qquad \Theta=\frac{kT}{1.013\eta L^3}\left(L/l_p\right)^{3/2}$ | 872<br>873 |

Note: $\widetilde{R}\equiv qR$, where $q=4\pi n\lambda_0^{-1}\sin(\theta/2)$ is magnitude of the scattering vector; $\eta$ is shear viscosity of the medium and $kT$ is thermal energy; $\mathrm{J}_1(x)$ is Bessel function of the first kind.

and $Kc/R_v(\theta)$ is plotted vs. $\sin^2(\theta/2)$. For a nonpolarized or horizontally polarized primary beam, $R_v(\theta)$, in the left-hand side of Equation 411 is to be replaced by $2R_u(\theta)/(1+\cos^2\theta)$ or $R_h(\theta)/\cos^2\theta$, respectively.

The radii of gyration for a sphere of radius $R_s$, for a thin rod-like particle of length $L$, for a Gaussian coil containing $N$ segments of length $l$, and for a thin disk of radius $R_d$ are given by:[847, 849,861]

$$\left\langle R_g^2 \right\rangle = \frac{3}{5}R_s^2 \quad (\text{sphere}) \tag{412a}$$

$$\left\langle R_g^2 \right\rangle = \frac{1}{12}L^2 \quad (\text{rod-like particle}) \tag{412b}$$

$$\left\langle R_g^2 \right\rangle = \frac{1}{6}Nl^2 \quad (\text{Gaussian coil}) \tag{412c}$$

$$\left\langle R_g^2 \right\rangle = \frac{1}{2}R_d^2 \quad (\text{thin disk}) \tag{412d}$$

The radius of gyration for a wormlike chain of length $L$, persistent length $l_p$, and diameter $d$ was found to be[861]

$$\left\langle R_g^2 \right\rangle = L^2\left\{\frac{1}{3}\tilde{l}_p - \tilde{l}_p^2 + 2\tilde{l}_p^4\left[\tilde{l}_p^{-1} - 1 + \exp\left(-\frac{1}{\tilde{l}_p}\right)\right]\right\} + \frac{d^2}{8} \quad (\text{wormlike chain}) \tag{413}$$

where $\tilde{l}_p = l_p / L$. For a random coil ($\tilde{l}_p \ll 1$, $l_p = l/2$, $L = Nl$, and $d \ll L$), Equation 413 reduces to Equation 412c. In the other limiting case of $\tilde{l}_p \gg 1$, Equation 413 reduces to the result for a cylinder of length $L$ and diameter $d$:

$$\left\langle R_g^2 \right\rangle = \frac{1}{12}L^2 + \frac{1}{8}d^2 \quad (\text{cylinder}) \tag{414}$$

This consideration can be further generalized to account for the interaction between the particles (see Section 5.9.1.4, below).

### 5.9.1.3 Theory of Mie

If the condition in Equation 406 is violated, the RDG theory is not valid. A solution of the scattering problem for particles arbitrary in size has been found only for several particular shapes. Mie[874] succeeded in finding a complete general solution of the Maxwell equations for a sphere in a periodic electromagnetic field. The refractive indexes of the sphere, $n_p$, and of the medium, $n_m$, are considered to be complex numbers (i.e., the theory is applicable to light-absorbing substances, including metals):

$$n_j^2(\omega) = \varepsilon_j(\omega) - i\frac{4\pi\chi_j(\omega)}{\omega} \quad \text{or} \quad n_j(\omega) = \tilde{n}_j(\omega) - ik_j(\omega); \qquad j = p \text{ or } m \qquad (415)$$

Here, $\varepsilon_j(\omega)$ and $\chi_j(\omega)$ are the dielectric permittivity and the electrical conductivity, respectively, for a given circular frequency, $\omega$, of the field, while $\tilde{n}_j$ and $k_j$ are the real and the imaginary parts, respectively, of the refractive index.

As shown by Mie[874] and Debye,[875] the electromagnetic field of the light scattered by a sphere can be presented as an infinite series over associated Legendre polynomials, $P_n^1(\cos\theta)$, multiplied by spherical Bessel functions, $h_n^{(2)}(2\pi r/\lambda)$. The coefficients in this series must be determined from the boundary conditions and afterwards can be used to calculate the angular dependence of the amplitude and polarization of the scattered field. Different boundary conditions were imposed in the case of conducting or dielectric materials of the sphere and of the medium.

The numerical calculation of the complete problem presents a formidable task, and a number of practical recommendations for appropriate simplifications are given in the specialized literature.[847-849] Typically, the final result of such calculations is presented in terms of the efficiency factors for absorption and scattering, $Q_{abs}$ and $Q_{sca}$. The magnitudes of $Q_{abs}$ and $Q_{sca}$ depend on $\lambda$, $\tilde{n}$, $k$, $\theta$, and the particle size. For nonabsorbing particles ($k_p$=0), $Q_{abs}$=0; for nonscattering particles ($\tilde{n}_p = \tilde{n}_m$), $Q_{sca}$=0. The efficiency factors can be directly related to the absorbance and turbidity of the suspension (see Section 5.9.1.7). A similar approach was used to investigate the scattering from coated spheres; long circular, elliptic, and parabolic cylinders; flat disks; spheroids; and others (see References 847, 848, and 876).

The theory of Mie[874] is used also in the laser diffraction method for particle size analysis.[877] In this method, the light scattered by the particles is collected over a range of angles (usually between 1° and 20°) in the forward direction. The corresponding experimental setup is usually referred to as Fourier optics. The method is applied to relatively large particles (typically between 0.3 and 600 μm) when the scattered light in a forward direction (projected on a screen) presents a combination of concentric fringes. The angular intensity distribution of the scattered light is analyzed to deduce the particle size distribution. For particles of diameter above several micrometers, the diffraction pattern is usually interpreted by simpler approximate theories, like that of the Fraunhofer diffraction.[877]

### 5.9.1.4 Interacting Particles

#### *5.9.1.4.1 Fluctuation theory of static light scattering*

All discussion up to here has been based on the assumption that the scatterers are independent; however, in most of cases this assumption is not justified. A general approach

for calculating $R(\theta)$ for a suspension of small interacting particles was proposed by Einstein.[878] He related the fluctuations in the polarizability of suspension with the fluctuations of the particle concentration. The final result reads:

$$R_j(\theta) = \frac{4\pi^2 n_m^2 \left(\frac{dn}{dc}\right)^2}{\lambda_0^4 N_A} c P_j(\theta) \left[\frac{\partial(\Pi / N_A kT)}{\partial c}\right]^{-1} \qquad j = v,u,h \tag{416}$$

where $\Pi(c)$ is the osmotic pressure of the suspension. For a low particle concentration, the osmotic pressure is expanded in series with respect to the particle concentration:

$$\frac{\Pi}{N_A kT} = A_1 c + A_2 c^2 + A_3 c^3 + \ldots \qquad j = v,u,h \tag{417}$$

where $A_i$ are virial coefficients ($A_1 = 1/M$). Then, the relationship between $c$ and $R(\theta)$ can be rewritten in the form:[879]

$$\frac{Kc}{R_j(\theta)} P_j(\theta) = \frac{1}{M} + 2A_2 c + \ldots \quad j = v,u,h \tag{418}$$

where $P_j(\theta)$ is given by Equation 402, depending on the polarization of the incident light. As seen from this expression, the particle mass can be determined by measuring $R(\theta)$ at several concentrations and extrapolating the result toward $c$=0. The intercept of the obtained straight line (at small concentrations) is equal to $1/M$, while the slope provides the second osmotic virial coefficient, $A_2$, which is a measure of the interparticle interactions.

The system of large interacting particles requires a modification of the Einstein approach, because one should account for correlations in the position of the scattering subunits within a given particle, along with correlations in the positions of different particles. If the condition in Equation 406 is satisfied, one can decompose these correlations into two different terms to obtain[880]

$$R_j(\theta) = K_1 \rho P_j(\theta) S(\rho, q); \qquad K_1 = \frac{4\pi^2 n_m^2 \left(\frac{dn}{d\rho}\right)^2}{\lambda_0^4 N_A} \qquad j = v,u,h \tag{419}$$

where the particle form factor $P_j(\theta)$ is the same as for noninteracting particles, while the structure factor $S(\rho,q)$, accounts for the interactions. By definition, the static structure factor is

$$S(\rho, q) = 1 + \rho \int_0^\infty 4\pi r^2 [g(r) - 1] \frac{\sin qr}{qr} dr \tag{420}$$

where $g(r)$ is the pair radial distribution function.

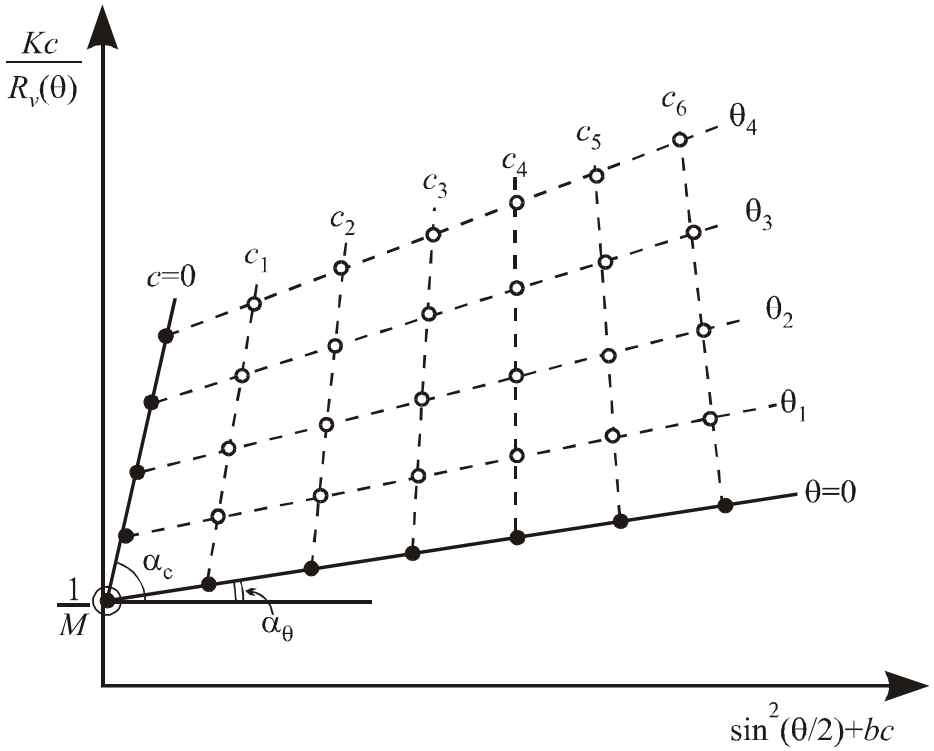


**FIGURE 72.** Schematic presentation of the Zimm-plot[881] (method of double extrapolation). The data from measurements at several concentrations ($c_1$ to $c_6$) and scattering angles ($\theta_1$ to $\theta_4$) are presented by empty circles. Then, extrapolation to $c = 0$ for each angle and to $\theta = 0$ for each concentration is numerically performed (see the black dots). Both lines, $c = 0$ and $\theta = 0$, should meet the ordinate at the point $M^{-1}$, where $M$ is the particle mass. The slope angle of the line $c = 0$ is equal to $\alpha_c = \tan^{-1}\left[\left(4\pi n/\lambda_0\right)^2\left\langle R_g^2\right\rangle/3M\right]$, while the slope angle of the line $\theta = 0$ is equal to $\alpha_\theta = \tan^{-1}\left(2A_2\right)$.

For small particles, $g(r)$ is substantially different from unity only at interparticle distances $r << q^{-1}$. Then, the structure factor is equal to the inverse osmotic compressibility of the suspension:[880]

$$S(\rho,q) \approx 1 + \rho\int_0^\infty 4\pi r^2\left[g(r)-1\right] \equiv \left[\frac{\partial(\Pi/kT)}{\partial\rho}\right]_T^{-1} \tag{421}$$

and Equation 419 reduces to the Einstein expression, Equation 416, with $\rho$ (instead of $c$) being used as a measure of the particle concentration - note that Equation 416 does not depend on the particular choice of the concentration definition.

*5.9.1.4.2 Zimm-plot (method of double extrapolation)*

The substitution of Equation 410 in Equation 418 suggests a graphical procedure for interpretation of light scattering data from suspensions of large interacting particles of arbitrary shape. Keeping the leading terms we obtain:

$$\frac{Kc}{R_v(\theta)}=\frac{1}{M}\left[1+\frac{16}{3}\left(\frac{\pi n}{\lambda_0}\right)^2 \sin^2(\theta/2)\left\langle R_g^2\right\rangle\right]+2A_2c+... \quad (422)$$

Based on this formula, Zimm[881] suggested plotting $Kc/R_v(\theta)$ against $[\sin^2(\theta/2)+bc]$, where $b$ is an arbitrary constant usually chosen to satisfy the condition $bc_{max}\sim1$. This method requires measurements at different concentrations and scattering angles. The data are presented as a grid of points (Figure 72) which allows extrapolation (1) to zero angle for each used concentration, and (2) to zero concentration for each scattering angle. Finally, the extrapolated points for zero concentration (at different angles) are extrapolated to zero angle, and the points for zero angle (at different concentrations) are extrapolated to zero concentration. In the ideal case, the two extrapolated curves must cut the ordinate $Kc/R_v(\theta)$ at the same point, which is the inverse mass of the particle. Respectively, the initial slope of the curve $c$=0 provides the square radius of gyration, $\left\langle R_g^2\right\rangle$, while the initial slope of the curve $\theta$=0 gives the second osmotic virial coefficient, $A_2$.

For non-polarized or horizontally polarized incident beams, $R_v(\theta)$ in Equation 422 is to be replaced by $2R_u(\theta)/(1+\cos^2\theta)$ or $R_h(\theta)/\cos^2\theta$, respectively.

*5.9.1.4.3 Interpretation of the second osmotic virial coefficient*

Generally speaking, positive values of $A_2$ mean net repulsion between the particles, while negative values of $A_2$ correspond to attraction. For more detailed analysis of the values of the second osmotic virial coefficient, the use of other definitions of the particle concentration is more convenient. The common virial expansion:[11]

$$\frac{\Pi}{kT}=\rho+\frac{1}{2}\beta_2\rho^2+... \quad (423)$$

defines another second virial coefficient, $\beta_2$, which has the dimensions of volume and is widely used in statistical thermodynamics. The coefficients, $A_2$ and $\beta_2$, are interconnected through the relationship:

$$\beta_2=2\frac{M^2}{N_A}A_2 \quad (424)$$

For the central interaction between the particles, one can rigorously show that:[11,880]

$$\beta_2=\int_0^\infty[1-g(r)]4\pi r^2dr=\int_0^\infty\left[1-\exp\left(-\frac{W(r)}{kT}\right)\right]4\pi r^2dr \quad (425)$$

where $r$ is the distance between the centers of mass of the particles, and $W(r)$ is the pair interaction energy. More general expressions for $\beta_2$ in the case of anisodiametrical particles is also available.[11,880] The usage of $\beta_2$ is convenient when the experimental results about the

particle interactions must be compared to theoretical calculations. For hard spheres, $\beta_2$ is equal to $8V_p$, where $V_p$ is the particle volume. This fact was used by some authors to define so-called effective volume of the particle through the measured second virial coefficient:[314,324]

$$V_{\mathrm{EFF}} = \frac{1}{8}\beta_2 = \frac{1}{4}\frac{A_2 M^2}{N_A}; \quad A_2, \beta_2 > 0 \tag{426}$$

Note that $V_{\mathrm{EFF}}$ could be substantially different from the actual particle volume, $V_p$, if long-range interactions between the particles are present. The counterpart of Equation 422 in terms of $\rho$ and $\beta_2$ reads:

$$\frac{K_1 \rho}{R_v(\theta)} = \left[1 + \frac{16}{3}\left(\frac{\pi n}{\lambda_0}\right)^2 \sin^2(\theta/2)\left\langle R_g^2 \right\rangle\right] + \beta_2 \rho + \ldots; \quad K_1 = \frac{4\pi^2 n_m^2}{\lambda_0^4}\left(\frac{dn}{d\rho}\right)^2 \tag{427}$$

In the case of microemulsions and suspensions of spherical particles, it is usually more convenient to use the volume fraction, $\phi$, of the dispersed particles as a measure of their concentration.[882-887] By using the fact that $\phi = \rho V_p$, one can obtain the virial expansion:

$$\frac{\Pi}{kT} = B_1 \phi + B_2 \phi^2 + \ldots; \quad B_1 = \frac{1}{V_p} \text{ and } B_2 = \frac{\beta_2}{2V_p^2} \tag{428}$$

The light scattering data can be interpreted by using the equation:

$$\frac{K_2 \phi}{R_v(\theta)} = \frac{1}{V_p}\left[1 + \frac{16}{3}\left(\frac{\pi n}{\lambda_0}\right)^2 \sin^2(\theta/2)\left\langle R_g^2 \right\rangle\right] + 2B_2 V_p \phi; \qquad K_2 = \frac{4\pi^2 n_m^2}{\lambda_0^4}\left(\frac{dn}{d\phi}\right)^2 \tag{429}$$

Therefore, the double extrapolation procedure in these variables provides the real volume of the particles, $V_p$. The quantity $2B_2V_p$ is dimensionless and often denoted in the literature as $\lambda_V$ (see Section 5.9.2.4, below). For hard spheres, $\lambda_V = 8$.

### 5.9.1.5 Depolarization of Scattered Light

The polarization of the incident beam is denoted by subscripts *v*, *h*, or *u* for vertically polarized, horizontally polarized, or nonpolarized light, respectively. Generally, the Rayleigh constant can be considered as consisting of two components, $R^V$ and $R^H$, corresponding to the vertical and horizontal directions of the electrical field of the scattered light (Figure 70). Therefore, one can define six quantities: $R_v^V, R_h^V, R_u^V, R_v^H, R_h^H$, and $R_u^H$, the values of which provide information about the size, shape, and anisotropy of the scattering particles.[888-890] Depending on the polarization of the incident light, it is accepted to define three depolarization coefficients:

$$\Delta_v = \frac{R_v^H}{R_v^V}, \Delta_h = \frac{R_h^H}{R_h^V}$$
$$\Delta_u = \frac{R_u^H}{R_u^V} = \frac{R_v^H + R_h^H}{R_v^V + R_h^V} = \frac{1+\Delta_h}{1+\Delta_v^{-1}} \tag{430}$$

Usually, $\Delta_v$, $\Delta_h$, and $\Delta_u$ refer to a scattering angle $\theta$=90° and small concentrations, $c \to 0$ (the scattering from the solvent is subtracted). The values of $\Delta_v$, $\Delta_h$, and $\Delta_u$ can be used to determine the type of the suspended particles (see Table 10). Note that the inherent particle anisotropy is reflected in the value of $\Delta_v$, while $\Delta_u$ contains a contribution from the particle size as well.

**Table 10. Depolarization Coefficients of Different Types of Particles[888,889]**

| Particles | $\Delta_v$ | $\Delta_h$ | $\Delta_u$ |
|---|---|---|---|
| small, isotropic | 0 | not defined | 0 |
| small, anisotropic | (0 – 1) | 1 | (0 – 1) |
| large, isotropic | 0 | ∞ | (0 – 1) |
| large, anisotropic | (0 – 1) | 1 | (0 – 1) |

One can define the so-called optical anisotropy of the particles

$$\delta^2 = \frac{(\alpha_1 - \alpha_2)^2 + (\alpha_2 - \alpha_3)^2 + (\alpha_3 - \alpha_1)^2}{(\alpha_1 + \alpha_2 + \alpha_3)^2} \tag{431}$$

where $\alpha_1$, $\alpha_2$, and $\alpha_3$ are the polarizabilities of the particle along its three main axes. As shown by Cabannes[888] for particles arbitrary in size:

$$\delta^2 = \frac{10\Delta_u}{6 - 7\Delta_u} \tag{432}$$

In the particular case of small particles and $\theta$=90°, one has:

$$P_v(90^\circ) = \frac{3 + 3\Delta_v}{3 - 4\Delta_v}; \; R_v(90^\circ) = cKM\frac{3 + 3\Delta_v}{3 - 4\Delta_v} \tag{433a}$$

$$P_u(90^\circ) = \frac{6 + 6\Delta_u}{6 - 7\Delta_u}; \; R_u(90^\circ) = \frac{1}{2}cKM\frac{6 + 6\Delta_u}{6 - 7\Delta_u} \tag{433b}$$

Comparison of Equations 402, 405, and 433b shows that in the case of small anisotropic molecules, one has an additional multiplier $\left(\frac{6 + 6\Delta u}{6 - 7\Delta u}\right)$ called the *Cabannes' factor*.

Therefore, the correct determination of the particle mass in such systems requires measurements of both, $R(90°)$ and $\Delta(90°)$.

#### 5.9.1.6 Polydisperse Samples

The light scattering methods provide statistically averaged quantities when applied to polydisperse samples (e.g., micellar or polymer solutions). The case of independent scatterers can be rigorously treated[862,881] by using the mass distribution function of the particles, $f(M)$. By definition, $dm=f(M)dM$ is the mass of particles in the range between $M$ and $(M+dM)$, scaled by the total particle mass. As shown by Zimm,[881] the scattering law in such a system can be presented similarly to the case of monodisperse particles (see Equation 405):

$$\left[\frac{Kc}{R_j(\theta)}\right]^{-1} = \int_0^\infty f(M) M P_j(\theta, M) dM = \langle M \rangle_m \left\langle P_j(\theta) \right\rangle_m \qquad j = u, v, h \tag{434}$$

where $c$ is the total particle concentration, while the averaged molecular mass, $\langle M\rangle_m$, and form factor, $\langle P(\theta)\rangle_m$, are defined as:

$$\langle M \rangle_m = \int_0^\infty M f(M) dM \ , \qquad \left\langle P_j(\theta) \right\rangle_m = \frac{1}{\langle M \rangle_m} \int_0^\infty f(M) M P_j(\theta, M) dM \tag{435}$$

For small scattering angles, $P_v(\theta,M) \to 1 - \frac{1}{3} q^2 \left\langle R_g^2(M) \right\rangle$, where $\left\langle R_g^2(M) \right\rangle$ is the squared radius of gyration of particles having mass $M$. Substituting this expression in Equation 434, one obtains:[881]

$$\left[\frac{Kc}{R_V(\theta)}\right]_{\theta \to 0}^{-1} = \langle M \rangle_m \left( 1 - \frac{1}{3} q^2 \int_0^\infty f(M) \left\langle R_g^2(M) \right\rangle M \, dM \right) \tag{436}$$

This expression can be used as a starting point for analysis of the scattered light intensity by polydisperse samples. If the shape of the particles is known (that is, $\left\langle R_g^2(M) \right\rangle$ is a known function; see Equation 412), one can determine two parameters characterizing the distribution $f(M)$ (e.g., its mean value and standard deviation) from the experimentally measured intercept and slope of the line, $[cK/R_v(\theta)]^{-1}$ vs. $q^2$. For small particles, $P(\theta \to 0, M) \approx 1$ and:

$$\left[\frac{Kc}{R(\theta)}\right] \approx 1 / \langle M \rangle_m \tag{437}$$

Therefore, in this case, one can determine the mass averaged particle mass (Equation 435).

### 5.9.1.7 Turbidimetry

Instead of measuring the intensity of the scattered light at a given angle, θ, one can measure the extinction of the incident beam propagating through the suspension.[853,879] The method is called *turbidimetry* and was widely used in the past, because the necessary equipment was essentially the same as that for measuring the absorption of light by colored solutions. Usually, non-polarized light is used in these experiments; hence, the following consideration corresponds to nonpolarized incident beams.

The turbidity, $\tau[\mathrm{m}^{-1}]$, of a suspension is defined through a counterpart of Beer-Lambert's equation:[848,849]

$$I(x) = I_0 \exp(-\tau x) \tag{438}$$

On the other hand, the turbidity can be calculated by integrating the scattered light in all directions and dividing by the intensity of the incident beam:

$$\tau = \int_{\theta=0}^{\pi} \int_{\varphi=0}^{2\pi} \frac{\langle I_s(\theta) \rangle_t}{\langle I_0 \rangle_t} r^2 \sin\theta \, d\theta \, d\varphi = 2\pi \int_0^{\pi} R_u(\theta) \sin\theta \, d\theta \tag{439}$$

For suspension of noninteracting scatterers, it is convenient to introduce so-called dissipation factor, $Q$:

$$Q = \frac{3}{8} \int_0^{\pi} P_v(\theta)\left(1 + \cos^2\theta\right) \sin\theta \, d\theta \tag{440}$$

Also, for noninteracting particles we have (see Equations 402 and 407):

$$R_u(\theta) \equiv R_u(0) P_u(\theta) = R_u(0) P_v(\theta) \left( \frac{1 + \cos^2\theta}{2} \right) \tag{441}$$

Therefore, τ can be expressed as:

$$\tau = \frac{8\pi}{3} Q \, R_u(0) = \frac{16\pi}{3} Q \, \frac{R_u(90^\circ)}{P_v(90^\circ)} = \frac{8\pi}{3} QcKM \tag{442}$$

Note that for small particles $P_v(\theta) = 1$, $Q = 1$, and $\tau = (8\pi/3)cKM$. This simpler case can be generalized to suspensions of interacting particles and the final result reads:[879]

$$\tau = \frac{\frac{8}{3}\pi K c}{\frac{1}{M} + 2A_2 c} \tag{443}$$

Therefore, for small particles, $Kc/\tau$ is a linear function of $c$ in the low concentration range, and the intercept and slope of the straight line allow us to calculate $M$ and $A_2$, respectively.

The above consideration was for particles not absorbing light. If the particles do absorb light, one must use the Mie theory (Section 5.9.1.3). Equation 438 is modified to read:[847-849]

$$I(x) = I_0 \exp[-(\xi + \tau)x] \tag{444}$$

and the absorbance, $\xi$, and the turbidity, $\tau$, of a suspension containing spherical particles of radius $R$ are determined from:

$$\xi = \pi R^2 \rho Q_{abs} \text{ and } \tau = \pi R^2 \rho Q_{sca} \tag{445}$$

where $Q_{abs}$ and $Q_{sca}$ must be numerically calculated as mentioned in Section 5.9.1.3.

### 5.9.2 DYNAMIC LIGHT SCATTERING

We represent here only the basic methods and equations used for DLS data analysis. Detailed description of the subject can be found in the available monographs.[891-897]

#### 5.9.2.1 DLS by Monodisperse, Noninteracting Spherical Particles

In the DLS methods, the time fluctuations of the intensity of the scattered light, $I_s(t)$, are analyzed. These fluctuations are caused by the translational and rotational Brownian motion of the particles, which leads to perpetual variation of the particle configuration with the resulting change in the interference pattern of the scattered light. The time course of the detector signal (which is proportional to $I_s(t)$) can be analyzed by two different devices.

*5.9.2.1.1 Spectrum analyzer*

This equipment is used when the intensity of the scattered light is high and an analog output from the photomultiplier tube (the detector) is available. The power spectrum, $P(q,\omega)$, of the output signal is extracted. For instance, in the case of translational diffusion of monodisperse spherical particles:

$$P^{(2)}(q,\omega) = \frac{2q^2 D/\pi}{\omega^2 + (2q^2 D)^2} + \delta(\omega) \tag{446}$$

where $D$ is the translational diffusion coefficient of the particles and $\delta(x)$ is the Dirac-delta function. According to Equation 446, the power spectrum is Lorentzian, centered at $\omega=0$ with a half-width equal to $2q^2D$. From the value of $D$, one can calculate the hydrodynamic radius of the particle, $R_h$, by means of the Stokes-Einstein formula:

$$R_h = \frac{kT}{6\pi\eta D} \tag{447}$$

where $\eta$ is the shear viscosity of the disperse medium.

*5.9.2.1.2 Correlator*

This type of instrument is aimed at calculating the autocorrelation function of the intensity of the scattered light, defined as:

$$g^{(2)}(q,\tau) \equiv \frac{1}{\langle I_s \rangle_t^2} \lim_{T\to\infty} \frac{1}{2T} \int_{-T}^{T} I_s(t) I_s(t+\tau) dt = \langle I_s(t) I_s(t+\tau) \rangle_t / \langle I_s \rangle_t^2 \tag{448}$$

An important advantage of the correlators is that they are capable of working even with very low intensities of the scattered light, when each photon is separately counted by the detector. From a theoretical viewpoint, $P^{(2)}(q,\omega)$ and $g^{(2)}(q,\tau)$ provide essentially the same information, because for a stationary random process (as in the case with diffusion) these two quantities are Fourier transforms of each other (Wiener-Khintchine theorem):[880]

$$g^{(2)}(q,\tau) = \int_{-\infty}^{+\infty} P^{(2)}(\omega) \cos(\omega\tau) d\omega \tag{449a}$$

$$P^{(2)}(q,\omega) = \frac{1}{2\pi} \int_{-\infty}^{+\infty} g^{(2)}(\tau) \cos(\omega\tau) d\tau \tag{449b}$$

Therefore, $g^{(2)}(q,\tau)$ can be calculated if $P^{(2)}(q,\omega)$ is experimentally determined and vice versa. In the particular case of translational diffusion of monodisperse spherical particles (see Equation 446):

$$g^{(2)}(q,\tau) = \int_{-\infty}^{+\infty} \left[ \delta(\omega) + \frac{2q^2 D/\pi}{\omega^2 + (2q^2 D)^2} \right] \cos(\omega\tau) d\omega = 1 + \exp(-2q^2 D\tau) \tag{450}$$

In reality, the experiment provides the function:

$$G^{(2)}(q,\tau) = 1 + F\exp(-2q^2 D\tau) \tag{451}$$

where the factor $F$ accounts for the spatial coherence of the scattering volume and depends on the aperture of the detector. If the detector radius is $\sim\lambda r/b$ ($r$ is the distance between the scattering volume and the detector, $b$ is the radius of the scattering volume, and $\lambda^2 r^2/\pi b^2$ is the coherence area),[898] $F$ is close to unity. For a larger radius of the detector, $F$ would be orders of magnitude smaller, and the signal/noise ratio will be also small.

Equations 446 and 450 are applicable in the so-called homodyne method (or self-beating method), where only scattered light is received by the detector.[891-896] In some cases, it is also desirable to capture by the detector a part of the incident beam which has not undergone the scattering process. This method is called *heterodyne* (or method of the local oscillator) and sometimes provides information that is not accessible by the homodyne method.[892] It can be shown that if the intensity of the scattered beam is much lower than that

of the detected nonscattered (incident) beam, the detector measures the autocorrelation function of the electrical field of the scattered light defined as:

$$g^{(1)}(q,\tau) \equiv \left\langle E_s^*(t) E_s(t+\tau) \right\rangle / \left\langle I_s \right\rangle_t \tag{452}$$

where $E_s(t)$ is the intensity of the electrical field of the light and the asterisk indicates complex conjugation. The counterparts of Equations 446 and 450 in the heterodyne method read:

$$P^{(1)}(q,\omega) = \frac{q^2 D/\pi}{\omega^2 + \left(q^2 D\right)^2} \tag{453a}$$

$$g^{(1)}(q,\tau) = \exp\left(-q^2 D\tau\right) \tag{453b}$$

In this case, the Wiener-Khintchine theorem, Equation 449, is also valid if $g^{(2)}(q,\tau)$ is replaced by $g^{(1)}(q,\tau)$ and $P^{(2)}(q,\omega)$ by $P^{(1)}(q,\omega)$. In addition, for the diffusion process, $g^{(1)}(q,\tau)$ and $g^{(2)}(q,\tau)$ are interrelated by the Siegert equation:

$$g^{(2)}(q,\tau) = 1 + \left| g^{(1)}(q,\tau) \right|^2 \tag{454}$$

If charged particles are placed in an external, constant electrical field (e.g., in electrophoretic equipment), they acquire a drift velocity, $\mathbf{V}_{EL}$, which is superimposed upon the diffusion. The respective power spectrum in the heterodyne method is[899]

$$P^{(1)}(q,\omega) = \frac{1}{2}\left[ \frac{q^2 D/\pi}{(\omega + \mathbf{q}.\mathbf{V}_{EL})^2 + \left(q^2 D\right)^2} + \frac{q^2 D/\pi}{(\omega - \mathbf{q}.\mathbf{V}_{EL})^2 + \left(q^2 D\right)^2} \right] \tag{455a}$$

where $\mathbf{q}$ is the scattering vector equal to the difference between the scattered and incident wavevectors $\left( |\mathbf{q}| = \frac{4\pi n}{\lambda_0} \sin(\theta/2) \right)$. Therefore, the power spectrum is a sum of two Lorentzians which are shifted in frequency, but their half-width remains determined by the translational diffusion coefficient. The autocorrelation function in this case is

$$g^{(1)}(q,\tau) = \exp\left(-q^2 D\tau\right) \cos\left[(\mathbf{q}.\mathbf{V}_{EL})\tau\right] \tag{455b}$$

Equations 455a and 455b show that, in principle, from one experiment one can simultaneously determine $D$ and $V_{EL}$. In practice, a series of experiments at different intensities of the external field, $E$, is performed, and the linear function $V_{EL}$ vs. $E$ is plotted. The slope of the resulting line gives the electrophoretic mobility, $\mu_{EL} \equiv V_{EL} / E$. In a similar way the velocity of aerodynamic fluxes can be studied by using tracer particles (laser doppler anemometry).[900]

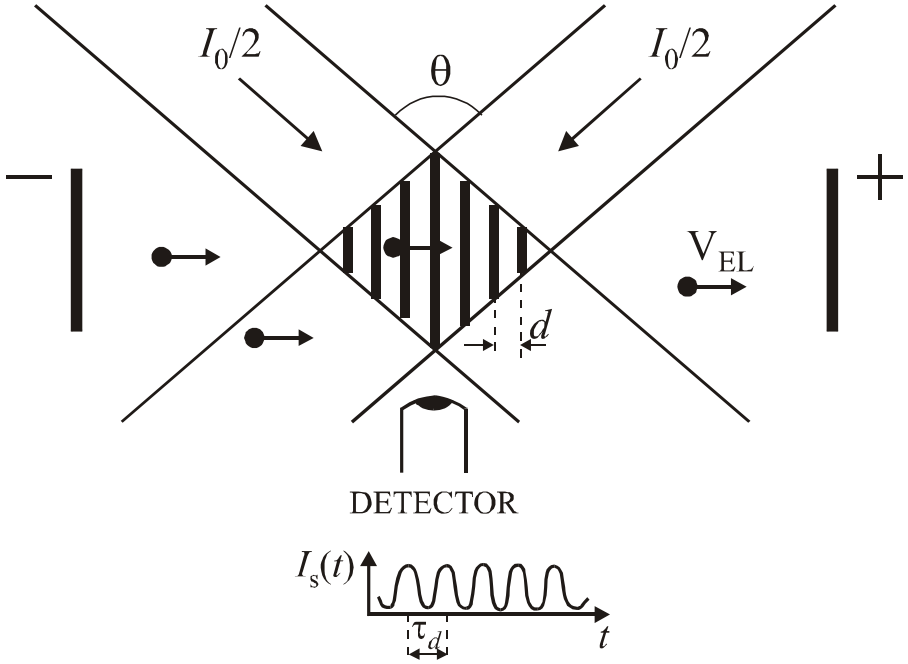


**FIGURE 73.** The method of crossed beams for measurement of particle drift velocity, $V_{EL}$. The incident laser beam of intensity $I_0$ is split into two coherent beams by using an optical prism (not shown in the figure). Then, the two beams meet each other in the scattering volume and form an interference pattern. The distance between the bright planes of this pattern is $d = \lambda_0/[2n\sin(\theta/2)]$. The particles, moving under the action of applied electrical potential, give rise to pulses of scattered light when passing through the bright planes. The time interval, $\tau_d$, between two consecutive pulses, created by a given particle, is $\tau_d = d/V_{EL}$. Since $d$ is known and $\tau_d$ is measured from the autocorrelation function of the scattered light, one can calculate the drift velocity, $V_{EL}$.

The scattering geometry used in most of the commercial equipment for measuring the electrophoretic mobility of particles[901] is shown schematically in Figure 73. The incident laser beam is split into two parts of equal intensity, which are afterwards crossed in the scattering volume. At the crossing point a pattern of consecutive dark and bright interference planes is formed, due to the mutual coherence of the beams. Therefore, when the particle (driven by the external electrical field) crosses the bright planes, it scatters light which is received by the detector as a sequence of pulses. The time interval between the two pulses of light, scattered by one and the same particle, depends on the distance between the interference planes (determined by the geometry of the crossing beams) and on the particle velocity. The corresponding autocorrelation function of the intensity of the scattered light is a damped cosine function, the period of which allows one to calculate the particle drift velocity and electrophoretic mobility. A modification[901] of the equipment allows one to measure relatively low mobilities with high precision, which is particularly important for nonaqueous dispersions.

#### 5.9.2.2 DLS by Polydisperse, Noninteracting Spherical Particles

For polydisperse samples of noninteracting particles, the autocorrelation function (or the power spectrum) presents a superposition of the respective functions of the individual species, weighted by the intensities of light scattered by them. Several procedures have been employed to analyze the signal from polydisperse samples. The most straightforward procedure[902] is the method of cumulants, in which the log of the measured correlation function is expanded in series:

$$\ln\left[g^{(1)}(q,\tau)\right] = \sum_{n=1}^{\infty} K_n(q)\frac{(-\tau)^n}{n!} \tag{456}$$

The first cumulant, $K_1(q) = \lim_{\tau\to 0}\dfrac{d\ln g^{(1)}(q,\tau)}{d\tau}$, defines an effective diffusion coefficient:

$$D_{\mathrm{EFF}} = \frac{K_1(q)}{q^2} \tag{457}$$

For noninteracting particles, $D_{\mathrm{EFF}}$ presents the so-called $z$-average diffusion coefficient, $\langle D\rangle_z$:

$$D_{\mathrm{EFF}} = \langle D\rangle_z \equiv \frac{\int_0^{\infty} f(M)M\,P(q,M)D(M)\,dM}{\int_0^{\infty} f(M)M\,P(q,M)\,dM} \tag{458}$$

The second cumulant, $K_2(q) = \lim_{\tau\to 0}\dfrac{d^2\ln g^{(1)}(q,\tau)}{d\tau^2}$, provides information about the polydispersity of the sample:

$$\frac{K_2(q)}{q^4} = \langle D^2\rangle_z - \langle D\rangle_z^2 \tag{459}$$

The higher order cumulants, $K_3$ and $K_4$, are measures of the distribution asymmetry and flatness, respectively. It is usually difficult to determine reliably $K_3$ and $K_4$.

The mean hydrodynamic radius, calculated from $D_{\mathrm{EFF}}$, is given by:

$$\langle R_h\rangle = \frac{kT}{6\pi\eta\langle D\rangle_z} = \frac{\int_0^{\infty} f(M)M\,P(q,M)\,dM}{\int_0^{\infty} f(M)M\,P(q,M)R_h^{-1}(M)\,dM} \tag{460}$$

The main advantage of the cumulant method is that it does not require any assumption about the particular shape of the size distribution. The main drawback of this method is that a

variety of rather different distributions may have similar values of $K_1$ and $K_2$. Therefore, one cannot obtain reliable information about the size distribution only from DLS data. The cumulant method is most suitable when the size distribution is known to be monomodal and relatively narrow.

For polymodal or wide distributions the histogram method[903-911] (or the exponential sampling method) is more representative. In this method, the particle size distribution is presented by a finite number of discrete sizes, each of them being an adjustable fraction of the total concentration. Then, the correlation function is calculated and compared with the measured one. The relative amplitude of each size class is varied to give the best agreement between the calculated and the experimental functions. Although conceptually simple, the histogram method is not straightforward, because a given correlation function can be described by an infinite variety of particle distributions (ill-posed mathematical problem). To overcome this difficulty, one must invoke independent criteria to restrict the population of possible solutions and to choose "the most reasonable" one. Several procedures were proposed and realized as computer programs, the most widely used of them being CONTIN,[894,904] nonnegative least squares (NNLS),[905] singular value analysis,[907] maximum entropy,[910] regularization technique,[911] and several others.[906,908,909] For more thorough and reliable results, multi-angle measurements and combined analysis of the data from SLS and DLS on the basis of Mie theory are recommended.

#### 5.9.2.3 DLS by Nonspherical Particles

In diluted suspensions, translation and rotation of the particles can be considered as statistically independent. Then, the correlation function of the scattered light can be presented as being composed of two parts[912] - phase autocorrelation function, $C_\Phi(q,\tau)$, accounting for the translational diffusion, and amplitude autocorrelation function, $C_B(\tau)$, determined by the particle rotation:

$$g^{(1)}(q,\tau) = C_B(\tau)\, C_\Phi(q,\tau) \tag{461}$$

where, by definition,

$$C_B(\tau) \equiv \langle B^*(0)B(\tau)\rangle_t \,/\, \langle B(0)^2\rangle_t \tag{462}$$

$B(t)$ is the scattering amplitude of a particle, which depends on the particle polarizability at given orientation. $B(t)$ changes with time due to reorientation of the particle. If the scatterers are spherical, $B(t)$ is constant and $C_B(\tau)=1$. Note that $C_B(\tau)$ does not depend on the scattering angle and can be calculated if the polarizability tensor and the rotational diffusion tensor of the particles are known. The calculation of $C_\Phi(q,\tau)$ requires averaging of the translational

diffusion tensor of the particle over all possible orientations in order to obtain the averaged translational diffusion coefficient.

The polarizability of cylindrically symmetrical particles (rod-shaped or ellipsoidal particles) can be characterized by isotropic ($\alpha$) and anisotropic ($\beta$) parts of the polarizability tensors:[892]

$$\alpha \equiv \frac{1}{3}\left(\alpha_{\mathrm{II}} + 2\alpha_{\mathrm{I}}\right), \qquad \beta \equiv \left(\alpha_{\mathrm{II}} - \alpha_{\mathrm{I}}\right) \tag{463}$$

where $\alpha_{\mathrm{II}}$ and $\alpha_{\mathrm{I}}$ are the polarizabilities in directions parallel and perpendicular, respectively, to the symmetry axis. The autocorrelation function for small, monodisperse, cylindrically symmetrical particles has the form:[892]

$$g_v^{(1)V}(q,\tau) = \alpha^2 \exp\left(-q^2 D\tau\right) + \frac{4}{45}\beta^2 \exp\left[-\left(q^2 D + 6\Theta\right)\tau\right] \tag{464}$$

where $\Theta$ is the rotational diffusion coefficient; the subscript "*v*" and the superscript "*V*" denote vertically polarized incident and scattered beams, respectively. Since $g_v^{(1)V}$ consists of two exponents (the second one being difficult for precise determination, because it is weaker in magnitude and decays more rapidly compared to the first one), it is preferable to perform measurements also in depolarized light:[892,912]

$$g_v^{(1)H}(q,\tau) = \frac{\beta^2}{15} \exp\left[-\left(q^2 D + 6\Theta\right)\tau\right] \tag{465}$$

which presents one exponent depending on both, $D$ and $\Theta$.

For long rod-like particles, the autocorrelation function is a sum of exponentials[893]

$$g_v^{(1)V}(\tau) = \sum_{l=0,l\,even}^{\infty} B_l \exp\left\{-\left[q^2 D + l(l+1)\Theta\right]\tau\right\} \tag{466}$$

The amplitude coefficients $B_l$ are defined through spherical Bessel functions and can be calculated if the particle length is specified. The extraction of the value of $\Theta$ from the experimentally obtained correlation function obeying Equation 466 is a formidable task, which makes it very difficult to deduce reliably results for large particles from only DLS. In such systems, the electro-optical methods[854-856] are more accurate for measurement of $\Theta$.

If a homodyne method is used, the measured autocorrelation function $g^{(2)}(q,\tau)$ can be interpreted by using the Siegert relation, Equation 454. The translational and rotational diffusion coefficients for several specific shapes of the particles are given in Table 9. The respective power spectrum functions can be calculated by using the Fourier transform, Equation 449b.

#### 5.9.2.4 Effect of the Particle Interactions

The diffusion coefficient of the particles in suspension depends on concentration of particles due to the interparticle interactions.[913-917] Furthermore, one should distinguish the self-diffusion (or tracer diffusion) coefficient, $D_S$, from the collective diffusion (or mutual diffusion) coefficient, $D_C$. The self-diffusion coefficient accounts for the motion of a given particle and can be formally defined as an autocorrelation function of the particle velocity:[880,913]

$$D_S = \frac{1}{3}\int_0^\infty \langle \mathbf{V}(0).\mathbf{V}(\tau)\rangle \, d\tau \tag{467}$$

where the brackets denote the averaging over the stochastic particle motion. The mean-square displacement, $\langle \Delta r^2(t)\rangle$, of a given particle is given by:[913]

$$\left\langle \Delta r^2(t)\right\rangle = 6D_S t; \quad \text{for} \quad t >> \tau_{Br} \equiv M / 6\pi\eta R_h \tag{468}$$

where $\tau_{Br}$ is the characteristic time of the Brownian motion of a particle of mass $M$ and hydrodynamic radius, $R_h$. The collective diffusion coefficient is a collective property of the suspension and characterizes the evolution of small concentration gradients in the linear approximation (Fick's low):[913]

$$\frac{\partial \rho}{\partial t} = -D_C \Delta\rho \tag{469}$$

Hence, $D_C$ is the quantity determined in conventional, gradient diffusion measurements. For noninteracting particles (very diluted suspension) $D_S = D_C$.

As discussed above, DLS experiment provides the autocorrelation function $g^{(1)}(q,\tau)$ or some other quantity which contains equivalent information ($g^{(2)}(q,\tau)$ or $P(q,\omega)$). Similar to the case of noninteracting particles, one can define an effective diffusion coefficient:

$$D_{EFF}(q,\rho) \equiv K_1 / q^2 \tag{470}$$

where $K_1(q,\rho)$ is the first cumulant of the autocorrelation function. It was shown[913,917] that the low-$q$ limit of $D_{EFF}$ coincides with $D_C$:

$$D_C(\rho) = \lim_{q\to 0}\left[D_{EFF}(q,\rho)\right]; \quad qR_h < 1 \tag{471}$$

while the high-$q$ limit of $D_{EFF}(q,\rho)$ provides the so-called short-time self-diffusion coefficient:[913]

$$D_S^S(\rho) = D_{EFF}(q,\rho); \quad \text{for} \quad qR_h >> 1 \tag{472}$$

More general expressions for $D_{EFF}(q,\rho)$ at intermediate values of $q$ are also available,[894,897,917-922] in terms of the static structure factor, $S(q,\rho)$, and the so-called dynamic structure factor, $F(q,\rho,\tau)$:[913]

$$D_{\mathrm{EFF}}(q,\rho) = -\frac{1}{S(q,\rho)}\lim_{\tau\to 0}\left[\frac{\partial F(q,\rho,\tau)/q^2}{\partial\tau}\right]_{q,\rho} \equiv \frac{H(q,\rho)}{S(q,\rho)} \tag{473}$$

By definition, the dynamic structure factor accounts for the correlations between the positions of the particles at different moments of time:[913]

$$F(q,\rho,\tau) \equiv \frac{1}{N}\sum_{k=1}^{N}\sum_{j=1}^{N}\left\langle \exp\left\{i\mathbf{q}\cdot\left[\mathbf{r}_k(0)-\mathbf{r}_j(\tau)\right]\right\}\right\rangle \tag{474}$$

where $\mathbf{q}$ is the scattering vector, and $\mathbf{r}_k(t)$ is the position of particle $k$ in the moment $t$. Both functions, $F(q,\rho,\tau)$ and $H(q,\rho)$, include contributions from hydrodynamic interactions between the particles. Note that $F(q,\rho,\tau=0) \equiv S(q,\rho)$, while for noninteracting Brownian particles:[892,913]

$$F(q,\tau) = \left\langle \exp\left[-i\mathbf{q}\cdot\Delta\mathbf{r}(\tau)\right]\right\rangle = \exp\left(-q^2 D_0\,\tau\right) \tag{475}$$

where $D_0$ is the diffusion coefficient at negligible interparticle interactions.

An important consequence of Equations 471, 473, 474, and 421 can be derived at the low-$q$ limit:[913]

$$D_C(\rho) = \frac{(\partial\Pi/\partial\rho)}{f(\rho)} \tag{476}$$

where $(\partial\Pi/\partial\rho)$ is the osmotic compressibility, and $f(\rho)=H^{-1}(q=0,\rho)$ is the friction (drag) coefficient of the particles in the suspension. Equation 476 represents the generalized Stokes-Einstein relation. Equations 471 and 472 show that one can determine (at least in principle) $D_C(\rho)$ and $D_S^S(\rho)$ by measuring the first cumulant, $K_1(q,\rho)$, at different scattering angles. On the other hand, $D_S$ and $D_C$ can be calculated in numerical experiments performed by Monte Carlo or Brownian dynamics methods.[923,924]

As shown by Batchelor[914] and Felderhof,[916] to the first order in the volume fraction, $\phi$, the diffusion coefficients, $D_C$ and $D_S^S$, can be presented as:

$$D_{\mathrm{C}} = D_0\left[1+\lambda_{\mathrm{C}}\Phi\right] \tag{477}$$

$$D_{\mathrm{S}}^{\mathrm{S}} = D_0\left[1+\lambda_{\mathrm{A}}\Phi\right] \tag{478}$$

where $D_0$ is the diffusion coefficient at infinite dilution, while $\lambda_C$ and $\lambda_A$ are coefficients which depend on the interparticle interactions (including the hydrodynamic ones).

Felderhof[916] succeeded in presenting $\lambda_C$ as a sum of several terms, each of them being an explicit integral over the pair distribution function, $g(r)$ (see also References 921 and 925):

$$\lambda_C = \lambda_V + \lambda_O + \lambda_A + \lambda_S + \lambda_D \tag{479}$$

$$\lambda_V = 3\int_0^\infty dx[1-g(x)]x^2 \tag{480a}$$

$$\lambda_O = -3\int_0^\infty dx[1-g(x)]x \tag{480b}$$

$$\begin{aligned}\lambda_A = \frac{3}{2}\int_0^\infty dx\Big[&-2.5x^{-4}+2.25x^{-6}+5.3334x^{-8}-61.42x^{-10}\\&-94.24x^{-12}+134.58x^{-14}-248.46x^{-16}\\&-1587.4x^{-18}+727.2x^{-20}+O\left(x^{-22}\right)\Big]g(x)x^2\end{aligned} \tag{480c}$$

$$\begin{aligned}\lambda_S = \int_0^\infty dx\Big[&18.75x^{-7}-7.5x^{-9}-89.39x^{-11}+215.5x^{-13}+843.8x^{-15}\\&+435.9x^{-17}+4164x^{-19}+O\left(x^{-21}\right)\Big]g(x)x^2\end{aligned} \tag{480d}$$

$$\lambda_D = 1 \tag{480e}$$

where $x = r/R$, and $R$ is the particle radius. Comparison of Equation 480a with Equation 425 shows that $\lambda_V$ presents another definition of the second osmotic virial coefficient:

$$\lambda_V = \frac{\beta_2}{V_p} = 2B_2V_p = \frac{2M^2}{N_AV_p}A_2, \tag{481}$$

$\lambda_O$ stems from the far-field (Oseen) hydrodynamic interaction, while $\lambda_A$, $\lambda_S$, and $\lambda_D$ account for the near-field hydrodynamics.[916]

Note that Equations 480a, 480b, and 480e are exact, while in Equations 480c and 480d the terms up to $x^{-20}$ in a series expansion are taken into account. For hard spheres, one can calculate[926] $\lambda_V^{HS} = 8, \lambda_O^{HS} = -6, \lambda_A^{HS} = -1.831, \lambda_S^{HS} = 0.285,$ and $\lambda_C^{HS} = 1.454$. DLS experiments[927] with suspension of sterically stabilized silica particles in organic solvents (used as a model of hard sphere dispersion) gave $\lambda_C^{HS} = 1.4 \pm 0.2$, which is in a good agreement with the theoretical value. A numerical algorithm for calculation of the next terms in the expansions in Equations 480c and 480d was developed,[925] but usually the first several terms (up to $x^{-7}$) are enough to calculate precisely $\lambda_A$ and $\lambda_C$. $\lambda_k$ ($k = V, O, A, S, C$) were calculated for simple functions modeling the pair interaction energy (sticky potential, square-well potential, etc.), and some of the results are shown in Table 11.

**Table 11. Expressions for the Correction Factors, $\lambda_V$, $\lambda_O$, $\lambda_C$ and $\lambda_A$, for Different Types of Interaction Between Spherical Particles.**

| Type of interaction | $\lambda_V$ | $\lambda_O$ | $\lambda_C$ | $\lambda_A$ | Ref. |
|---|---|---|---|---|---|
| 1. Hard spheres<br>$W(r)=\begin{cases}0\ ; & r\ge 2R\\ +\infty; & r<2R\end{cases}$<br>a) non-slip boundary condition<br>b) perfect slip boundary condition | <br><br>+ 8.00<br><br>+ 8.00 | <br><br>- 6.00<br><br>- 4.00 | <br><br>+ 1.454<br><br>+ 3.511 | <br><br>- 1.8315<br>-0.562 | 926 |
| 2. Sticky hard spheres<br>$g(r)=\begin{cases}1; & r>2R\\ 1+\dfrac{R}{6\tau}; & r=2R\\ 0; & r<2R\end{cases}$<br>$\tau$-stickiness parameter | + 8 - (2/$\tau$) | - 6 + (1/$\tau$) | 1.454 - (1.125/$\tau$) | 1.8315-(0.295/$\tau$) | 928 |
| 3. Weakly charged particles<br>$W(r)=\begin{cases}\dfrac{(Ze)^2}{4\pi\varepsilon_0\varepsilon}\dfrac{\exp[\kappa(2R-r)]}{r(1+\kappa R)^2}; & r\ge 2R\\ +\infty; & r<2R\end{cases}$ | $8+\dfrac{Z^2L_B}{R}\dfrac{(1+2\kappa R)}{(1+\kappa R)^2}\dfrac{3}{(\kappa R)^2}$ | $-6-\dfrac{Z^2L_B}{R}\dfrac{1}{(1+\kappa R)^2}\dfrac{3}{\kappa R}$ | $1.45+\dfrac{Z^2L_B}{R}\dfrac{1}{(1+\kappa R)}\dfrac{3}{(\kappa R)^2}$ | $-1.83+\dfrac{Z^2L_B}{R}\dfrac{\exp(2\kappa R)}{(1+\kappa R)^2}\times$<br>$\times\left[\dfrac{15}{6}\mathrm{E}_3(2\kappa R)-\dfrac{27}{18}\mathrm{E}_5(2\kappa R)\right]$ | 929 |

Note: Z is the number of charges per particle, $L_B = e^2/(4\pi\varepsilon_0\varepsilon kT)$ is Bjerrum length, $\mathrm{E}_n(x)\equiv\int_0^\infty \dfrac{e^{-xt}}{t^n}dt$ ($n$ = 1, 2, 3, ...) is integral exponent function.

The important case of charged particles, interacting through electrostatic and van der Waals forces was analyzed by several authors.[922,929-933] It was shown[921,929] that the contribution of the near-field terms ($\lambda_A$, $\lambda_S$, and $\lambda_D$) is negligible for electrostatically repelling particles when the collective diffusivity is concerned. For weakly charged particles (low surface potential and small size), explicit formulae for the coefficients were obtained[929] (see Table 11). For strongly charged particles and in the cases when the van der Waals attraction is operative, one needs numerical procedures to calculate $\lambda_k$.[921,929] This approach allows one to determine the particle charge (or electrical potential) from the measured values of $\lambda_V$ (by SLS) or $\lambda_C$ (by DLS) if the particle size and the ionic strength are known.[929,930]

At low ionic strength ($\kappa R \sim 1$), other effects connected with the finite diffusivity of the small ions in the electrical double layer surrounding the particle are present.[929,934,935] The noninstantaneous diffusion of the small ions (with respect to the Brownian motion of the colloid particle) could lead to detectable reduction of the single particle diffusion coefficient, $D_0$, from the value predicted by the Stokes-Einstein relation, Equation 447. For spherical particles, the relative decrease in the value of $D_0$ is largest at $\kappa R \approx 1$ and could be around 10 to 15 %. As shown in the normal-mode theory,[919] the finite diffusivity of the small ions also affects the concentration dependence of the collective diffusion coefficient of the particles. Belloni et al.[931] obtained an explicit expression for the contribution of the small ions in $\lambda_C$:

$$\Delta\lambda_{\mathrm{SI}} = \frac{Z^2 L_B}{R} \frac{1}{(1+\kappa R)^2} \frac{3}{(\kappa R)^2} \frac{D_0}{D_{\mathrm{SI}}} \tag{482}$$

where $Z$ is the number of charges per particle, $L_B = e^2/(4\pi\varepsilon_0\varepsilon kT)$ is the Bjerrum length, and $D_{\mathrm{SI}}$ is the diffusion coefficient of the small ions. The ratio of $\Delta\lambda_{\mathrm{SI}}$ and the electrostatic part in $\lambda$ (see Table 11):

$$\frac{\Delta\lambda_{\mathrm{SI}}}{\lambda_C^{\mathrm{EL}}} = \frac{1}{(1+\kappa R)} \frac{D_0}{D_{\mathrm{SI}}} \approx \frac{1}{(1+\kappa R)} \frac{R_{\mathrm{SI}}}{R} \tag{483}$$

shows[929] that the relative contribution of the small ions is above 10 % only when the particles are small ($R \leq 4$nm) and at a not very high ionic strength ($\kappa R \sim 1$). This could be the case with protein molecules and charged spherical micelles. Otherwise, the effect of the finite diffusivity of the small ions is negligible in comparison with the effect of the direct particle-particle electrostatic interaction.

#### 5.9.2.5 Concentrated Dispersions: Photon Cross-Correlation Techniques, Fiber Optics DLS, and Diffusing Wave Spectroscopy

A major drawback of the conventional DLS experiment is that the dispersion must be transparent for the light beam. For micrometer-sized particles, this requires concentrations below $10^{-5}$ vol %. Often the concentration of the samples is higher and their dilution for

investigation is not desirable. The autocorrelation function of multiply scattered light is difficult to interpret and to extract subsequent information about the particle size. Several powerful techniques have been proposed aimed at overcoming this problem and extending the application of DLS to more concentrated suspensions.

One obvious way to reduce the contribution of the multiple light scattering is to use a very thin sample cell of an optical path length below 100 μm.[936,937] Alternatively, Phillies[938,939] suggested using a more complex optical system comprising two laser beams and two detectors focussed in the same sample volume and having exactly the same scattering vector (in direction and magnitude). The signals from the two detectors are cross-correlated by using a photon correlator. It has been shown[938-941] that the signals from the two detectors are correlated only for the light that is scattered once (single scattering), whereas the contributions from double and higher-order multiple scattering are uncorrelated. Therefore, when the signals from the two detectors (single + multiple scattering) are cross-correlated, only the signal corresponding to single scattering from the particles gives a contribution into the time dependence of the cross-correlation function. As a result, one obtains a time correlation function from turbid samples, which is similar to those obtained from transparent samples and can be interpreted in the same way. Several other cross-correlation schemes were suggested by Schätzel[941] and some of them have found realization in practice.[941-945] In the two-color dynamic light scattering (TCDLS),[941-944] two laser beams of different colors are used and the angles between the incident beams and the detectors (all in the same plane) are chosen in such a way as to define equal scattering vectors. In the three-dimensional light scattering (3DDLS)[941,945] two incident beams of the same wavelength enter the sample from slightly above and slightly below the average scattering plane. The two detectors are also placed above and below the average scattering plane, respectively, so that the third dimension is used to achieve equal scattering vectors in the 3DDLS method. Both techniques have proven to suppress efficiently the multiple scattering in concentrated latex dispersions (see, e.g., the recent review by Pusey[942]). Furthermore, it was shown[945] that the same cross-correlation techniques can be used to eliminate the multiple scattering in SLS experiments. These techniques can be applied to turbid samples, for which the contribution of the single light scattering is a detectable fraction (> 1%) of the total intensity of the scattered light.

Two different techniques have been developed for studying even more concentrated (opaque) colloidal dispersions. The fiberoptic DLS or fiberoptical quasi-elastic light scattering (FOQELS) was proposed by Tanaka and Benedek[946] and has undergone substantial development during the last years.[947-951] In this method, an optical fiber is applied to guide the incident beam toward the suspension and to collect the scattered light. Since the same fiber is used for particle illumination and for collecting the scattered light, the optical path is the shortest possible, and the contribution of the multiple scattering is enormously reduced. The main problem with the first versions of FOQELS equipment was that the detected signal

presented a superposition of homodyne and heterodyne components, the second being created by the light reflected from the front face of the optical fiber.[952] The relative contribution of the homodyne component increased with the particle concentration and this lead to ambiguity in data interpretation. Several improvements were proposed[953-955] to avoid the detection of this backward reflected light. A schematic of the version developed by Wiese and Horn[954] is shown in Figure 74. The laser beam 1 enters the fiber optic Y-coupler and illuminates the particles through fiber 2, which is submerged in the dispersion. The back-scattered light re-enters optical fiber 2 and through fiber 3 reaches the detector. The front face of the optical fiber is inclined at an angle of 10° with respect to the optical axis, in order to reduce the intensity of the back-reflected beam, which otherwise would act as a local oscillator. With this equipment, very concentrated dispersions (up to 40 %) can be studied.[954] Another type of miniaturized fiber probe, comprising two optical fibers (one for illumination, and the other one for receiving the scattered light), was proposed for *in situ* process control by Dhadwal et al.[955] The use of single-mode fibers (whose core diameter is of the order of the light wavelength) is another innovation which facilitates the data interpretation in FOQELS experiments.[954,955] In the last years, the fiber optic DLS transformed into a useful tool for studying concentrated particle dispersions.

The diffusing wave spectroscopy[956-959] (DWS) is another useful technique for studying the dynamics of opaque dispersions. The key feature of the DWS experiment is the measurement of the autocorrelation function $g^{(2)}(\tau)$ of a light that has undergone multiple scattering. Both configurations, forward scattering and backward scattering, were studied (see Figure 75). To derive a theoretical expression for $g^{(2)}(\tau)$, the transport of light in the concentrated dispersion is considered[958,959] as a diffusion process (this explains the term "diffusion wave spectroscopy"). The path of each photon in the dispersion is modeled by random, multiple scattering from a sequence of particles. The attenuation of the temporal light correlation due to the Brownian motion of the particles is calculated for each light path. The contributions of all paths are then summed up (by using appropriate averaging procedure) to calculate the autocorrelation function. Therefore, it is essential to have many scattering events for each photon before its detection by the photomultiplier. In this multiple scattering regime, the characteristic time is determined by the cumulative effect of many particles and is much shorter, compared to the single scattering regime.[959] Thus, the time scale in this experiment is much faster, and the particle motion is studied over length scales much smaller than $\lambda$. The experimental equipment for DWS is practically the same as that for conventional DLS. The main difficulties with the method arise when the autocorrelation function must be interpreted to extract information about the particle dynamics. The method was applied[959-970] to several complex colloidal systems (liquid-like concentrated dispersions, colloidal crystals, foams, emulsions, particles in porous media and under shear) and many non-trivial results have been obtained.

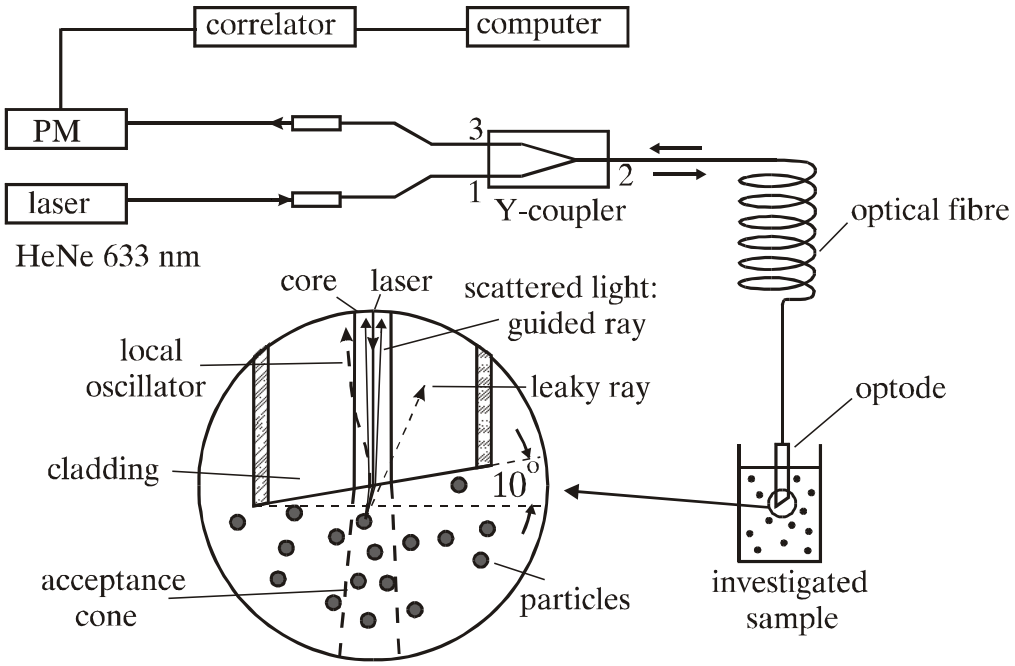


**FIGURE 74.** Schematics of experimental setup for fiber-optic DLS. Laser beam 1 illuminates the particles through the *Y*-coupler and fiber 2, which is submerged in the dispersion. The back-scattered light re-enters fiber 2, and through fiber 3 it reaches the detector. The front face of fiber 2 is cut at 10° with respect to the optical axis (the inset) to reduce the intensity of the back-reflected beam, which otherwise would act as a local oscillator reaching the detector. (Modified from Wiese, H. and Horn, D., *J. Chem. Phys.*, 94, 6429, 1991.)

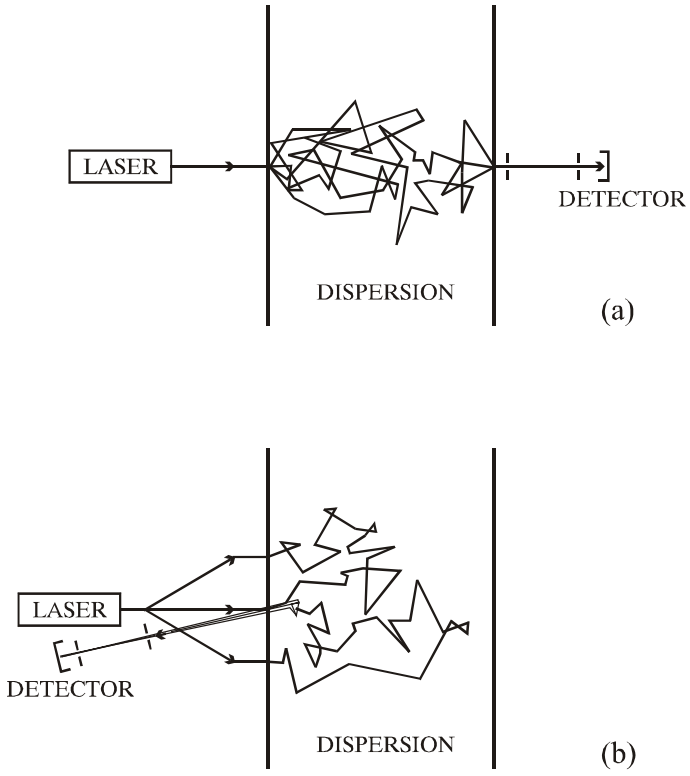


**FIGURE 75.** Diffusion wave spectroscopy (DWS). The light reaches the detector after multiple acts of scattering from dispersed particles. The optical path of the light in the dispersion is modeled as a result of random diffusion motion. Forward (a) or backward (b) scattered light can be analyzed.

### 5.9.3 Application of Light Scattering Methods to Colloidal Systems

The aim of this section is to illustrate the most typical applications of LS methods to dispersions and micellar surfactant solutions.

#### 5.9.3.1 Surfactant Solutions

*5.9.3.1.1 Critical micellar concentration, aggregation number, second virial coefficient*

The application of LS methods for investigating micellar solutions started with the studies of Debye.[971] He showed that from measurements of the turbidity as a function of the surfactant concentration one can determine the critical micellar concentration (CMC), the micellar mass (and the corresponding aggregation number, $\nu_a$), and the second osmotic virial coefficient, $A_2$. For larger micelles, additional information about the micellar size and shape was obtained.[972] Later numerous studies have provided valuable information about CMC, $\nu_a$ and $A_2$ for a variety of nonionic and ionic surfactants.[973-978] Currently SLS is a routine method for determination of these quantities. Nevertheless, the information obtained by SLS from micellar solutions must be handled with some care,[979-981] because one of the main assumptions of the SLS theory (i.e., that the properties of the micelles, $\nu_a$ and $A_2$, remain constant with the micellar concentration) was shown to be not entirely fulfilled for these systems. This is particularly important for more concentrated surfactant solutions, where transitions in micellar size and shape may take place.

*5.9.3.1.2 Diffusion coefficient, size, shape, and polydispersity of micelles*

Dynamic light scattering has the advantage that valuable information about the micellar diffusion coefficient,[982] $D$, and hydrodynamic radius, $R_h$, could be obtained at fixed surfactant concentration. Moreover, the effect of intermicellar interactions is less pronounced for the values of $D$ and $R_h$, than the values measured by SLS. The combination of SLS and DLS allows one to determine the size, shape and polydispersity of micelles. Such systematic studies[930,982,983] were performed for sodium dodecylsulfate micelles at large ionic strength (0.15 M to 0.6 M NaCl) and variable temperature (10°C to 85°C) to reveal the transition from small spherical to large rod-shaped micelles. A comparison of $\langle R_g \rangle$ (determined by SLS) with $R_h$ (determined by DLS) was used to verify the rod-like shape of micelles. More refined analyzes[984-986] included the effects of the micellar polydispersity and flexibility of the rod-like micelles. The persistent length of the SDS rods was determined[982] to be ~ 70 nm; of cetylpyridinum bromide rods,[987,988] ~ 25 to 40 nm; of hexadecyltrimethylammonium salicylate,[989] ~ 100 to 150 nm; of sodium dodecyl dioxyethylenesulfate,[990] ~ 165 to 190 nm. Such studies provide data which are used as a test of the thermodynamic theories of the growth of rod-like micelles.[991]

*5.9.3.1.3 Intermicellar interactions*

The concentration dependencies of $R(\theta)$ and $D_{EFF}$ were used[930,992-994] to investigate the interactions between SDS micelles at different electrolyte concentrations. Corti an Degiorgio[930] interpreted the measured values of $A_2$ and $\lambda_C$ by using a model accounting for the electrostatic repulsion and van der Waals attraction between the micelles. In this way, the Hamaker constant and the micellar charge were determined. The assumption that the micelles do not change in size and shape in the studied range of electrolyte concentrations was questioned later by Mazer.[982] Indeed, Corti and Degiorgio[930] and Dorshow et al.[992] needed a rather large value of the Hamaker constant to describe the attraction between the micelles. Several other studies[932,993,994] were directed to determine the micellar charge and its variation with the electrolyte concentration; however; some of them were based on approximated formulae for the electrostatic interaction energy between the micelles, assuming low electrical surface potential. The typical surface potential of SDS micelles is[995] ~ 60 to 70 mV, and more complex and rigorous approaches[921,996] must be used to describe correctly the electrostatic interaction. The accumulated LS data suggests that very often the observed concentration dependencies present a result of the combined action of intermicellar interactions and changes of the micellar size and shape. Mazer[982] concludes that for SDS micelles the intermicellar interactions prevail only at low and moderate electrolyte concentrations (≤ 0.2 *M* NaCl).

A combination of SLS and DLS methods was used[997] to investigate the behavior of nonionic micellar solutions in the vicinity of their cloud point. It had been known for many years that at a high temperature the micellar solutions of polyoxyethylene-alkyl ether surfactants ($C_nEO_m$) separate into two isotropic phases. The solutions become opalescent with the approach of the cloud point, and several different explanations of this phenomenon were proposed. Corti and Degiorgio[997] measured the temperature dependence of $D_{EFF}$ and $\langle I_S \rangle_t$ and found that they can be described as a result of critical phase separation, connected with intermicellar attraction and long-range fluctuations in the local micellar concentration. Far from the cloud point, the micelles of nonionic surfactants with a large number of ethoxy-groups ($m \sim 30$) may behave as hard spheres.[324]

*5.9.3.1.4 Microemulsions*

Microemulsions are another type of system which has been intensively studied by LS methods.[882-887,998-1001] Vrij and co-workers[882,998] used SLS to determine the volume of water-in-oil microemulsion droplets and the second osmotic virial coefficient. Two interesting conclusions from their studies were drawn:[998] (1) the van der Waals forces between the water cores of the droplets (if considered to be nondeformable spheres) are too weak to explain the observed strong attraction, and (2) the minimal distance between the centers of mass of two droplets upon collision is smaller than the droplet diameter. Similar observations were made by other authors and were explained by using several different models. Calje et al.[998] and

Lemaire et al.[999] assumed that the aforementioned effects were due to mutual overlap of the surfactant monolayers covering the droplets. Denkov et al.[886] argued that the droplets may deform upon collision and showed that the attraction between deformable droplets is stronger compared to that between hard spheres of the same Hamaker constant. Auvrey[1002] and Fletcher et al.[1003,1004] attributed the observed effects to the coalescence (fusion) of some fraction of the droplets. The droplet fusion also could be connected to the observed[1005,1006] sharp increase of the electric conductivity of water-in-oil microemulsions at a given threshold value of the droplet volume fraction (percolation model) and to the observed[1007] exchange of water-soluble fluorescent probes between droplets. The presence of droplet aggregates was demonstrated[1008, 1009] by electro-optic birefringence, and their lifetime was estimated in some cases. Although a number of other experimental methods were invoked to analyze the structure and dynamics of microemulsions, the nature of the interdroplet interactions is by no means well understood.[887] A critical behavior of microemulsions was observed[1010] at certain conditions.

LS methods (often in combination with other experimental methods) are widely used for the investigation of complex surfactant systems such as mixed micelles,[1011,1012] block copolymer micelles,[1013,1014] iridescent lamellar phases,[1015,1016] complexes between micelles and polymers,[1017-1020] aggregates of biosurfactants[1021-1023] (micelles and vesicles), and many others.

The scattering of light from interfaces[1024, 1025] and thin liquid films[1026,1027] provides other possibilities for studying surfactant systems. LS from interfaces covered with surfactant monolayers allowed investigation of the interfacial tension and of the rheological properties of the monolayers. Such measurements were successfully applied[1024] for measurement of ultra-low interfacial tension, as well as the bending constant of surfactant monolayers in microemulsion systems. SLS and DLS from liquid films were used[1026,1027] for measurement of the interaction forces between the film surfaces as a function of the film thickness.

### 5.9.3.2 Dispersions

#### *5.9.3.2.1 Size, shape, and polydispersity of particles*

The classical application of SLS to dispersions is for determination of the particle size, shape and polydispersity.[847,848] Earlier studies were restricted to diluted samples of noninteracting particles with size comparable to the light wavelength. Substantial progress has been achieved during the last decades in the application of LS methods to more difficult samples. The invention of DLS allowed the precise determination of particle size in the nanometer range. On the other side, the application of the laser diffraction method[877,1028] extended the upper limit of measurable particle size up to several hundred micrometers. A variety of theoretical procedures has been proposed[903-911] to solve the inverse scattering problem and to determine

more reliably the particle size distribution from LS data. Several theoretical approaches were developed to handle data from SLS[1029-1031] and DLS[956-961,1032] experiments on concentrated samples, where the multiple scattering is substantial. Alternatively, the cross-correlation techniques[938-945] and fiber optic probes were applied[948-955] to avoid the multiple scattering in concentrated suspensions. A new types of theories, based on extensive computer calculations, emerged in 1970s for description of the light scattering from large arbitrary shaped particles - the extended boundary condition method[1033,1034] (EBCM) and the coupled dipole method[1035, 1036] (CDM). All these new directions are rapidly developing and they substantially enlarge the area of application of LS methods.

*5.9.3.2.2 Static and dynamic structure factors*

Static and dynamics LS experiments have played a very important role for a deeper understanding of the structure and dynamics of suspensions containing strongly interacting particles.[913,1037-1051] A number of theoretical approaches, based on modern statistical theories, were proposed for calculation of the static and dynamic structure factors of monodisperse[913,922,917-919] and polydisperse suspensions.[1052-1054] The hydrodynamic and electrostatic interactions between charged particles have been subjects of particular interest. The experimentally attainable quantities, such as pair distribution function and effective diffusion coefficients, were used as test probes for the rapidly developing theories. The importance of different factors (particle and electrolyte concentrations, particle charge, etc.) for the phase transitions in suspensions have been systematically investigated. The liquid-like and colloidal crystal states were found to have distinct features, which can be quantitatively studied by LS experiments. An excellent review of this topic is given by Pusey and Tough.[913]

The kinetics of crystallization of colloidal suspensions at high particle concentration and/or low ionic strength is another phenomenon which has been the subject of intensive experimental studies.[1045-1051,1055,1056] The time scale of the crystallization process in suspensions is much slower (compared to that in atomic liquids), which makes it available for direct measurement by LS methods. The induction time, the crystallization rate, and the structure and size distribution of the growing crystallites have been studied as functions of different factors. The structure of the colloid crystals is conventionally studied by Bragg-diffraction[1039,1045] or Kossel lines analysis.[1047-1049]

Substantial interest has been raised the problem of the structure and dynamics of suspensions in shear hydrodynamic fields.[1057-1065] The experiments showed that both shear-induced melting and shear-induced ordering can be observed at different particle volume fractions and shear rates. The nonequilibrium microstructure of the suspension under shear can be investigated in these experiments and compared with the predictions from analytical theories and computer simulations.

*5.9.3.2.3 Kinetics of coagulation and structure of the formed aggregates*

During the last decade, a substantial progress has been achieved in our understanding of coagulation phenomenon (see also Section 5.6). Light scattering, electron microscopy, and other experimental methods,[1066,1067] in combination with extensive numerical experiments and theoretical work,[1068-1070] revealed that the aggregates formed upon the coagulation of colloidal particles have a fractal-type structure,[1071] i.e., they exhibit size-scale invariance. The fractal dimension of the aggregates (which is a measure of their compactness) depends on the specific regime of aggregation. Two limiting regimes of colloid aggregation can be distinguished: diffusion-limited aggregation (DLA), which corresponds to barrierless (rapid) coagulation, and reaction-limited aggregation (RLA), in which the repulsive barrier in the pair interaction energy is around several $kT$ (slow coagulation). In DLA, the coagulation rate is limited solely by the time between the collisions of the particles due to the diffusion. In RLA, a large number of collisions is required before two particles can stick together, which leads to much slower aggregation rate. Computer simulations and analytical theories[1072] predict that for DLA the clusters formed have a fractal dimension $d_f \approx 1.8$ and the average mass of the aggregates must be a linear function of time,[1073] $\langle M \rangle \propto t$ (see, e.g., Equation 328). In contrast, for RLA[1074,1075] $d_f \approx 2.1$ and $\langle M \rangle \propto \exp(k_a t)$,[1076] where the aggregation constant $k_a$ depends on the sticking probability and the time between collisions. The size distribution of the formed aggregates is also different in the two regimes.[1077] All these theoretical predictions were verified[1078-1080] by SLS and DLS methods on colloid particles of different material (silica, polystyrene, gold, hematite). The results about the size distribution of the aggregates were scaled[1078] on a single master curve, whose shape was found to be independent of the regime of aggregation and the material of the particles. The fractal approach and the light scattering techniques have found also a wide application for analysis of the protein aggregation and the early stages of protein crystallization.[1081-1085]

## ACKNOWLEDGMENT

The authors are indebted to Miss M. Paraskova for typing the text and drawing the figures.

## REFERENCES


1. Jungermann, E., *Cationic Surfactants,* Marcel Dekker, New York, 1970.
2. Lucassen-Reynders, E.H., *Anionic Surfactants – Physical Chemistry of Surfactant Action*, Marcel Dekker, New York, 1981.
3. Schick, M.J., *Nonionic Surfactants: Physical Chemistry,* Marcel Dekker, New York, 1986.
4. Gibbs, J.W., *The Scientific Papers of J.W. Gibbs*, Vol. 1, Dover, New York, 1961.
5. Ono, S. and Kondo, S., Molecular theory of surface tension in liquids, in *Handbuch der Physik,* Vol. 10, Flügge, S., Ed., Springer, Berlin, 1960.
6. Adamson, A.W. and Gast, A.P. *Physical Chemistry of Surfaces*; Sixth Edition, Wiley, New York, 1997.
7. Freundlich, H., *Colloid and Capillary Chemistry*, Methuen, London, 1926.
8. Langmuir, I., *J. Amer. Chem. Soc.,* 40, 1361, 1918.
9. Volmer, M., *Z. Physikal. Chem.,* 115, 253, 1925.
10. Frumkin, A., *Z. Physikal. Chem.,* 116, 466, 1925.
11. Hill, T.L., *An Introduction to Statistical Thermodynamics*, Addison-Wesley, Reading, MA, 1962.
12. Lucassen-Reynders, E.H., *J. Phys. Chem*., 70, 1777, 1966.
13. Borwankar, R.P. and Wasan, D.T., *Chem. Eng. Sci.,* 43, 1323, 1988.
14. Derjaguin, B.V., *Theory of Stability of Colloids and Thin Liquid Films,* Plenum Press, Consultants Bureau, New York, 1989.
15. Shchukin, E.D., Pertsov, A.V., and Amelina, E.A., *Colloid Chemistry*, Moscow Univ. Press, Moscow, 1982 (Russian); Elsevier, 2001 (English).
16. Zeldowitch, J., *Acta Physicochim. (USSR)*, 1, 961, 1934.
17. Halsey, G. and Taylor, H.S., *J. Chem. Phys.,* 15, 624, 1947.
18. Gurkov, T.G., Kralchevsky, P.A., and Nagayama, K., *Colloid Polym. Sci.,* 274, 227, 1996.
19. Butler, J.A.V., *Proc. Roy. Soc. Ser. A,* 135, 348, 1932.
20. Fainerman, V.B. and Miller, R., *Langmuir*, 12, 6011, 1996.
21. Vaughn, M.W. and Slattery, J. C., *J. Colloid Interface Sci.,* 195, 1, 1997.
22. Makievski, A.V., Fainerman, V.B., Bree, M., Wüstneck, R., Krägel, J., and Miller, R., *J. Phys. Chem. B,* 102, 417, 1998.
23. Landau, L.D. and Lifshitz, E.M., *Statistical Physics,* Part 1, Pergamon, Oxford, 1980.
24. Hachisu, S., *J. Colloid Interface Sci.,* 33, 445, 1970.
25. Kalinin, V.V. and Radke, C.J., *Colloids Surf. A,* 114, 337, 1996.
26. Warszyński, P., Barzyk, W., Lunkenheimer, K., and Fruhner, H., *J. Chys Chem.*, *B,* 102, 10948, 1998.

27. Kralchevsky, P.A., Danov, K.D., Broze, G., and Mehreteab, A., *Langmuir,* 15, 2351, 1999.

28. Prosser, A.J. and Frances, E.I., *Colloids Surf. A,* 178, 1, 2001.

29. Kirkwood, J.G. and Oppenheim, I., *Chemical Thermodynamics*, McGraw-Hill, New York, 1961.

30. Robinson, R.A. and Stokes, R.H., *Electrolyte Solutions,* Butterworths, London, 1959.

31. Gouy, G., *J. Phys. Radium,* 9, 457, 1910.

32. Davies, J. and Rideal, E., *Interfacial Phenomena,* Academic Press, New York, 1963.

33. Grahame, D.C., *Chem. Rev.,* 41, 441, 1947.

34. Israelachvili, J.N., *Intermolecular and Surface Forces*, Academic Press, London, 1992.

35. Kralchevsky, P.A. and Nagayama, K., *Particles at Fluid Interfaces and Membranes*, Elsevier, Amsterdam, 2001.

36. Matijevič, E. and Pethica, B.A., *Trans. Faraday Soc.,* 54, 1382, 1958.

37. van Voorst Vader, F., *Trans. Faraday Soc.*, 56, 1067, 1960.

38. Tajima, K., *Bul. Chem. Soc. Jpn,* 44, 1767, 1971.

39. Stern, O., *Ztschr. Elektrochem.,* 30, 508, 1924.

40. Tajima, K., Muramatsu, M., and Sasaki, T., *Bul. Chem. Soc. Jpn*, 43, 1991, 1970.

41. Tajima, K., *Bul. Chem. Soc. Jpn*, 43, 3063, 1970.

42. Danov, K.D., Kolev, V.L, Kralchevsky, P.A., Broze, G., and Mehreteab, A., manuscript in preparation.

43. Cross, A.W. and Jayson, G.G., *J. Colloid Interface Sci.*, 162, 45, 1994.

44. Johnson, S.B., Drummond, C.J., Scales, P.J., and Nishimura, S., *Langmuir,* 11, 2367, 1995.

45. Alargova, R.G., Danov, K.D., Petkov, J.T., Kralchevsky, P.A., Broze, G., and Mehreteab, A., *Langmuir,* 13, 5544, 1997.

46. Rathman, J.F. and Scamehorn, J.F., *J. Phys. Chem.*, 88, 5807, 1984.

47. Berr, S.S., Coleman, M.J., Marriot, J., and Johnson Jr., J.S., *J. Phys. Chem*., 90, 6492, 1986.

48. Rosen, M.J., *Surfactants and Interfacial Phenomena*, Wiley, New York, 1989.

49. Clint, J., *Surfactant Aggregation*, Chapman & Hall, London, 1992.

50. Alargova, R.G., Danov, K.D., Kralchevsky, P.A., Broze, G., and Mehreteab, A., *Langmuir,* 14, 4036, 1998.

51. Dimov, N.K., Kolev, V.L., Kralchevsky, P.A., Lyutov, L.G., Brose, G., and Mehreteab, A., *J. Colloid Interface Sci*., 256, 23 (2002).

52. Valkovska, D.S., Danov, K.D., and Ivanov, I.B., *Colloids Surf. A,* 175, 179, 2000.

53. Danov, K.D., Kralchevsky, P.A., and Ivanov, I.B., in *Encyclopedic Handbook of Emulsion Technology*, Sjöblom, J., Ed., Marcel Dekker, New York, 2001, chap. 26.

54. Dukhin, S.S., Kretzschmar, G., and Miller, R., *Dynamics of Adsorption at Liquid Interfaces*, Elsevier, Amsterdam, 1995.

55. Eastoe, J. and Dalton, J.S., *Adv. Colloid Interface Sci.,* 85, 103, 2000.

56. Lord Rayleigh, *Proc. Roy. Soc. (Lond.)*, 29, 71, 1879.

57. N. Bohr, *Phil. Trans. Roy. Soc. (Lond.)*, *A*, 209, 281, 1909.

58. Defay, R. and Pétré, G., Dynamic surface tension, in *Surface and Colloid Science,* Vol. 3, Matijevič, E., Ed., Wiley, New York, 1971, p. 27.

59. Miller, R. and Kretzschmar, G., *Adv. Colloid Interface Sci*., 37, 97, 1991.

60. Wantke, K.-D., Lunkenheimer, K., and Hempt, C., *J. Colloid Interface Sci.*, 159, 28, 1993.

61. Chang, C.-H. and Franses, E.I., *J. Colloid Interface Sci.*, 164, 107, 1994.

62. Johnson, D.O. and Stebe, K.J., *J. Colloid Interface Sci.*, 182, 525, 1996.

63. Horozov, T. and Arnaudov, L., *J. Colloid Interface Sci.*, 219, 99, 1999.

64. Horozov, T. and Arnaudov, L., *J. Colloid Interface Sci.*, 222, 146, 2000.

65. van den Tempel, M. and Lucassen-Reynders, E.H., *Adv. Colloid Interface Sci.*, 18, 281, 1983.

66. Langevin, D., *Colloids Surf.*, 43, 121, 1990.

67. Lemaire, C. and Langevin, D., *Colloids Surf.*, 65, 101, 1992.

68. Grigorev, D.O., Krotov, V.V., and Noskov, B.A., *Colloid J.*, 56, 562, 1994.

69. Mysels, K.J., *Colloids Surf.*, 43, 241, 1990.

70. Kralchevsky, P.A., Radkov, Y.S., and Denkov, N.D., *J. Colloid Interface Sci.*, 161, 361, 1993.

71. Fainerman, V.B., Miller, R., and Joos, P., *Colloid Polym. Sci.*, 272, 731, 1994.

72. Fainerman, V.B. and Miller, R., *J. Colloid Interface Sci.*, 176, 118, 1995.

73. Horozov, T.S., Dushkin, C.D., Danov, K.D., Arnaudov, L.N., Velev, O.D., Mehreteab, A., and Broze, G., *Colloids Surf. A*, 113, 117, 1996.

74. Mishchuk, N.A., Dukhin, S.S., Fainerman, V.B., Kovalchuk, V.I., and Miller, R., *Colloids Surf. A*, 192, 157, 2001.

75. van den Bogaert, R. and Joos, P., *J. Phys. Chem.*, 83, 17, 1979.

76. Möbius, D. and Miller R., Eds., *Drops and Bubbles in Interfacial Research*, Elsevier, Amsterdam, 1998.

77. Jho, C. and Burke, R., *J. Colloid Interface Sci.*, 95, 61, 1983.

78. Joos, P. and van Hunsel, J., *Colloid Polym. Sci.* 267, 1026, 1989.

79. Fainerman, V.B. and Miller, R., *Colloids Surf. A*, 97, 255, 1995.

80. Miller, R., Bree, M., and Fainerman, V.B., *Colloids Surf. A,* 142, 237, 1998.

81. Senkel, O., Miller, R., and Fainerman, V.B., *Colloids Surf. A*, 143, 517, 1998.

82. Bain, C.D., Manning-Benson, S., and Darton, R.C., *J. Colloid Interface Sci.,* 229, 247, 2000.

83. Rotenberg, Y., Boruvka, L., and Neumann, A.W., *J. Colloid Interface Sci.,* 37, 169, 1983.

84. Makievski, A.V., Loglio, G., Krägel, J., Miller, R., Fainerman, V.B., and Neumann, A.W., *J. Phys. Chem.,* 103, 9557, 1999.

85. Joos, P., *Dynamic Surface Phenomena,* VSP BV, AH Zeist, The Netherlands, 1999.

86. Ward, A.F.H. and Tordai, L., *J. Chem. Phys.*, 14, 453, 1946.

87. Miller, R., *Colloid Polym. Sci.*, 259, 375, 1981.

88. McCoy, B.J., *Colloid Polym. Sci.*, 261, 535, 1983.

89. Hansen, R.S., *J. Chem Phys.,* 64, 637, 1960.

90. Filippov, L.K., *J. Colloid Interface Sci.*, 164, 471, 1994.

91. Daniel, R. and Berg, J.C., *J. Colloid Intrface Sci.,* 237, 294, 2001.

92. Sutherland, K.L., *Austr. J. Sci. Res.*, A5, 683, 1952.

93. Abramowitz, M. and Stegun, I.A., *Handbook of Mathematical Functions,* Dover, New York, 1965.

94. Korn, G.A. and Korn, T.M., *Mathematical Handbook*, McGraw-Hill, New York, 1968.

95. Danov, K.D., Kolev, V.L., Kralchevsky, P.A., Broze, G., and Mehreteab, A., *Langmuir,* 16, 2942, 2000.

96. Dukhin, S.S., Miller, R., and Kretzschmar, G., *Colloid Polym. Sci.*, 261, 335, 1983.

97. Dukhin, S.S. and Miller, R., *Colloid Polym. Sci.,* 272, 548, 1994.

98. MacLeod, C. and Radke, C.J., *Langmuir,* 10, 3555, 1994.

99. Vlahovska, P.M., Danov, K.D., Mehreteab, A., and Broze, G., *J. Colloid Interface Sci.*, 192, 194, 1997.

100. Danov, K.D., Vlahovska, P.M., Kralchevsky, P.A., Broze, G., and Mehreteab, A., *Colloids Surf. A*, 156, 389, 1999.

101. Diamant, H. and Andelman, D., *J. Phys. Chem.,* 100, 13732, 1996.

102. Diamant, H., Ariel, G., and Andelman, D., *Colloids Surf. A,* 183-185, 259, 2001.

103. Nayfeh, A.H., *Perturbation Methods*, Wiley, New York, 1973.

104. Danov, K.D., Kolev, V.L., Arnaudov, L.N., Kralchevsky, P.A., Broze, G., and Mehreteab, A., manuscript in preparation.

105. Durbut, P., Surface Activity, in *Handbook of Detergents,* Part A, Broze, G., Ed., Marcel Dekker, New York, 1999, chap. 3.

106. Bond, W.N. and Puls, H.O., *Phil. Mag.*, 24, 864, 1937.

107. Doss, K.S.G., *Koll. Z.*, 84, 138, 1938.

108. Blair, C.M., *J. Chem. Phys.*, 16, 113, 1948.

109. Ward, A.F.H., *Surface Chemistry*, London, 1949.

110. Dervichian, D.G., *Koll. Z.*, 146, 96, 1956.

111. Hansen, R.S. and Wallace, T., *J. Phys. Chem.*, 63, 1085, 1959.

112. Baret, J.F., *J. Phys. Chem.*, 72, 2755, 1968.

113. Baret, J.F., *J. Chem. Phys.*, 65, 895, 1968.

114. Baret, J.F., *J. Colloid Interface Sci.*, 30, 1, 1969.

115. Borwankar, R.P. and Wasan, D.T., *Chem. Eng. Sci.*, 38, 1637, 1983.

116. Dong, C., Hsu, C.-T., Chin, C.-Y., and Lin, S.-Y., *Langmuir,* 16, 4573, 2000.

117. Laplace, P.S., *Traité de mécanique céleste*; Suppléments au Livre X, 1805, 1806.

118. Bakker, G., Kapillatytät und oberflächenspannung, in *Handbuch der Experimentalphysik,* Band 6, Akademische Verlagsgesellschaft, Leipzig, 1928.

119. Princen, H.M., The equilibrium shape of interfaces, drops, and bubbles, in *Surface and Colloid Science*, Vol. 2, Matijevic, E., Ed., Wiley, New York, 1969, p. 1.

120. Finn, R., *Equilibrium Capillary Surfaces*, Springer-Verlag, New York, 1986.

121. Weatherburn, C.E., *Differential Geometry in Three Dimensions*, Cambridge, 1930.

122. McConnell, A.J., *Application of Tensor Analysis,* Dover, New York, 1957.

123. Young, T., *Philos. Trans. Roy. Soc. Lond.*, 95, 55, 1805.

124. Jonson, R.E. and Dettre, Wettability and contact angles, in *Surface and Colloid Science,* Vol. 2, Matijevic, E., Ed., Wiley, New York, 1969, p. 85.

125. Starov, V.M., *Adv. Colloid Interface Sci.*, 39, 147, 1992.

126. Neumann, F., *Vorlesungen über die Theorie der Capillarität,* B.G. Teubner, Leipzig, 1894.

127. Ivanov, I.B., Kralchevsky, P.A., and Nikolov, A.D., *J. Colloid Interface Sci.*, 112, 97, 1986.

128. Hartland, S. and Hartley, R.W., *Axisymmetric Fluid-Liquid Interfaces,* Elsevier, Amsterdam, 1976.

129. Kralchevsky, P.A., Eriksson, J.C., and Ljunggren, S., *Adv. Colloid Interface Sci.*, 48, 19, 1994.

130. Tachev, K.D., Angarska, J.K., Danov, K.D., and Kralchevsky, P.A., *Colloids Surf. B*, 19, 61, 2000.

131. Meunier, J. and Lee, L.T., *Langmuir*, 7, 1855, 1991.

132. Dan, N., Pincus, P., and Safran, S.A., *Langmuir*, 9, 2768, 1993.

133. Kralchevsky, P.A., Paunov, V.N. Denkov, N.D., and Nagayama, K., *J. Chem. Soc. Faraday Trans.*, 91, 3415, 1995.

134. Petsev, D.N., Denkov, N.D., and Kralchevsky, P.A., *J. Colloid Interface Sci.*, 176, 201, 1995.

135. De Gennes, P.G. and Taupin, C., *J. Phys. Chem.*, 86, 2294, 1982.

136. Concus, P., *J. Fluid Mech.*, 34, 481, 1968.

137. Kralchevsky, P.A., Ivanov, I.B., and Nikolov, A.D., *J. Colloid Interface Sci.*, 112, 108, 1986.

138. Abramowitz, M. and Stegun, I.A., *Handbook of Mathematical Functions,* Dover, New York, 1965.

139. Jahnke, E., Emde, F., and Lösch, F., *Tables of Higher Functions,* McGraw-Hill, New York, 1960.

140. Lo, L.L., *J. Fluid Mech.*, 132, 65, 1983.

141. Derjaguin, B.V., *Dokl. Akad. Nauk USSR*, 51, 517, 1946.

142. Scheludko, A., *Proc. Koninkl. Nederl. Akad. Wet*., B65, 87, 1962.

143. Scheludko, A., *Adv. Colloid Interface Sci.*, 1, 391, 1967.

144. Dimitrov, A.S., Kralchevsky, P.A., Nikolov, A.D., and Wasan, D.T., *Colloids Surf.*, 47, 299, 1990.

145. J. Plateau, Experimental and theoretical researches on the figures of equilibrium of a liquid mass withdrawn from the action of gravity, in *The Annual Report of the Smithsonian Institution*, Washington D.C., 1863; pp. 207-285.

146. J. Plateau, The figures of equilibrium of a liquid mass, in *The Annual Report of the Smithsonian Institution*, Washington D.C., 1864; pp. 338-369.

147. J. Plateau, *Statique Expérimentale et Théoretique des Liquides Soumis aux Seules Forces Moléculaires*, Gauthier-Villars, Paris, 1873.

148. Zettlemoyer, A.C., *Nucleation,* Marcel Dekker, New York, 1969.

149. Abraham, E.F., *Homogeneous Nucleation Theory,* Academic Press, New York, 1974.

150. Thomson, W. (Lord Kelvin), *Proc. Roy. Soc.*, 9, 225, 1858; *Phil.Mag.*, 17, 61, 1859.

151. Lupis, C.H.P. *Chemical Thermodynamics of Matherials,* North-Holland, New York, 1983.

152. Lifshitz, I.M. and Slyozov, V.V., *Zh. Exp. Teor. Fiz.*, 35, 479, 1958 (in Russian).

153. Wagner, C., *Z. Electrochem.*, 35, 581, 1961.

154. Kalhweit, M., *Faraday Discuss. Chem. Soc.*, 61, 48, 1976.

155. Parbhakar, K., Lewandowski, J., and Dao, L.H., *J. Colloid Interface Sci.*, 174, 142, 1995.

156. Kabalnov, A.S., Pertzov, A.V., and Shchukin, E.D., *Colloids Surf.*, 24, 19, 1987.

157. Kabalnov, A.S. and Shchukin, E.D., *Adv. Colloid Interface Sci.*, 38, 69, 1992.

158. McClements, D.J., Dungan, S.R., German, J.B., and Kinsela, J.E., *Food Hydrocolloids*, 6, 415, 1992.

159. Weiss, J., Coupland, J.N., and McClements, D.J., *J. Phys. Chem*., 100, 1066, 1996.

160. Weiss, J., Canceliere, C., and McClements, D.J., *Langmuir*, 16, 6833, 2000.

161. Kabalnov, A.S., *Langmuir,* 10, 680, 1994.

162. Ivanov, I.B. and Kralchevsky, P.A., Mechanics and thermodynamics of curved thin liquid films, in *Thin Liquid Films,* Ivanov, I.B., Ed., Marcel Dekker, New York, 1988, p. 49.

163. Kralchevsky, P.A. and Ivanov, I.B., *J. Colloid Interface Sci.*, 137, 234, 1990.

164. Kralchevsky, P.A., Danov, K.D., and Ivanov, I.B., Thin liquid film physics, in *Foams: Theory, Measurements and Applications*, Prud'homme, R.K., Ed.; Marcel Dekker, New York, 1995, p. 1.

165. Rusanov, A.I., *Phase Equilibria and Surface Phenomena*, Khimia, Leningrad, 1967 (Russian); *Phasengleichgewichte und Grenzflächenerscheinungen,* Akademie Verlag, Berlin, 1978 (German).

166. Derjaguin, B.V. and Kussakov, M.M., *Acta Physicochem. USSR,* 10, 153, 1939.

167. Exerowa, D. and Scheludko, A., *Bull. Inst. Chim. Phys. Bulg. Acad. Sci.*, 4, 175, 1964.

168. Mysels, K.J., *J. Phys. Chem.*, 68, 3441, 1964.

169. Exerowa, D., *Commun. Dept. Chem. Bulg. Acad. Sci.*, 11, 739, 1978.

170. Kruglyakov, P.M., Equilibrium properties of free films and stability of foams and emulsions, in *Thin Liquid Films,* Ivanov, I.B., Ed., Marcel Dekker, New York, 1988, p. 767.

171. Martynov, G.A. and Derjaguin, B.V., *Kolloidn. Zh.*, 24, 480, 1962.

172. Toshev, B.V. and Ivanov, I.B., *Colloid Polym. Sci.*, 253, 558, 1975.

173. Ivanov, I.B. and Toshev, B.V., *Colloid Polym. Sci.*, 253, 593, 1975.

174. Frumkin, A., *Zh. Phys. Khim. USSR*, 12, 337, 1938.

175. de Feijter, J.A., Thermodynamics of thin liquid films, in *Thin Liquid Films,* Ivanov, I.B., Ed., Marcel Dekker, New York, 1988, p. 1.

176. Kralchevsky, P.A. and Ivanov, I.B., *Chem.Phys. Lett.,* 121**,** 111, 1985.

177. Nikolov, A.D., Kralchevsky, P.A., Ivanov, I.B., and Dimitrov, A.S., *AIChE Symposium Ser. 252,* Vol. 82, 82, 1986.

178. de Feijter, J.A. and Vrij, A., *J.Electroanal. Chem.*, 47, 9, 1972.

179. Kralchevsky, P.A. and Ivanov, I.B., *Chem.Phys. Lett.,* 121**,** 116, 1985.

180. Denkov, N.D., Petsev, D.N., and Danov, K.D., *J. Colloid Interface Sci.*, 176, 189, 1995.

181. Derjaguin, B.V., *Acta Physicochim. USSR,* 12, 181, 1940.

182. Princen, H.M. and Mason, S.G., *J. Colloid Sci.*, 20, 156, 1965.

183. Prins, A., *J. Colloid Interface Sci.*, 29, 177, 1969.

184. Clint, J.H., Clunie, J.S., Goodman, J.F., and Tate, J.R., *Nature* (*Lond.*), 223, 291, 1969.

185. Yamanaka, T., *Bull. Chem. Soc. Jap.*, 48, 1755, 1975.

186. Princen, H.M., *J. Phys. Chem.*, 72, 3342, 1968.

187. Princen, H.M. and Frankel, S., *J. Colloid Interface Sci.*, 35, 186, 1971.

188. Scheludko, A., Radoev, B., and Kolarov, T., *Trans. Faraday Soc.*, 64, 2213, 1968.

189. Haydon, D.A. and Taylor, J.L., *Nature (Lond.)*, 217, 739, 1968.

190. Kolarov, T. and Zorin, Z.M., *Kolloidn. Zh.*, 42, 899, 1980.

191. Kruglyakov, P.M. and Rovon, Yu.G., *Physical Chemistry of Black Hydrocarbon Films,* Nauka, Moskow, 1978 (in Russian).

192. Marinova, K.G., Gurkov, T.D., Dimitrova, T.D., Alargova, R.G., and Smith, D., *Langmuir*, 14, 2011, 1998.

193. Françon, M., *Progress in Microscopy,* Pergamon Press, London, 1961.

194. Beyer, H., *Theorie und Praxis der Interferenzmicroscopie,* Academische Verlagessellschaft, Leipzig, 1974.

195. Zorin, Z.M., *Kolloidn. Zh*., 39, 1158, 1977.

196. Zorin, Z., Platikanov, D., Rangelova, N., and Scheludko, A., in *Surface Forces and Liquid Interfaces*, Derjaguin, B.V., Ed., Nauka, Moscow, 1983, p. 200 (in Russian).

197. Nikolov, A.D., Kralchevsky, P.A., and Ivanov, I.B., *J. Colloid Interface Sci.*, 112, 122, 1986.

198. Lobo, L.A., Nikolov, A.D., Dimitrov, A.S., Kralchevsky, P.A., and Wasan, D.T., *Langmuir*, 6, 995, 1990.

199. Dimitrov, A.S., Nikolov, A.D., Kralchevsky, P.A., and Ivanov, I.B., *J. Colloid Interface Sci.*, 151, 462, 1992.

200. Picard, G., Schneider, J.E., and Fendler, J.H., *J. Phys. Chem.*, 94, 510, 1990.

201. Picard, G., Denicourt, N., and Fendler, J.H., *J. Phys. Chem.*, 95, 3705, 1991.

202. Skinner, F.K., Rotenberg, Y., and Neumann, A.W., *J. Colloid Interface Sci.*, 130, 25, 1989.

203. Dimitrov, A.S., Kralchevsky, P.A., Nikolov, A.D., Noshi, H., and Matsumoto, M., *J. Colloid Interface Sci.*, 145, 279, 1991.

204. Hadjiiski, A., Dimova, R., Denkov, N.D., Ivanov, I.B., and Borwankar, R., *Langmuir*, 12, 6665, 1996.

205. Ivanov, I.B., Hadjiiski, A., Denkov, N.D., Gurkov, T.D., Kralchevsky, P.A., and Koyasu, S., *Biophys. J.*, 75, 545, 1998.

206. Nicolson, M.M., *Proc. Camb. Phil. Soc*., 45, 288, 1949.

207. Chan, D.Y.C., Henry, J.D., and White, L.R., *J. Colloid Interface Sci*., 79, 410, 1981.

208. Paunov, V.N., Kralchevsky, P.A., Denkov, N.D., Ivanov, I.B., and Nagayama, K., *J. Colloid Interface Sci*., 157, 100, 1993.

209. Kralchevsky, P.A., Paunov, V.N., Ivanov, I.B., and Nagayama, K., *J. Colloid Interface Sci*., 151, 79, 1992.

210. Kralchevsky, P.A., Paunov, V.N., Denkov, N.D., Ivanov, I.B., and Nagayama, K., *J. Colloid Interface Sci*., 155, 420, 1993.

211. Kralchevsky, P.A. and Nagayama, K., *Langmuir*, 10, 23, 1994.

212. Kralchevsky, P.A. and Nagayama, K., *Adv. Colloid Interface Sci.*, 85, 145, 2000.

213. Denkov, N.D., Velev, O.D., Kralchevsky, P.A., Ivanov, I.B., Nagayama, K., and Yoshimura, H., *Langmuir,* 8, 3183, 1992.

214. Dimitrov, A.S., Dushkin, C.D., Yoshimura, H., and Nagayama, K., *Langmuir,* 10, 432, 1994.

215. Sasaki, M. and Hane, K., *J. Appl. Phys.,* 80, 5427, 1996.

216. Du, H., Chen, P., Liu, F., Meng, F.-D., Li, T.-J., and Tang, X.-Y., *Materials Chem. Phys.*, 51, 277, 1977.

217. Price, W.C., Williams, R.C., and Wyckoff, R.W.G., *Science*, 102, 277, 1945.

218. Cosslett, V.E. and Markham, R., *Nature*, 161, 250, 1948.

219. Horne, R.W. and Pasquali-Ronchetti, I., *J. Ultrastruct. Res.*, 47, 361, 1974.

220. Harris, J.R., *Micron Microscopica Acta*, 22, 341, 1991.

221. Yoshimura, H., Matsumoto, M., Endo, S., and Nagayama, K., *Ultramicroscopy*, 32, 265, 1990.

222. Yamaki, M., Higo, J., and Nagayama, K., *Langmuir*, 11, 2975, 1995.

223. Nagayama, K., *Colloids Surf. A,* 109, 363, 1996.

224. Burmeister, F., Schäfle, C., Keilhofer, B., Bechinger, C., Boneberg, J., and Leiderer, P., *Adv. Mater*., 10, 495, 1998.

225. Xia, Y., Tien, J., Qin, D., and Whitesides, G.M., *Langmuir,* 12, 4033, 1996.

226. Lindström, H., Rensmo, H., Sodergren, S., Solbrand, A., and Lindquist, S.E., *J. Phys. Chem.,* 100, 3084, 1996.

227. Matsushita, S., Miwa, T., and Fujishima, A., *Langmuir,* 13, 2582, 1997.

228. Murray, C.B., Kagan, C.R., and Bawendi, M.G., *Science,* 270, 1335, 1995.

229. Jap, B.K., Zulauf, M., Scheybani, T., Hefti, A., Baumeister, W., Aebi, U., and Engel, A., *Ultramicroscopy*, 46, 45, 1992.

230. De Rossi, D., Ahluwalia, A., and Mulè, M., *IEEE Eng. Med. Biol.*, 13, 103, 1994.

231. Kralchevsky, P.A. and Denkov, N.D., *Current Opinion Colloid Interface Sci*., 6, 383, 2001.

232. Gil, T., Ipsen, J.H., Mouritsen, O.G., Sabra, M.C., Sperotto, M.M., and Zuckermann, M.J., *Biochim. Biophys. Acta*, 1376, 245, 1998.

233. Mansfield, S.L., Gotch, A.J., and Harms, G.S., *J. Phys. Chem.*, *B*, 103, 2262, 1999.

234. Fisher, L.R. and Malloy A.R., *Annu. Rep. Prog. Chem.,* Sect. C, 95, 373, 1999.

235. Kralchevsky, P.A., Paunov, V.N., and Nagayama, K., *J. Fluid Mech.*, 299, 105, 1995.

236. Camoin, C., Roussel, J.F., Faure, R., and Blanc, R., *Europhys. Lett.*, 3, 449, 1987.

237. Velev, O.D., Denkov, N.D., Paunov, V.N., Kralchevsky P.A., and Nagayama, K., *Langmuir*, 9, 3702, 1993.

238. Dushkin, C.D., Kralchevsky, P.A., Yoshimura, H., and Nagayama, K., *Phys. Rev. Lett.*, 75, 3454, 1995.

239. Lucassen, J., *Colloids Surf.*, 65, 131, 1992.

240. Stamou, D., Duschl, C., and Johannsmann, D., *Phys. Rev.*, *E*, 62, 5263, 2000.

241. Kralchevsky, P.A., Denkov, N.D., and Danov, K.D., *Langmuir,* 17, 2001, 7694.

242. Bowden, N., Terfort, A., Carbeck, J., and Whitesides, G.M., *Science*, 276, 233, 1997.

243. Bowden, N., Choi, I.S., Grzybowski, B.A., and Whitesides, G.M., *J. Am. Chem. Soc.*, 121, 5373, 1999.

244. Velikov, K.P., Durst, F., and Velev, O.D. *Langmuir,* 14, 1148, 1998.

245. Sur, J. and Pak, H.K., *J. Korean Phys. Soc.*, 38, 582, 2001.

246. Danov, K.D., Pouligny, B., Angelova, M.I., and Kralchevsky, P.A., in *Studies in Surface Science and Catalysis,* Vol. 132, Iwasawa Y., Oyama N., and Kunieda H., Eds., Elsevier, Amsterdam, 2001; p. 519.

247. Danov, K.D., Pouligny, B., and Kralchevsky, P.A., *Langmuir,* 17, 2001, 6599.

248. Kralchevsky, P.A., Paunov, V.N., Denkov, N.D., and Nagayama, K., *J. Colloid Interface Sci.*, 167, 47, 1994.

249. Velev, O.D., Denkov, N.D., Paunov, V.N., Kralchevsky, P.A., and Nagayama, K., *J. Colloid Interface Sci.*, 167, 66, 1994.

250. Petkov, J.T., Denkov, N.D., Danov, K.D., Velev, O.D., Aust, R., and Durst, F., *J. Colloid Interface Sci.*, 172, 147, 1995.

251. Danov, K.D., Aust, R., Durst, F., and Lange, U., *J. Colloid Interface Sci.,* 175, 36, 1995.

252. Petkov, J.T., Danov, K.D., Denkov, N.D., Aust, R., and Durst, F., *Langmuir,* 12, 2650, 1996.

253. Petkov, J.T., Gurkov, T.D., and Campbell, B.E., *Langmuir,* 17, 4556, 2001.

254. Derjaguin, B.V., Churaev, N.V., and Muller, V.M., *Surface Forces,* Plenum Press: Consultants Bureau, New York, 1987.

255. Derjaguin, B.V., *Kolloid Zeits.*, 69, 155, 1934.

256. Attard, P. and Parker, J.L., *J. Phys. Chem.*, 96, 5086, 1992.

257. Tabor, D. and Winterton, R.H.S., *Nature*, 219, 1120, 1968.

258. Keesom, W.H., *Proc. Amst*., 15, 850, 1913.

259. Debye, P., *Physik*, 2, 178, 1920.

260. London, F., *Z. Physics*, 63, 245, 1930.

261. Hamaker, H.C., *Physics*, 4, 1058, 1937.

262. Usui, S., Sasaki, H., and Hasegawa, F., *Colloids Surf.*, 18, 53, 1986.

263. Lifshitz, E.M., *Soviet Phys. JETP (Engl. Transl.),* 2, 73, 1956.

264. Dzyaloshinskii, I.E., Lifshitz, E.M., and Pitaevskii, L.P., *Adv. Phys.*, 10, 165, 1961.

265. Nir, S. and Vassilieff, C.S., Van der Waals interactions in thin films, in *Thin Liquid Films,* Ivanov, I.B., Ed., Marcel Dekker, New York, 1988, p. 207.

266. Danov, K.D., Petsev, D.N., Denkov, N.D., and Borwankar, R., *J. Chem. Phys.*, 99, 7179, 1993.

267. Casimir, H.R. and Polder, D., *Phys. Rev.*, 73, 360, 1948.

268. Mahanty, J. and Ninham, B.W., *Dispersion Forces,* Academic Press, New York, 1976.

269. Moelwyn-Hughes, E.A., *Physical Chemistry*, Pergamon Press, London, 1961; chap. 21.

270. Langmuir, I., *J. Chem. Phys.*, 6, 873, 1938.

271. Tenchov, B.G. and Brankov, J.G., *J. Colloid Interface Sci.,* 109, 172, 1986.

272. Vassilieff, C.S., Tenchov, B.G., Grigorov, L.S., and Richmond, P., *J. Colloid Interface Sci.*, 93, 8, 1983.

273. Verwey, E.J.W. and Overbeek, J.Th.G., *The Theory of Stability of Liophobic Colloids,* Elsevier, Amsterdam, 1948.

274. Muller, V.M., *Kolloidn. Zh.*, 38, 704, 1976.

275. McCormack, D., Carnie, S.L., and Chan, D.Y.C., *J. Colloid Interface Sci.*, 169, 177, 1995.

276. Hogg, R., Healy, T.W., and Fuerstenau, D.W., *Trans. Faraday Soc.*, 62, 1638, 1966.

277. Usui, S., *J. Colloid Interface Sci.*, 44, 107, 1973.

278. Russel, W.B., Saville, D.A., and Schowalter, W.R., *Colloidal Dispersions,* University Press, Cambridge, 1989.

279. Debye, P. and Hückel, E., *Z. Phys.*, 24, 185, 1923.

280. McCartney, L.N. and Levine, S., *J. Colloid Interface Sci.*, 30, 345, 1969.

281. Derjaguin, B.V. and Landau, L.D., *Acta Physicochim. USSR,* 14, 633, 1941.

282. Efremov, I.F., Periodic colloidal structures, in *Colloid and Surface Science,* Vol. 8, Matijevic, E., Ed., Wiley, New York, 1976, p. 85.

283. Schultze, H., *J. Prakt. Chem.*, 25, 431, 1882.

284. Hardy, W.B., *Proc. Roy. Soc. (Lond.)*, 66, 110, 1900.

285. Guldbrand, L., Jönsson, B., Wennerström, H., and Linse, P., *J. Chem. Phys.,* 80, 2221, 1984.

286. Kjellander, R. and Marčelja, S., *J. Phys. Chem.,* 90, 1230, 1986.

287. Attard, P., Mitchell, D.J., and Ninham, B.W., *J. Chem. Phys.,* 89, 4358, 1988.

288. Kralchevsky, P.A. and Paunov, V.N., *Colloids Surf.,* 64, 245, 1992.

289. Danov, K.D., Kralchevsky, P.A., and Ivanov, I.B., in *Handbook of Detergents, Part A: Properties*, Broze, G., Ed., Marcel Dekker, New York, 1999, p. 303.

290. Marra, J., *J. Phys. Chem.*, 90, 2145, 1986.

291. Marra, J., *Biophys. J.*, 50, 815, 1986.

292. Kjellander, R., Marčelja, S., Pashley, R.M., and Quirk, J.P., *J. Phys. Chem.*, 92, 6489, 1988.

293. Kjellander, R., Marčelja, S., Pashley, R.M., and Quirk, J.P., *J. Chem. Phys.*, 92, 4399, 1990.

294. Khan, A., Jönsson, B., and Wennerström, H., *J. Phys. Chem.,* 89, 5180, 1985.

295. Kohonen, M.M., Karaman, M.E., and Pashley, R.M., *Langmuir*, 16, 5749, 2000.

296. Paunov, V.N. and Kralchevsky, P.A., *Colloids Surf.,* 64, 265, 1992.

297. Tadros, Th.F., Steric interactions in thin liquid films, in *Thin Liquid Films,* Ivanov, I.B., Ed., Marcel Dekker, New York, 1988, p. 331.

298. Patel, S.S. and Tirel, M., *Ann. Rev. Phys. Chem.*, 40, 597, 1989.

299. Ploehn, H.J. and Russel, W.B., *Adv. Chem. Eng.*, 15, 137, 1990.

300. de Gennes, P.G., *Scaling Concepts in Polymer Physics,* Cornell University Press, Ithaca, NY, 1979, chap. 3.

301. Dolan, A.K. and Edwards, S.F., *Proc. Roy. Soc. (Lond.)*, A337, 509, 1974.

302. Dolan, A.K. and Edwards, S.F., *Proc. Roy. Soc. (Lond.)*, A343, 627, 1975.

303. de Gennes, P.G., *C. R. Acad. Sci. (Paris)*, 300, 839, 1985.

304. de Gennes, P.G., *Adv. Colloid Intrface Sci.,* 27, 189, 1987.

305. Alexander, S.J., *Physique*, 38, 983, 1977.

306. Taunton, H.J., Toprakcioglu, C., Fetters, L.J., and Klein, J., *Macromolecules*, 23, 571, 1990.

307. Klein, J. and Luckham, P., *Nature*, 300, 429, 1982; *Macromolecules*, 17, 1041, 1984.

308. Luckham, P.F. and Klein, J., *J. Chem. Soc. Faraday Trans.*, 86, 1363, 1990.

309. Sonntag, H., Ehmka, B., Miller, R., and Knapschinski, L., *Adv. Colloid Interface Sci.*, 16, 381, 1982.

310. Horn, R.G. and Israelachvili, J.N., *Chem. Phys. Lett.*, 71, 192, 1980.

311. Nikolov, A.D., Wasan, D.T., Kralchevsky, P.A., and Ivanov, I.B., Ordered structures in thinning micellar foam and latex films, in *Ordering and Organisation in Ionic Solutions,* Ise N. and Sogami, I., Eds., World Scientific, Singapore, 1988.

312. Nikolov, A.D. and Wasan, D.T., *J. Colloid Interface Sci.*, 133, 1, 1989.

313. Nikolov, A.D., Kralchevsky, P.A., Ivanov, I.B., and Wasan, D.T., *J. Colloid Interface Sci.,* 133, 13, 1989.

314. Nikolov, A.D., Wasan, D.T., Denkov, N.D., Kralchevsky, P.A., and Ivanov, I.B., *Prog. Colloid Polym. Sci.*, 82, 87, 1990.

315. Wasan, D.T., Nikolov, A.D., Kralchevsky, P.A., and Ivanov, I.B., *Colloids Surf.*, 67, 139, 1992.

316. Asakura, S. and Oosawa, F., *J. Chem. Phys.*, 22, 1255, 1954; *J. Polym. Sci.*, 33, 183, 1958.

317. de Hek, H. and Vrij, A., *J. Colloid Interface Sci.*, 84, 409, 1981.

318. Snook, I.K. and van Megen, W., *J. Chem. Phys.*, 72, 2907, 1980.

319. Kjellander, R. and Marčelja, S., *Chem Phys Lett.*, 120, 393, 1985.

320. Tarazona, P. and Vicente, L., *Mol. Phys.*, 56, 557, 1985.

321. Evans, R., and Parry, A.O., *J. Phys. Condens. Matter*, 2, SA15, 1990.

322. Henderson, J.R., *Mol. Phys.*, 59, 89, 1986.

323. Henderson, D., *J. Colloid Interface Sci.*, 121, 486, 1988.

324. Kralchevsky, P.A. and Denkov, N.D. *Chem. Phys. Lett.*, 240, 385, 1995; *Prog. Colloid Polymer Sci.*, 98, 18, 1995.

325. Carnahan, N.F. and Starling, K.E., *J. Chem. Phys.*, 51, 635, 1969.

326. Kjellander, R. and Sarman, S., *Chem. Phys. Lett.*, 149, 102, 1988.

327. Beresford-Smith, B. and Chan, D.Y.C., *Chem. Phys. Lett*., 92, 474, 1982.

328. Richetti, P. and Kékicheff, P., *Phys. Rev. Lett.*, 68, 1951, 1992.

329. Karlström, G., *Chem. Scripta*, 25, 89, 1985.

330. Bondy, C., *Trans. Faraday Soc.*, 35, 1093, 1939.

331. Patel, P.D. and Russel, W.B., *J. Colloid Interface Sci.*, 131, 192, 1989.

332. Aronson, M.P., *Langmuir*, 5, 494, 1989.

333. van Lent, B., Israels, R., Scheutjens, J.M.H.M., and Fleer, G.J., *J. Colloid Interface Sci.*, 137, 380, 1990.

334. Joanny, J.F., Leibler, L., and de Gennes, P.G., *J. Polym. Sci.*, 17, 1073, 1979.

335. Evans, E. and Needham, D., *Macromolecules*, 21, 1822, 1988.

336. Johnnott, E.S., *Phil. Mag.*, 70, 1339, 1906.

337. Perrin, R.E., *Ann. Phys.*, 10, 160, 1918.

338. Bruil, H.G. and Lyklema, J., *Nature*, 233, 19, 1971.

339. Friberg, S., Linden, St.E., and Saito, H., *Nature*, 251, 494, 1974.

340. Keuskamp, J.W. and Lyklema, J., *ACS Symp. Ser.*, 8, 191, 1975.

341. Kruglyakov, P.M., *Kolloidn. Zh.*, 36, 160, 1974.

342. Kruglyakov, P.M. and Rovin, Yu.G., *Physical Chemistry of Black Hydrocarbon Films,* Nauka, Moscow, 1978 [in Russian].

343. Manev, E., Sazdanova, S.V., and Wasan, D.T., *J. Dispersion Sci. Technol.*, 5, 111, 1984.

344. Basheva, E.S., Nikolov, A.D., Kralchevsky, P.A., Ivanov, I.B., and Wasan, D.T., in *Surfactants in Solution,* Vol. 12, Mittal, K.L., and Shah, D.O., Eds., Plenum Press, New York, 1991, p. 467.

345. Bergeron, V. and Radke, C.J., *Langmuir*, 8, 3020, 1992.

346. Kralchevsky, P.A., Nikolov, A.D., Wasan, D.T., and Ivanov, I.B., *Langmuir*, 6, 1180, 1990.

347. Claesson, P.M., Kjellander, R., Stenius, P., and Christenson, H.K., *J. Chem. Soc. Faraday Trans. I,* 82, 2735, 1986.

348. Parker, J.L., Richetti, P., and Kékicheff, P., *Phys. Rev. Lett.*, 68, 1955, 1992.

349. Basheva, E.S., Danov, K.D., and Kralchevsky, P.A., *Langmuir,* 13, 4342, 1997.

350. Dushkin, C.D., Nagayama, K., Miwa, T., and Kralchevsky, P.A., *Langmuir*, 9, 3695, 1993.

351. Pollard, M.L. and Radke, C.J., *J. Chem. Phys.*, 101, 6979, 1994.

352. Chu, X.L., Nikolov, A.D., and Wasan, D.T., *Langmuir*, 10, 4403, 1994.

353. Chu, X.L., Nikolov, A.D., and Wasan, D.T., *J. Chem. Phys.*, 103, 6653, 1995.

354. Stanley, H.E. and Teixeira, J., *J. Chem. Phys.*, 73, 3404, 1980.

355. Israelachvili, J.N. and Adams, G.E., *J. Chem. Soc. Faraday Trans. 1,* 74, 975, 1978.

356. Israelachvili, J.N. and Pashley, R.M., *Nature*, 300, 341, 1982.

357. Pashley, R.M., *J. Colloid Interface Sci.*, 80, 153, 1981.

358. Pashley, R.M., *J. Colloid Interface Sci.*, 83, 531, 1981.

359. Healy, T.W., Homolam, A., James, R.O., and Hunter, R.J., *Faraday Discuss. Chem Soc.*, 65, 156, 1978.

360. Marčelja, S. and Radič, N., *Chem. Phys Lett.*, 42, 129, 1976.

361. Schibi, D. and Ruckenstein, E., *Chem. Phys Lett.*, 95, 435, 1983.

362. Attard, P. and Batchelor, M.T., *Chem. Phys. Lett.*, 149, 206, 1988.

363. Jönsson, B. and Wennerström, H., *J. Chem. Soc. Faraday Trans. 2*, 79, 19, 1983.

364. Leikin, S. and Kornyshev, A.A., *J. Chem. Phys.*, 92**,** 6890, 1990.

365. Israelachvili, J.N. and Wennerström, H., *J. Phys. Chem.*, 96, 520, 1992.

366. Henderson, D. and Lozada-Cassou, M., *J. Colloid Interface Sci.*, 114, 180, 1986; *J. Colloid Interface Sci.*, 162, 508, 1994.

367. Basu, S. and Sharma, M.M., *J. Colloid Interface Sci.*, 165, 355, 1994.

368. Paunov, V.N., Dimova, R.I., Kralchevsky, P.A., Broze, G., and Mehreteab, A., *J. Colloid Interface Sci.,* 182, 239, 1996.

369. Booth, F., *J. Chem. Phys.*, 19, 391, 1951.

370. Bikerman, J.J., *Philos. Mag.*, 33, 384, 1942.

371. Rowlinson, J.S., Development of theories of inhomogeneous fluids, in *Fundamentals of Inhomogeneous Fluids,* Henderson, D., Ed., Marcel Dekker, New York, 1992.

372. Claesson, P., Carmona-Ribeiro, A.M., and Kurihara, K., *J. Phys. Chem.*, 93, 917, 1989.

373. Horn, R.G., Smith, D.T., and Haller, W., *Chem. Phys. Lett.,* 162, 404, 1989.

374. Tchaliovska, S., Herder, P., Pugh, R., Stenius, P., and Eriksson, J.C., *Langmuir*, 6, 1533, 1990.

375. Pashley, R.M., McGuiggan, P.M., Ninham, B.W., and Evans, D.F., *Science*, 229, 1088, 1985.

376. Rabinovich, Y.I. and Derjaguin, B.V., *Colloids Surf.*, 30, 243, 1988.

377. Parker, J.L., Cho, D.L., and Claesson, P.M., *J. Phys. Chem.*, 93, 6121, 1989.

378. Christenson, H.K., Claesson, P.M., Berg, J., and Herder, P.C., *J. Phys. Chem.*, 93, 1472, 1989.

379. Christenson, H.K., Fang, J., Ninham, B.W., and Parker, J.L., *J. Phys. Chem.*, 94, 8004, 1990.

380. Ducker, W.A., Xu, Z., and Israelachvili, J.N., *Langmuir*, 10, 3279, 1994.

381. Eriksson J.C., Ljunggren, S., and Claesson, P.M., *J. Chem. Soc. Faraday Trans. 2,* 85, 163, 1989.

382. Joesten, M.D. and Schaad, L.J., *Hydrogen Bonding,* Marcel Dekker, New York, 1974.

383. Stillinger, F.H. and Ben-Naim, A., *J. Chem. Phys.*, 47, 4431, 1967.

384. Conway, B.E., *Adv. Colloid Interface Sci.*, 8, 91, 1977.

385. Kuzmin, V.L. and Rusanov, A.I., *Kolloidn. Z.*, 39, 455, 1977.

386. Dubrovich, N.A., *Kolloidn. Z.*, 57, 275, 1995.

387. Christenson, H.K. and Claesson, P.M., *Science*, 239, 390, 1988.

388. Parker, J.L., Claesson, P.M., and Attard, P., *J. Phys. Chem.*, 98, 8468, 1994.

389. Carambassis, A., Jonker, L.C., Attard, P., and Rutland, M.W., *Phys. Rev. Lett.*, 80, 5357, 1998.

390. Mahnke, J., Stearnes, J., Hayes, R.A., Fornasiero, D., and Ralston, J., *Phys. Chem. Chem. Phys.*, 1, 2793, 1999.

391. Considine, R.F., Hayes, R.A., and Horn, R.G., *Langmuir*, 15, 1657, 1999.

392. Considine, R.F. and Drummond, C., *Langmuir*, 16, 631, 2000.

393. Attard, P., *Langmuir,* 16, 4455, 2000.

394. Yakubov, G.E., Butt, H.-J., and Vinogradova, O., *J. Phys. Chem. B*, 104, 3407, 2000.

395. Ederth, T., *J. Phys Chem. B*, 104, 9704, 2000.

396. Ishida, N., Sakamoto, M., Miyahara, M., and Higashitani, K., *Langmuir,* 16, 5681, 2000.

397. Ishida, N., Inoue, T., Miyahara, M., and Higashitani, K., *Langmuir,* 16, 6377, 2000.

398. Tanford, C., *The Hydrophobic Effect,* Wiley, New York, 1980.

399. Leckband, D.E., Israelachvili, J.N., Schmitt, F.-J., and Knoll, W., *Science,* 255, 1419, 1992.

400. Helfrich, W., *Z. Naturforsch.*, 33a, 305, 1978.

401. Servuss, R.M. and Helfrich, W., *J. Phys. (France),* 50, 809, 1989.

402. Fernandez-Puente, L., Bivas, I., Mitov, M.D., and Méléard, P., *Europhys. Lett.*, 28, 181, 1994.

403. Safinya, C.R., Roux, D., Smith, G.S., Sinha, S.K., Dimon, P., Clark, N.A., and Bellocq, A.M., *Phys. Rev. Lett.*, 57, 2718, 1986.

404. McIntosh, T.J., Magid, A.D., and Simon, S.A., *Biochemistry*, 28, 7904, 1989.

405. Abillon, O. and Perez, E., *J. Phys. (France),* 51, 2543, 1990.

406. Evans, E.A. and Skalak, R., *Mechanics and Thermodynamics of Biomembranes,* CRC Press, Boca Raton, Florida, 1980.

407. Aniansson, G.A.E., Wall, S.N., Almgren, M., Hoffman, H., Kielmann, I., Ulbricht, W., Zana, R., Lang. J., and Tondre, C., *J. Phys. Chem.*, 80, 905, 1976.

408. Aniansson, G.A.E., *J. Phys. Chem.*, 82, 2805, 1978.

409. Dimitrova, T.D., Leal-Calderon, F., Gurkov, T.D., and Campbell, B., *Langmuir*, 17, 8069, 2001.

410. Bird, R.B., Stewart, W.E., and Lightfoot, E.N., *Transport Phenomena*, Wiley, New York, 1960.

411. Germain, P., *Mécanique des Milieux Continus*, Masson et Cie, Paris, 1962.

412. Batchelor, G.K., *An Introduction of Fluid Mechanics*, Cambridge University Press, London, 1967.

413. Slattery, J.C., *Momentum, Energy, and Mass Transfer in Continua*, R.E. Krieger, Huntington, New York, 1978.

414. Landau, L.D. and Lifshitz, E.M., *Fluid Mechanics*, Pergamon Press, Oxford, 1984.

415. Barnes, H.A., Hutton, J.F., and Walters, K., *An Introduction to Rheology*, Elsevier, Amsterdam, 1989.

416. Walters, K., Overview of macroscopic viscoelastic flow, in *Viscoelasticity and Rheology*, Lodge, A.S., Renardy, M., and Nohel, J.A., Eds., Academic Press, London, 1985, p. 47.

417. Boger, D.V., *Ann. Rev. Fluid Mech.*, 19, 157, 1987.

418. Barnes, H.A., *J. Rheol.*, 33, 329, 1989.

419. Navier, M., *Mém. de l'Acad. d. Sci.*, 6, 389, 1827.

420. Stokes, G.G., *Trans. Cambr. Phil. Soc.*, 8, 287, 1845.

421. Happel, J. and Brenner, H., *Low Reynolds Number Hydrodynamics with Special Applications to Particulate Media*, Prentice-Hall, Englewood Cliffs, New York, 1965.

422. Kim, S. and Karrila, S.J., *Microhydrodynamics: Principles and Selected Applications*, Butterworth-Heinemann, Boston, 1991.

423. Reynolds, O., *Phil. Trans. Roy. Soc. (Lond.)*, A177, 157, 1886.

424. Lamb, H., *Hydrodynamics*, Cambridge University Press, London, 1963.

425. Felderhof, B.U., *J. Chem. Phys.*, 49, 44, 1968.

426. Sche, S. and Fijnaut, H.M., *Surface Sci.*, 76, 186, 1976.

427. Maldarelli, Ch. and Jain, R.K., The hydrodynamic stability of thin films, in *Thin Liquid Films*, Ivanov, I.B., Ed., Marcel Dekker, New York, 1988, p. 497.

428. Valkovska, D.S. and Danov, K.D., *J. Colloid Interface Sci.*, 241, 400, 2001.

429. Taylor, P., *Proc. Roy. Soc. (Lond.)*, A108, 11, 1924.

430. Dimitrov, D.S. and Ivanov, I.B., *J. Colloid Interface Sci.*, 64, 97, 1978.

431. Ivanov, I.B., Dimitrov, D.S., Somasundaran, P., and Jain, R.K., *Chem. Eng. Sci.*, 40, 137, 1985.

432. Ivanov, I.B. and Dimitrov, D.S., Thin film drainage, in *Thin Liquid Films*, Ivanov, I.B., Ed., Marcel Dekker, New York, 1988, p. 379.

433. O'Neill, M.E. and Stewartson, K., *J. Fluid Mech.*, 27, 705, 1967.

434. Goldman, A.J., Cox, R.G., and Brenner, H., *Chem. Eng. Sci.*, 22, 637, 1967.

435. Goldman, A.J., Cox, R.G., and Brenner, H., *Chem. Eng. Sci.*, 22, 653, 1967.

436. Levich, V.G., *Physicochemical Hydrodynamics*, Prentice-Hall, Englewood Cliffs, New Jersey, 1962.

437. Edwards, D.A., Brenner, H., and Wasan, D.T., *Interfacial Transport Processes and Rheology*, Butterworth-Heinemann, Boston, 1991.

438. Charles, G.E. and Mason, S.G., *J. Colloid Sci.*, 15, 236, 1960.

439. Danov, K.D., Denkov, N.D., Petsev, D.N., Ivanov, I.B., and Borwankar, R., *Langmuir*, 9, 1731, 1993.

440. Danov, K.D., Valkovska, D.S., and Ivanov, I.B., *J. Colloid Interface Sci.*, 211, 291, 1999.

441. Hartland, S., Coalescence in dense-packed dispersions, in *Thin Liquid Films*, Ivanov, I.B., Ed., Marcel Dekker, New York, 1988, p. 663.

442. Hetsroni, G., Ed., *Handbook of Multiphase System*, Hemisphere Publishing, New York, 1982, pp. 1-96.

443. Davis, A.M.J., Kezirian, M.T., and Brenner, H., *J. Colloid Interface Sci.*, 165, 129, 1994.

444. Brenner, H., *Chem. Eng. Sci.*, 18, 1, 1963.

445. Brenner, H., *Chem. Eng. Sci.*, 19, 599, 1964; *Chem. Eng. Sci.*, 19, 631, 1964.

446. Brenner, H. and O'Neill, M.E., *Chem. Eng. Sci.*, 27, 1421, 1972.

447. Van de Ven, T.G.M., *Colloidal Hydrodynamics*, Academic Press, London, 1988.

448. Jeffery, G.B., *Proc. Lond. Math. Soc.*, 14, 327, 1915.

449. Stimson, M. and Jeffery, G.B., *Proc. R. Soc. (Lond.)*, A111, 110, 1926.

450. Cooley, M.D.A. and O'Neill, M.E., *Mathematika*, 16, 37, 1969.

451. Cooley, M.D.A. and O'Neill, M.E., *Proc. Cambridge Philos. Soc.*, 66, 407, 1969.

452. Davis, M.H., *Chem. Eng. Sci.*, 24, 1769, 1969.

453. O'Neill, M.E. and Majumdar, S.R., *Z. Angew. Math. Phys.*, 21, 164, 1970; *Z. Angew. Math. Phys.*, 21, 180, 1970.

454. Davis, M.H., *Two Unequal Spheres in a Slow Linear Shear Flow*, Rept. NCAR-TN/STR-64, National Center for Atmospheric Research, Bolder, CO, 1971.

455. Batchelor, G.K., *J. Fluid Mech.*, 74, 1, 1976.

456. Davis, R.H. and Hill, N.A., *J. Fluid Mech.*, 236, 513, 1992.

457. Batchelor, G.K., *J. Fluid Mech.*, 119, 379, 1982.

458. Batchelor, G.K. and Wen, C.-S., *J. Fluid Mech.*, 124, 495, 1982.

459. Jeffrey, D.J. and Onishi, Y., *J. Fluid Mech.*, 139, 261, 1984.

460. Fuentes, Y.O., Kim, S., and Jeffrey, D.J., *Phys. Fluids*, 31, 2445, 1988; *Phys. Fluids*, A1, 61, 1989.

461. Stokes, G.G., *Trans. Cambridge Phil. Soc.*, 1, 104, 1851.

462. Exerowa, D. and Kruglyakov, P. M., *Foam and Foam Films: Theory, Experiment, Application*, Elsevier, New York, 1998.

463. Ivanov, I.B., Radoev, B.P., Traykov, T.T., Dimitrov, D.S., Manev, E.D., and Vassilieff, C.S., *Proceedings of the International Conference on Colloid Surface Science*, Wolfram, E., Ed., Akademia Kiado, Budapest, 1975, p. 583.

464. Denkov, N.D., Petsev, D.N., and Danov, K.D., *Phys. Rev. Let.*, 71, 3226, 1993.

465. Valkovska, D.S., Danov, K.D., and Ivanov, I.B., *Colloid Surf. A*, 156, 547, 1999.

466. Davis, R.H., Schonberg, J.A., and Rallison, J.M., *Phys. Fluids*, A1, 77, 1989.

467. Chi, B.K. and Leal, L.G., *J. Fluid Mech.*, 201, 123, 1989.

468. Ascoli, E.P., Dandy, D.S., and Leal, L.G., *J. Fluid Mech.*, 213, 287, 1990.

469. Yiantsios, S.G. and Davis, R.H., *J. Fluid Mech.*, 217, 547, 1990.

470. Zhang, X. and Davis, R.H., *J. Fluid Mech.*, 230, 479, 1991.

471. Chesters, A.K., *Trans. Inst. Chem. Engrs. A*, 69, 259, 1991.

472. Yiantsios, S.G. and Davis, R.H., *J. Colloid Interface Sci.*, 144, 412, 1991.

473. Yiantsios, S.G. and Higgins, B.G., *J. Colloid Interface Sci.*, 147, 341, 1991.

474. Joye, J.-L., Hirasaki, G.J., and Miller, C.A., *Langmuir*, 8, 3083, 1992.

475. Joye, J.-L., Hirasaki, G.J., and Miller, C.A., *Langmuir*, 10, 3174, 1994.

476. Abid, S. and Chestrers, A.K., *Int. J. Multiphase Flow*, 20, 613, 1994.

477. Li, D., *J. Colloid Interface Sci.*, 163, 108, 1994.

478. Saboni, A., Gourdon, C., and Chesters, A.K., *J. Colloid Interface Sci.*, 175, 27, 1995.

479. Rother, M.A., Zinchenko, A.Z., and Davis, R.H., *J. Fluid Mech.*, 346, 117, 1997.

480. Singh, G., Miller, C.A., and Hirasaki, G.J., *J. Colloid Interface Sci.*, 187, 334, 1997.

481. Cristini, V., Blawzdziewicz, J., and Loewenberg, M., *J. Fluid Mech.*, 366, 259, 1998.

482. Bazhlekov, I.B., Chesters, A.K., and van de Vosse, F.N., *Int. J. Multiphase Flow*, 26, 445, 2000.

483. Bazhlekov, I.B., van de Vosse, F.N., and Chesters, A.K., *Journal of Non-Newtonian Fluid Mechanics*, 93, 181, 2000.

484. Chesters, A.K. and Bazhlekov, I.B., *J. Colloid Interface Sci.*, 230, 229-243, 2000.

485. Boulton-Stone, J.M. and Blake, J.R., *J. Fluid Mech.*, 254, 437, 1993.

486. Frankel, S. and Mysels, K., *J. Phys. Chem.*, 66, 190, 1962.

487. Velev, O.D., Constantinides, G.N., Avraam, D.G., Payatakes, A.C., and Borwankar, R.P., *J. Colloid Interface Sci.*, 175, 68, 1995.

488. Exerowa, D., Nikolov, A., and Zacharieva, M., *J. Colloid Interface Sci.*, 81, 419, 1981.

489. de Vries, A.J., *Rec. Trav. Chim. Pays-Bas.*, 77, 441, 1958.

490. Vrij, A., *Discuss. Faraday Soc.*, 42, 23, 1966.

491. Ivanov, I.B., Radoev, B.P., Manev, E.D., and Sheludko, A.D., *Trans. Faraday Soc.*, 66, 1262, 1970.

492. Gumerman, R.J. and Homsy, G.M., *Chem. Engng. Commun.*, 2, 27, 1975.

493. Malhotra, A.K. and Wasan, D.T., *Chem. Engng. Commun.*, 48 35, 1986.

494. Valkovska, D. S., Danov, K.D., and Ivanov, I.B., *Adv. Colloid Interface Sci.*, 96, 101, 2002.

495. Manev, E.D., Sazdanova, S.V., and Wasan, D.T., *J. Colloid Interface Sci.*, 97, 591, 1984.

496. Ivanov, I.B., *Pure Appl. Chem.*, 52, 1241, 1980.

497. Aveyard, R., Binks, B.P., Fletcher, P.D.I., and Ye, X., *Prog. Colloid Polymer Sci.*, 89, 114, 1992.

498. Velev, O.D., Gurkov, T.D., Chakarova, Sv.K., Dimitrova, B.I., and Ivanov, I.B., *Colloids Surf. A*, 83, 43, 1994.

499. Dickinson, E., Murray, B.S., and Stainsby, G., *J. Chem. Soc. Faraday Trans.*, 84, 871, 1988.

500. Ivanov, I.B., Lectures at INTEVEP, Petroleos de Venezuela, Caracas, June 1995.

501. Ivanov, I.B. and Kralchevsky, P.A., *Colloid Surf. A*, 128, 155, 1997.

502. Basheva, E.S., Gurkov, T.D., Ivanov, I.B., Bantchev, G.B., Campbell, B., and Borwankar, R.P., *Langmuir*, 15, 6764, 1999.

503. Boussinesq, M.J., *Ann. Chim. Phys.*, 29, 349, 1913; *Ann. Chim. Phys.*, 29, 357, 1913.

504. Aris, R., *Vectors, Tensors, and the Basic Equations of Fluid Mechanics*, Prentice Hall, Englewood Cliffs, NJ, 1962.

505. Brenner, H. and Leal, L.G., *J. Colloid Interface Sci.*, 62, 238, 1977.

506. Brenner, H. and Leal, L.G., *J. Colloid Interface Sci.*, 65, 191, 1978.

507. Brenner, H. and Leal, L.G., *AIChE J.*, 24, 246, 1978.

508. Brenner, H. and Leal, L.G., *J. Colloid Interface Sci.*, 88, 136, 1982.

509. Stone, H.A., *Phys. Fluids*, A2, 111, 1990.

510. Valkovska, D.S. and Danov, K.D., *J. Colloid Interface Sci.*, 223, 314, 2000.

511. Stoyanov, S.D. and Denkov, N.D., *Langmuir*, 17, 1150, 2001.

512. Feng, S.-S., *J. Colloid Interface Sci.*, 160, 449, 1993.

513. Stebe, K.J. and Maldarelli, Ch., *Phys. Fluids*, A3, 3, 1991.

514. Stebe, K.J. and Maldarelli, Ch., *J. Colloid Interface Sci.*, 163, 177, 1994.

515. Scriven, L.E., *Chem. Eng. Sci.*, 12, 98, 1960.

516. Scriven, L.E. and Sternling, C.V., *J. Fluid Mech.*, 19, 321, 1964.

517. Slattery, J.C., *Chem. Eng. Sci.*, 19, 379, 1964; *Chem. Eng. Sci.*, 19, 453, 1964.

518. Slattery, J.C., *I&EC Fundam.*, 6, 108, 1967.

519. Slattery, J.C., *Interfacial Transport Phenomena*, Springer-Verlag, New York, 1990.

520. Barton, K.D. and Subramanian, R.S., *J. Colloid Interface Sci.*, 133, 214, 1989.

521. Feuillebois, F., *J. Colloid Interface Sci.*, 131, 267, 1989.

522. Merritt, R.M. and Subramanian, R.S., *J. Colloid Interface Sci.*, 131, 514, 1989.

523. Mannheimer, R.J. and Schechter, R.S., *J. Colloid Interface Sci.*, 12, 98, 1969.

524. Pintar, A.J., Israel, A.B., and Wasan, D.T., *J. Colloid Interface Sci.*, 37, 52, 1971.

525. Gardner, J.W. and Schechter, R.S., *Colloid Interface Sci.*, 4, 98, 1976.

526. Li, D. and Slattery, J.C., *J. Colloid Interface Sci.*, 125, 190, 1988.

527. Tambe, D.E. and Sharma, M.M., *J. Colloid Interface Sci.*, 147, 137, 1991.

528. Tambe, D.E. and Sharma, M.M., *J. Colloid Interface Sci.*, 157, 244, 1993.

529. Tambe, D.E. and Sharma, M.M., *J. Colloid Interface Sci.*, 162, 1, 1994.

530. Horozov, T., Danov, K., Kralchevsky, P., Ivanov, I., and Borwankar, R., A local approach in interfacial rheology: theory and experiment, in First World Congress on Emulsion, Paris, 3-20, 137, 1993.

531. Danov, K. D., Ivanov, I. B., and Kralchevsky, P. A., Interfacial rheology and emulsion stability, in Second World Congress on Emulsion, Paris, 2-2, 152, 1997.

532. de Groot, S.R. and Mazur, P., *Non-equilibrium Thermodynamics*, Interscience, New York, 1962.

533. Moeckel, G.P., *Arch. Rat. Mech. Anal.*, 57, 255, 1975.

534. Rushton, E. and Davies, G.A., *Appl. Sci. Res.*, 28, 37, 1973.

535. Haber, S., Hetsroni, G., and Solan, A., *Int. J. Multiphase Flow*, 1, 57, 1973.

536. Reed, L.D. and Morrison, F.A., *Int. J. Multiphase Flow*, 1, 573, 1974.

537. Hetsroni, G. and Haber, S., *Int. J. Multiphase Flow*, 4, 1, 1978.

538. Morrison, F.A. and Reed, L.D., *Int. J. Multiphase Flow*, 4, 433, 1978.

539. Beshkov, V.N., Radoev, B.P., and Ivanov, I.B., *Int. J. Multiphase Flow*, 4, 563, 1978.

540. Murdoch, P.G. and Leng, D.E., *Chem. Eng. Sci.*, 26, 1881, 1971.

541. Reed, X.B., Riolo, E., and Hartland, S., *Int. J. Multiphase Flow*, 1, 411, 1974; *Int. J. Multiphase Flow*, 1, 437, 1974.

542. Ivanov, I.B. and Traykov, T.T., *Int. J. Multiphase Flow*, 2, 397, 1976.

543. Traykov, T.T. and Ivanov, I.B., *Int. J. Multiphase Flow*, 3, 471, 1977.

544. Lu, C.-Y.D. and Cates, M.E., *Langmuir*, 11, 4225, 1995.

545. Jeelany, S.A.K. and Hartland, S., *J. Colloid Interface Sci.*, 164, 296, 1994.

546. Zapryanov, Z., Malhotra, A.K., Aderangi, N., and Wasan, D.T., *Int. J. Multiphase Flow*, 9, 105, 1983.

547. Malhotra, A.K. and Wasan, D.T., *Chem. Eng. Commun.*, 55, 95, 1987.

548. Malhotra, A.K. and Wasan, D.T., Interfacial rheological properties of adsorbed surfactant films with applications to emulsion and foam stability, in *Thin Liquid Films*, Ivanov, I.B., Ed., Marcel Dekker, New York, 1988, p. 829.

549. Singh, G., Hirasaki, G.J., and Miller, C.A., *J. Colloid Interface Sci.*, 184, 92, 1996.

550. Traykov, T.T., Manev, E.D., and Ivanov, I.B., *Int. J. Multiphase Flow*, 3, 485, 1977.

551. Bancroft, W.D., *J. Phys. Chem.*, 17, 514, 1913.

552. Griffin, J., *Soc. Cosmet. Chem.*, 5, 4, 1954.

553. Davies, J.T., in Proceedings of the 2nd International Congress on Surface Activity, Vol. 1, Butterworths, London, 1957, p. 426.

554. Shinoda, K. and Friberg, S., *Emulsion and Solubilization*, Wiley, New York, 1986.

555. Davis, H.T., Factors determining emulsion type: HLB and beyond, in Proc. First World Congress on Emulsion 19-22 Oct. 1993, Paris, 1993, p. 69.

556. Israelachvili, J., The history, applications and science of emulsion, in Proc. First World Congress on Emulsion 19-22 Oct. 1993, Paris, 1993, p. 53.

557. Kralchevsky, P.A., *J. Colloid Interface Sci.*, 137, 217, 1990.

558. Gompper, G. and Schick, M., *Phys. Rev.*, B41, 9148, 1990.

559. Lerczak, J., Schick, M., and Gompper, G., *Phys. Rev.*, 46, 985, 1992.

560. Andelman, D., Cates, M.E., Roux, D., and Safran, S., *J. Chem. Phys.*, 87, 7229, 1987.

561. Chandra, P. and Safran, S., *Europhys. Lett.*, 17, 691, 1992.

562. Danov, K.D., Velev, O.D., Ivanov, I.B., and Borwankar, R.P., Bancroft rule and hydrodynamic stability of thin films and emulsions, in First World Congress on Emulsion 19-22 Oct. 1993, Paris, 1993, p. 125.

563. Kunieda, H., Evans, D.F., Solans, C., and Yoshida, *Colloids Surf.*, 47, 35, 1990.

564. Koper, G.J.M., Sager, W.F.C., Smeets, J., and Bedeaux, D., *J. Phys. Chem.*, 99**,** 13291, 1995.

565. Ivanov, I.B., Danov, K.D., and Kralchevsky, P.A., *Colloids Surf. A*, 152, 161, 1999.

566. Velev, O.D., Gurkov, T.D., and Borwankar, R.P., *J. Colloid Iterface Sci.*, 159, 497, 1993.

567. Velev, O.D., Gurkov, T.D., Ivanov, I.B., and Borwankar, R.P., *Phys. Rev. Lett.*, 75, 264, 1995.

568. Danov, K., Ivanov, I., Zapryanov, Z., Nakache, E., and Raharimalala, S., Marginal stability of emulsion thin film, in *Proceedings of the Conference of Synergetics, Order and Chaos*, Velarde, M., Ed., World Scientific, Singapore, 1988, p. 178.

569. Valkovska, D.S., Kralchevsky, P.A., Danov, K.D., Broze, G., and Mehreteab, A., *Langmuir*, 16, 8892, 2000.

570. Danov, K.D., Gurkov, T.D., Dimitrova, T.D., and Smith, D., *J. Colloid Interface Sci.*, 188, 313, 1997

571. Ivanov, I.B., Chakarova, S.K., and Dimitrova, B.I., *Colloids Surf.*, 22, 311, 1987.

572. Dimitrova, B.I., Ivanov, I.B., and Nakache, E., *J. Dispersion Sci. Technol.*, 9, 321, 1988.

573. Sternling, C.V. and Scriven, L.E., *AIChE J.*, 5, 514, 1959.

574. Lin, S.P. and Brenner, H.J., *J. Colloid Interface Sci.*, 85, 59, 1982.

575. Holly, F.J., in *Wetting, Spreading and Adhesion* , Padday, J.F., Ed., Accademic Press, New York, 1978, p. 439.

576. Castillo, J.L. and Velarde, M.G., *J. Colloid Interface Sci.*, 108, 264, 1985.

577. Davis, R.H., *Adv. Colloid Interface Sci.*, 43, 17, 1993.

578. Uijttewaal, W.S.J., Nijhof, E.-J., and Heethaar, R.M., *Phys. Fluids*, A5, 819, 1993.

579. Zapryanov, Z. and Tabakova, S., *Dynamics of Bubbles, Drops and Rigid Particles*, Kluwer Academic Publishers, London, 1999.

580. Lorentz, H.A., *Abhandl. Theoret. Phys.*, 1, 23, 1906.

581. Faxen, H., *Arkiv. Mat. Astron. Fys.,* 17, 27, 1923.

582. Wakiya, S., *J. Phys. Soc. Jpn,* 12, 1130, 1957.

583. Dean, W.R. and O'Neill, M.E., *Mathematika*, 10, 13, 1963.

584. O'Neill, M.E., *Mathematika*, 11, 67, 1964.

585. Cooley, M.D.A. and O'Neill, M.E., *J. Inst. Math. Appl.*, 4, 163, 1968.

586. Keh, H.J. and Tseng, C.H., *Int. J. Multiphase Flow*, 1, 185, 1994.

587. Schonberg, J. and Hinch, E.J., *J. Fluid Mech.*, 203, 517, 1989.

588. Ryskin, G. and Leal, L.G., *J. Fluid Mech.*, 148, 1, 1984; *J. Fluid Mech.*, 148, 19, 1984; *J. Fluid Mech.*, 148, 37, 1984.

589. Liron, N. and Barta, E., *J. Fluid Mech.*, 238, 579, 1992.

590. Shapira, M. and Haber, S., *Int. J. Multiphase Flow*, 14, 483, 1988.

591. Shapira, M. and Haber, S., *Int. J. Multiphase Flow*, 16, 305, 1990.

592. Yang, S.-M. and Leal, L.G., *J. Fluid Mech.*, 149, 275, 1984.

593. Yang, S.-M. and Leal, L.G., *Int. J. Multiphase Flow*, 16, 597, 1990.

594. Lebedev, A.A., *Zhur. Russ. Fiz. Khim.*, 48, 1916.

595. Silvey, A., *Phys. Rev.*, 7, 106, 1916.

596. Hadamar, J.S., *Comp. Rend. Acad. Sci. (Paris)*, 152, 1735, 1911.

597. Rybczynski, W., *Bull. Intern. Acad. Sci. (Cracovie)*, A, 1911.

598. He, Z., Dagan, Z., and Maldarelli, Ch., *J. Fluid Mech.*, 222, 1, 1991.

599. Danov, K.D., Aust, R., Durst, F., and Lange, U., *Chem. Eng. Sci.*, 50, 263, 1995.

600. Danov, K.D., Aust, R., Durst, F., and Lange, U., *Chem. Eng. Sci.*, 50, 2943, 1995.

601. Danov, K.D., Aust, R., Durst, F., and Lange, U., *Int. J. Multiphase Flow.*, 21, 1169, 1995.

602. Danov, K.D., Gurkov, T.D., Raszillier, H., and Durst, F., *Chem. Eng. Sci.*, 53, 3413, 1998.

603. Stoos, J.A. and Leal, L.G., *J. Fluid Mech.*, 217, 263, 1990.

604. Danov, K.D., Dimova, R.I., and Pouligny, B., *Phys. Fluids*, 12, 2711, 2000.

605. Dimova, R.I., Danov, K.D., Pouligny, B., and Ivanov, I.B., *J. Colloid Interface Sci.*, 226, 35, 2000.

606. Angelova, M.I. and Pouligny, B., *Pure Appl. Optics*, 2, 261, 1993.

607. Pouligny, B., Martinot-Lagarde, G., and Angelova, M.I., *Progr. Colloid Polym. Sci.*, 98, 280, 1995.

608. Dietrich, C., Angelova, M., and Pouligny, B., *J. Phys. II France*, 7, 1651, 1997.

609. Velikov, K., Dietrich, C., Hadjiski, A., Danov, K., and Pouligny, B., *Europhys. Lett.*, 40(4), 405, 1997.

610. Velikov, K., Danov, K., Angelova, M., Dietrich, C., and Pouligny, B., *Colloids Surf. A*, 149, 245, 1999.

611. Dimova, R., Dietrich, C., Hadjiisky, A., Danov, K., and Pouligny, B., *Eur. Phys. J. B*, 12, 589, 1999.

612. Danov, K.D., Pouligny, B., Angelova, M.I., and Kralchevsky, P.A., in *Studies in Surface Science and Catalysis*, Vol. 132, Elsevier, Amsterdam, 2001.

613. Hunter, R.J., *Foundation of Colloid Science*, Vol. 1, Clarendon Press, Oxford, 1987.

614. Hunter, R.J., *Foundation of Colloid Science*, Vol. 2, Clarendon Press, Oxford, 1989.

615. Einstein, A., *Ann. Phys.*, 19, 289, 1906.

616. Kubo, R., *Rep. Prog. Phys.*, 29, 255, 1966.

617. Einstein, A., *Ann. Phys.*, 34, 591, 1911.

618. Taylor, G.I., *Proc. Roy. Soc. A*, 138, 41, 1932.

619. Oldroyd, J.G., *Proc. Roy. Soc. A*, 232, 567, 1955.

620. Taylor, G.I., *Proc. Roy. Soc. A*, 146, 501, 1934.

621. Fröhlich, H. and Sack, R., *Proc. Roy. Soc. A*, 185, 415, 1946.

622. Oldroyd, J.G., *Proc. Roy. Soc. A*, 218, 122, 1953.

623. Batchelor, G.K., *J. Fluid Mech.*, 83, 97, 1977.

624. De Kruif, C.G., Van Iersel, E.M.F., Vrij, A., and Russel, W.B., *J. Chem. Phys.*, 83, 4717, 1985.

625. Loewenberg, M. and Hinch, E.J., *J. Fluid Mech.*, 321, 395, 1996.

626. Da Cunha, F.R. and Hinch, E.J., *J. Fluid Mech.*, 309, 211, 1996.

627. Li, X. and Pozrikidis, C., *J. Fluid Mech.*, 341, 165, 1997.

628. Loewenberg, M., *J. Fluids Eng.*, 120, 824, 1998.

629. Blawzdziewicz, J., Vajnryb, E., and Loewenberg, M., *J. Fluid Mech.*, 395, 29, 1999.

630. Ramirez, J.A., Zinchenko, A., Loewenberg, M., and Davis, R.H., *Chem. Eng. Sci.*, 54, 149, 1999.

631. Blawzdziewicz, J., Vlahovska, P., and Loewenberg, M., *Physica A*, 276, 50, 2000.

632. Breyannis, G. and Pozrikidis, C., *Theor. Comp. Fluid Dynam.*, 13, 327, 2000.

633. Li, X. and Pozrikidis, C., *Int. J. Multiphase Flow*, 26, 1247, 2000.

634. Rednikov, A.Y., Ryazantsev, Y.S., and Velarde, M.G., *Phys. Fluids*, 6, 451, 1994.

635. Velarde, M.G., *Phil. Trans. Roy. Soc., Math. Phys. Eng. Sci.*, 356, 829, 1998.

636. Danov K.D., *J. Colloid Interface Sci.*, 235, 144, 2001.

637. Barnes, H.A., Rheology of emulsions - a review, in Proc. First World Congress on Emulsion 19-22 Oct. 1993, Paris, 1993, p. 267.

638. Krieger, L.M. and Dougherty, T.J., *Trans. Soc. Rheol.*, 3, 137, 1959.

639. Wakeman, R., *Powder Tech.*, 11, 297, 1975.

640. Prud'home, R.K. and Khan, S.A., Experimental results on foam rheology, in *Foams: Theory, Measurements, and Applications*, Prud'home, R.K. and Khan, S.A., Eds., Marcel Dekker, New York, 1996, p. 217.

641. Tadros, T.F., Fundamental principles of emulsion rheology and their applications, in Proc. First World Congress on Emulsion 19-22 Oct. 1993, Paris, 1993, p. 237.

642. Pal, R., Bhattacharya, S.N., and Rhodes, E., *Can. J. Chem. Eng.*, 64, 3, 1986.

643. Edwards, D.A. and Wasan, D.T., Foam rheology: the theory and role of interfacial rheological properties, in *Foams: Theory, Measurements, and Applications*, Prud'home, R.K. and Khan, S.A., Eds., Marcel Dekker, New York, 1996, p. 189.

644. Wessel, R. and Ball, R.C., *Phys. Rev.*, A46, 3009, 1992.

645. Kanai, H., Navarrete, R.C., Macosko, C.W., and Scriven, L.E., *Rheol. Acta*, 31, 333, 1992.

646. Pal, R., *Chem. Eng. Comm.*, 98, 211, 1990.

647. Pal, R., *Colloids Surf. A*, 71, 173, 1993.

648. Prins, A., Liqiud flow in foams as affected by rheological surface properties: a contribution to a better understanding of the foaming behaviour of liquids, in *Hydrodynamics of Dispersed Media*, Hulin, J.P., Cazabat, A.M., Guyon, E., and Carmona, F., Eds., Elsevier/North-Holland, Amsterdam, 1990, p. 5.

649. Babak, V.G., *Colloids Surf. A*, 85, 279, 1994.

650. Yuhua, Y., Pal, R., and Masliyah, J., *Chem Eng. Sci.*, 46, 985, 1991.

651. Giesekus, H., Disperse systems: dependence of rheological properties on the type of flow with implications for food rheology, in *Physical Properties of Foods*, Jowitt, R. et al., Eds., Applied Science Publishers, 1983, chap. 13.

652. Turian, R. and Yuan, T.-F., *AIChE J.*, 23, 232, 1977.

653. Clarke, B., *Trans. Inst. Chem. Eng.*, 45, 251, 1967.

654. von Smoluchowsky, M., *Phys. Z.*, 17, 557, 1916.

655. von Smoluchowsky, M., *Z. Phys. Chem.*, 92, 129, 1917.

656. Wang, H. and Davis, R.H., *J. Colloid Interface Sci.*, 159, 108, 1993.

657. Rogers, J.R. and Davis, R.H., *Mettal. Trans.*, A21, 59, 1990.

658. Young, N.O., Goldstein, J.S., and Block, M.J., *J. Fluid Mech.*, 6, 350, 1959.

659. Fuchs, N.A., *Z. Phys.*, 89, 736, 1934.

660. Friedlander, S.K., *Smoke, Dust and Haze: Fundamentals of Aerosol Behaviour*, Wiley-Interscience, New York, 1977.

661. Singer, J.M., Vekemans, F.C.A., Lichtenbelt, J.W.Th., Hesselink, F.Th., and Wiersema, P.H., *J. Colloid Interface Sci.*, 45, 608, 1973.

662. Leckband, D.E., Schmitt, F.-J., Israelachvili, J.N., and Knoll, W., *Biochemistry*, 33, 4611, 1994.

663. Bak, T.A. and Heilmann, O., *J. Phys. A: Math. Gen.*, 24, 4889, 1991.

664. Martinov, G.A. and Muller, V.M., in *Research in Surface Forces*, Vol. 4, Plenum Press, Consultants Bureau, New York, 1975, p. 3.

665. Elminyawi, I.M., Gangopadhyay, S., and Sorensen, C.M., *J. Colloid Interface Sci.*, 144, 315, 1991.

666. Hartland, S. and Gakis, N., *Proc. Roy. Soc. (Lond.)*, A369, 137, 1979.

667. Hartland, S. and Vohra, D.K., *J. Colloid Interface Sci.*, 77, 295, 1980.

668. Lobo, L., Ivanov, I.B., and Wasan, D.T., *AIChE J.*, 39, 322, 1993.

669. Danov, K.D., Ivanov, I.B., Gurkov, T.D., and Borwankar, R.P., *J. Colloid Interface Sci.*, 167, 8, 1994.

670. van den Tempel, M., *Recueil*, 72, 433, 1953.

671. Borwankar, R.P., Lobo, L.A., and Wasan, D.T., *Colloid Surf.*, 69, 135, 1992.

672. Dukhin, S., Sæther, Ø., and Sjöblom, J., Coupling of coalescence and flocculation in dilute O/W emulsions, in *Encycloped Handbook of Emulsion Technology*, Sjöblom, J., Ed., Marcel Dekker, New York, 2001, p. 71.

673. Garrett, P.R., Ed., *Defoaming: Theory and Industrial Applications*, Marcel Dekker: New York, 1993.

674. Garrett, P.R., "The Mode of Action of Antifoams" in *Defoaming: Theory and Industrial Applications,* Marcel Dekker: New York, 1993, chap. 1.

675. Exerowa, D. and Kruglyakov, P.M., *Foams and Foam Films*, Elsevier: Amsterdam, 1998, chap. 9.

676. Wasan, D.T. and Christiano, S.P., in *Handbook of Surface and Colloid Chemistry*; Birdi, K.S., Ed., CRC Press: Boca Raton, 1997, p. 179.

677. Kralchevsky, P.A. and Nagayama, K., *Particles at Fluid Interfaces and Membranes*, Studies in Interface Science, Vol. 10; Elsevier: Amsterdam, 2001, chap. 14.

678. Basheva, E.S., Ganchev, D., Denkov, N.D., Kasuga, K., Satoh, N., and Tsujii, K., *Langmuir*, 16, 1000, 2000.

679. Basheva, E.S., Stoyanov S., Denkov, N.D., Kasuga, K., Satoh, N., and Tsujii, K., *Langmuir*, 17, 969, 2001.

680. Koczo, K., Koczone, J.K., and Wasan, D.T., *J. Colloid Interface Sci*., 166, 225, 1994.

681. Denkov, N.D., Cooper, P. and Martin, J.-Y., *Langmuir*, 15, 8514,1999.

682. Marinova, K. and Denkov, N.D., *Langmuir*, 17, 2426, 2001.

683. Denkov, N.D,. and Marinova K., Antifoaming action of oils, *Proceedings of the 3rd EuroConference on Foams, Emulsions and Applications*; Zitha, P., Banhart, J., and Verbist, G., Eds; MIT: Bremen, 2000, p. 199.

684. Denkov, N.D., Tcholakova, S., Marinova, K., and Hadjiiski, A., Role of oil spreading for the efficiency of mixed oil-solid antifoams, *Langmuir*, 2001; submitted.

685. Marinova, K.M., Denkov, N.D., Branlard, P., Giraud, Y., and Deruelle, M., Optimal hydrophobicity of silica in mixed oil-silica antifoams, *Langmuir*, 2001, submitted.

686. Arnaudov, L., Denkov, N.D., Surcheva, I., Durbut, P., Broze, G., and Mehreteab, A., *Langmuir*, 17, 6999, 2001.

687. Hadjiiski, A., Tcholakova, S., Denkov, N.D., Durbut, P., Broze, G., and Mehreteab, A., *Langmuir*, 17, 7011, 2001.

688. Denkov, N.D., *Langmuir*, 15, 8530, 1999.

689. Garrett, P.R., *J. Colloid Interface Sci.*, 76, 587, 1980.

690. Kulkarni, R.D., Goddard, E.D., and Kanner, B., *J. Colloid Interface Sci.*, 59, 468, 1977.

691. Kruglyakov, P.M., in *Thin Liquid Films: Fundamentals and Applications*, Ivanov, I.B., Ed., Surfactant Science Series, Vol. 29, Marcel Dekker: New York, 1988, chap. 11.

692. Bergeron, V., Fagan, M.E., and Radke C., *Langmuir*, 9, 1704, 1993.

693. Bergeron, V., Cooper, P., Fischer, C., Giermanska-Kahn, J., Langevin, D., and Pouchelon, A., *Colloids Surfaces A: Physicochem. Eng. Aspects*, 122, 103, 1997.

694. Koczo, K., Lloyd, L., and Wasan, D.T., *J. Colloid Interface Sci.*, 150, 492, 1992.

695. Kulkarni, R.D., Goddard, E.D., and Chandar, P., in *Foams: Theory, Measurements, and Applications*, Prud'homme R.K. and Khan, S.A., Eds.; Surfactant Science Series, Vol. 57; Marcel Dekker: New York, 1996, chap. 14.

696. Aveyard, R., Binks, B.P., Fletcher P.D.I.; Peck, T-G., and Garrett, P., *J. Chem. Soc. Faraday Trans.*, 89, 4313, 1993.

697. Hadjiiski, A., Tcholakova, S., Ivanov, I.B., Gurkov, T.D., and Leonard, E., *Langmuir*, 18, 127, 2002.

698. Hadjiiski, A., Denkov, N.D., Tcholakova, S., and Ivanov, I.B., Role of entry barriers in the foam destruction by oil drops, *Proceedings of the 13th Symposium on Surfactants in Solution*, Mittal K.L., Moudgil B., and Shah D., Eds.; Marcel Dekker: New York, 2002.

699. Lichtman, I.A., Sinka, J.V., and Evans, D.W., *Assoc. Mex. Tec. Ind. Celul. Pap. (Bol.)*, 15, 2632, 1975.

700. Ross, S., *J. Phys. Colloid Chem.*, 54, 429, 1950.

701. Jha, B.K., Christiano, S.P., and Shah, D.O., *Langmuir*, 16, 9947, 2000.

702. Garrett, P.R., Davis, J., and Rendall, H.M., *Colloids Surfaces A: Physicochem. Eng. Aspects*, 85, 159, 1994.

703. Denkov N.D., Marinova, K., Christova, C., Hadjiiski, A., and Cooper, P., *Langmuir*, 16, 2515, 2000.

704. Overbeek, J.Th.G., *Adv. Colloid Sci.*, 3, 97, 1950.

705. Overbeek, J.Th.G., in *Colloid Science*, Vol. 1, Kruyt, H.R., Ed., Elsevier, Amsterdam, 1952, p. 197.

706. Overbeek, J. Th. G. and Wiersema, P.H., in *Electrophoresis*, Bier, M., Ed., Vol. 2, Academic Press, New York, 1967, chap. 1.

707. Dukhin, S.S. and Derjaguin, B.V., in *Surface and Colloid Science*, Vol. 7, Matijevic, E., Ed., John Wiley, New York, 1974, chap. 3.

708. Derjaguin, B.V., Dukhin, S.S., and Shilov, V.N., *Adv. Colloid Interface Sci.*, 13, 141 and 153, 1980.

709. Uzgiris, E., *Adv. Colloid Interface Sci.*, 14, 75, 1981.

710. Saville, D.A., *Adv. Colloid Interface Sci.*, 16, 267, 1982.

711. O'Brien, R.W., *Adv. Colloid Interface Sci.*, 16, 281, 1982.

712. Mandel, M. and Odjik, T., *Ann. Rev. Phys. Chem.*, 35, 75, 1984.

713. Dukhin, S.S., *Adv. Colloid Interface Sci.*, 44, 1, 1993.

714. Dukhin, A.S. and Goetz, P.J., *Adv. Colloid Interface Sci.*, 92, 73, 2001.

715. Dukhin, S.S. and Shilov, V.N., *Dielectric Phenomena and the Double Layer in Disperse Systems and Polyelectrolytes*, Wiley, New York, 1974.

716. Hunter, R.J., *Zeta Potential in Colloid Science*, Academic Press, New York, 1981.

717. Hunter, R.J., *Foundations of Colloid Science*, Vol. 2, Clarendon Press, Oxford, 1989, chaps. 6 and 13.

718. Ohshima, H. and Furusawa, K., Eds., *Electrical Phenomena at Interfaces: Fundamentals, Measurements, and Applications*, 2nd Ed., Marcel Dekker, New York, 1998.

719. Chew, W.C. and Sen, P.N., *J. Chem. Phys.*, 77, 2042, 1982.

720. Loeb, A.L., Wiersema, P.H., and Overbeek, J.Th.G., *The Electric Double Layer Around a Spherical Colloidal Particle*, MIT Press, Cambridge (Mass.), 1961.

721. Dukhin, S.S., Semenikhin, N.M., and Shapinskaia, L.M., *Dokl. Akad. Nauk SSSR*, 193, 385, 1970.

722. Stokes, A.N., *J. Chem. Phys.*, 65, 261, 1976.

723. Ohshima, H., Healy, T.W., and White L.R., *J. Colloid Interface Sci.*, 90, 17, 1982.

724. Ohshima, H., Electrical double layer, in *Electrical Phenomena at Interfaces: Fundamentals, Measurements, and Applications*, 2nd Ed., Ohshima, H. and Furusawa, K., Eds., Marcel Dekker, New York, 1998, chap. 1.

725. Ohshima, H., *J. Colloid Interface Sci.*, 171, 525, 1995.

726. von Smoluchowski, M., in *Handbuch der Electrizität und des Magnetismus*, Vol. 2, Barth, Leipzig, 1921, p. 366.

727. Bikerman, J.J., *Trans. Faraday Soc.*, 36, 154, 1940.

728. O'Brien, R.W., *J. Colloid Interface Sci.*, 110, 477, 1986.

729. Bowen, W.R. and Jacobs, P.M., *J. Colloid Interface Sci.*, 111, 223, 1986.

730. Sasaki, H., Muramatsu, A., Arakatsu, H., and Usui, S., *J. Colloid Interface Sci.*, 142, 266, 1991.

731. Nishimura, S., Tateyama, H., Tsunematsu, K., and Jinnai, K., *J. Colloid Interface Sci.*, 152, 359, 1992.

732. Furusawa, K., Sasaki, H., and Nashima, T., Electro-osmosis and streaming potential measurements, in *Electrical Phenomena at Interfaces: Fundamentals, Measurements, and Applications*, 2nd Ed., Ohshima, H. and Furusawa, K., Eds., Marcel Dekker, New York, 1998, chap.9.

733. Usui, S., Imamura, Y., and Sasaki, H., *J. Colloid Interface Sci.*, 118, 335, 1987.

734. Scales, P.J., Healy, T.W., and Evans, D.F., *J. Colloid Interface Sci.*, 124, 391, 1988; Scales, P.J., Grieser, F., and Healy, T.W., *Langmuir*, 6, 582, 1989.

735. Van den Hoven, Th.J.J. and Bijsterbosch, B.H., *Colloids Surfaces*, 22, 187, 1987.

736. von Smoluchowksi, M., *Z. Phys. Chem*., 92, 129, 1918.

737. Hückel, E., *Phys. Z.*, 25, 204, 1924.

738. Henry, D.C., *Proc. R. Soc. London*, A133, 106, 1931.

739. Henry, D.C., *Trans. Faraday Soc.*, 44, 1021, 1948.

740. Overbeek, J.Th.G., *Kolloid Beih.*, 54, 287 and 364, 1943.

741. Booth, F., *Proc R. Soc. London*, A203, 514, 1950.

742. Wiersema, P.H., Loeb, A.L., and Overbeek, J.Th.G., *J. Colloid Interface Sci.*, 22, 78, 1966.

743. O'Brien, R.W. and White, L.R., *J. Chem. Soc. Faraday Trans. 2*, 74, 1607, 1978.

744. O'Brien, R.W. and Hunter, R.J., *Canad. J. Chem*., 59, 1878, 1981.

745. Ohshima, H., Healy, T.W., White, L.R., and O'Brien, R.W., *J. Chem. Soc. Faraday Trans. 2*, 79, 1613, 1983; 80, 1299 and 1643, 1984.

746. Ohshima, H., *J. Colloid Interface Sci.*, 168, 269, 1994.

747. Ohshima, H., *J. Colloid Interface Sci.*, 239, 587, 2001.

748. Stigter, D., *J. Phys. Chem.*, 82, 1417 and 1424, 1978.

749. Van der Drift, W.P.J.T., de Keizer, A., and Overbeek, J.Th.G., *J. Colloid Interface Sci.*, 71, 67 and 79, 1979.

750. Ohshima, H., *J. Colloid Interface Sci.*, 180, 299, 1996.

751. Hermans, J.J., *J. Polym. Sci.*, 18, 527, 1955.

752. Overbeek, J.Th.G. and Stigter, D., *Rec. Trav. Chim.*, 75, 543, 1956.

753. Imai, N. and Iwasa, K., *Israel J. Chem.*, 11, 223, 1973.

754. Koopal, L.K. and Lyklema, J., *Disc. Faraday Soc.*, 59, 230, 1975; *J. Electroanal. Chem.*, 100, 895, 1979.

755. Brooks, D.E. and Seaman, G.V.F., *J. Colloid Interface Sci.*, 43, 670, 1973; *J. Colloid Interface Sci.*, 43, 687, 1973; *J. Colloid Interface Sci.*, 43, 700, 1973; *J. Colloid Interface Sci.*, 43, 714, 1973.

756. Ohshima, H. and Kondo, T., *J. Colloid Interface Sci.*, 116, 305, 1987; *J. Colloid Interface Sci.*, 135, 443, 1990; 163, 474, 1994.

757. Ohshima, H., Interfacial electrokinetic phenomena, in *Electrical Phenomena at Interfaces: Fundamentals, Measurements, and Applications*, 2nd Ed., Ohshima, H. and Furusawa, K., Eds., Marcel Dekker, New York, 1998, chap. 2.

758. Ohshima, H., *J. Colloid Interface Sci.*, 233, 142, 2001.

759. Churaev, N.V. and Nikologorskaja, *Colloids Surfaces*, 59, 71, 1991.

760. Furusawa, K., Chen, Q., and Tobori, N., *J. Colloid Interface Sci.*, 137, 456, 1990.

761. Levine, S. and Neale, G.H., *J. Colloid Interface Sci.*, 47, 520, 1974; *J. Colloid Interface Sci.*, 49, 332, 1974.

762. Happel, J., *Amer. Inst. Chem. Eng. J.*, 4, 197, 1958.

763. Kuwabara, S., *J. Phys. Soc. Jpn*, 14, 527, 1959.

764. Deggelmann, M., Palberg, T., Hagenbüchle, M., Maier, E.E., Krause, R., Graf, C., and Weber, R., *J. Colloid Interface Sci.*, 143, 318, 1991.

765. Kozak, M.W. and Davis, E.J., *J. Colloid Interface Sci.*, 127, 497, 1989; *J. Colloid Interface Sci.*, 129, 166, 1989.

766. Ohshima, H., *J. Colloid Interface Sci.*, 188, 481, 1997.

767. Zukoski, C.F. and Saville, D.A., *J. Colloid Interface Sci.*, 115, 422, 1987.

768. Mangelsdorf, C.S. and White, L.R., *J. Chem. Soc. Faraday Trans.*, 88, 3567, 1992; *J. Colloid Interface Sci.*, 160, 275, 1993.

769. Gaigalas, A.K., Woo, S., and Hubbard, J.B., *J. Colloid Interface Sci.*, 136, 213, 1990.

770. Ohshima, H., *J. Colloid Interface Sci.*, 179, 431, 1996.

771. Ohshima, H., *J. Colloid Interface Sci.*, 185, 131, 1997.

772. Schätzel, K., Weise, W., Sobotta, A., and Drewel, M., *J. Colloid Interface Sci.*, 143, 287, 1991.

773. Abramson, H.A., Moyer, L.S., and Gorin, M.H., *Electrophoresis of Proteins*, Reinhold, New York, 1942.

774. Tiselius, A., *Trans. Faraday Soc.*, 33, 524, 1937.

775. Imai, T., Otani, W., and Oka, K., *J. Phys. Chem.*, 94, 853, 1990.

776. Kameyama, K. and Takagi, T., *J. Colloid Interface Sci.*, 140, 517, 1990.

777. Imai, T., *J. Phys. Chem.*, 94, 5953, 1990.

778. Imai, T. and Kohsaka T., *J. Phys. Chem.*, 96, 10030, 1992.

779. Imai, T. and Hayashi N., *Langmuir*, 9, 3385, 1993.

780. Imae, T., Electrostatic and electrokinetic properties of micelles, in *Electrical Phenomena at Interfaces: Fundamentals, Measurements, and Applications*, 2nd Ed., Ohshima, H. and Furusawa, K., Eds., Marcel Dekker, New York, 1998, chap. 28.

781. Anderson, J.L., *J. Colloid Interface Sci.*, 105, 45, 1985.

782. Fair, M.C. and Anderson, J.L., *J. Colloid Interface Sci.*, 127, 388, 1989.

783. Yoon, B.J. and Kim, S., *J. Colloid Interface Sci.*, 128, 275, 1989.

784. Yoon, B.J., *J. Colloid Interface Sci.*, 142, 575, 1991.

785. von Smoluchowski, M., *Bull. Akad. Sci. Cracovie, Sci. Math. Natur.*, 1, 182, 1903.

786. Booth, F., *J. Chem. Phys.*, 22, 1956, 1954.

787. Ohshima, H., Healy, T.W., White, L.R., and O'Brien, R.W., *J. Chem. Soc. Faraday Trans. 2*, 80, 1299, 1984.

788. Levine, S., Neale, G., and Epstein, N., *J. Colloid Interface Sci.*, 57, 424, 1976.

789. Mazur, P. and Overbeek, J.Th.G., *Rec. Trav. Chim.*, 70, 83, 1951.

790. De Groot, S.R., Mazur, P., and Overbeek, J.Th.G., *J. Chem. Phys.*, 20, 1825, 1952.

791. Maxwell, J.C., *Electricity and Magnetism*, Oxford University Press (Clarendon), London, 1873.

792. Fricke, H., *Phys. Rev.*, 24, 575, 1924; 26, 682, 1925.

793. Dukhin, S.S., *Electroconductivity and Electrokinetic Properties of Disperse Systems*, Naukova Dumka, Kiev, 1975, chap. 2 (in Russian).

794. O'Brien, R.W., *J. Colloid Interface Sci.*, 81, 234, 1981.

795. O'Brien, R.W. and Perrins, W.T., *J. Colloid Interface Sci.*, 99, 20, 1984; *J. Colloid Interface Sci.*, 110, 447, 1986.

796. Ohshima, H., Healy, T.W., and White, L.R., *J. Chem. Soc. Faraday Trans. 2*, 79, 1613, 1983.

797. De Lacey, E.H.B. and White, L.R., *J. Chem. Soc. Faraday Trans. 2*, 77, 2007, 1981.

798. O'Brien, R.W., *J. Colloid Interface Sci.*, 113, 81, 1986.

799. Debye, P. and Falkenhagen, H., *Phys. Ztschr.*, 29, 121 and 401, 1928.

800. Hinch, E.J., *J. Chem. Soc. Faraday Trans 2*, 80, 535, 1984.

801. Midmore, B.R., Hunter, R.J., and O'Brien, R.W., *J. Colloid Interface Sci.*, 120, 210, 1987; *J. Colloid Interface Sci.*, 123, 486, 1988.

802. Myers, D.F. and Saville, D.A., *J. Colloid Interface Sci.*, 131, 448, 1989.

803. Shubin, V.E., Hunter, R.J., and O'Brien, R.W., *J. Colloid Interface Sci.*, 159, 174, 1993.

804. Grosse, C., Arroyo, F.J., Shilov, V.N., and Delgado, A.V., *J. Colloid Interface Sci.*, 242, 75, 2001.

805. Enderby, J.A., *Proc. Phys. Soc.*, A207, 321, 1951.

806. Booth, F. and Enderby, J.A., *Proc. Phys. Soc.*, A208, 351, 1952.

807. Marlow, B.J., Fairhurst, D., and Pendse, H.P., *Langmuir*, 4, 611, 1988.

808. Hozumi, Y. and Furusawa, K., *Colloid Polym. Sci.*, 268, 469, 1990.

809. Durand Vidal, S., Simonin, J.P., Turq, P., and Bernard, Q., *Progress Colloid Polym. Sci.*, 98, 184, 1995.

810. Debye, P., *J. Chem. Phys.*, 1, 13, 1933.

811. O'Brien, R.W., *J. Fluid Mech.*, 190, 71, 1988.

812. Rider, P.F. and O'Brien, R.W., *J. Fluid Mech.*, 257, 607, 1993.

813. Takeda, S., Tobori, N., Sugawara, H., and Furusawa, K., Dynamic electrophoresis, in *Electrical Phenomena at Interfaces: Fundamentals, Measurements, and Applications*, 2nd Ed., Ohshima, H. and Furusawa, K., Eds., Marcel Dekker, New York, 1998, chap. 13.

814. Gibb, S.E. and Hunter, R.J., *J. Colloid Interface Sci.*, 224, 99, 2000.

815. Kong, L., Beattie, J.K., and Hunter, R.J., *J. Colloid Interface Sci.*, 238, 70, 2001.

816. Rasmusson, M., *J. Colloid Interface Sci.*, 240, 432, 2001.

817. Dukhin, A.S., Shilov, V.N., Ohshima, H., and Goetz, P.J. *Langmuir*, 16, 2615, 2000.

818. Löbbus, M., Sohhfeld, J., van Leeuwen, H.P., Vogelsberger, W., and Lyklema, J, *J. Colloid Interface Sci.*, 229, 174, 2000.

819. Hunter, R.J., *J. Colloid Interface Sci.*, 22, 231, 1966.

820. Chan, D.Y.C. and Horn, R.G., *J. Chem. Phys.*, 83, 5311, 1985.

821. Israelachvili, J.N., *J. Colloid Interface Sci.*, 110, 263, 1986.

822. Dukhin, S.S. and Semenikhin, M.M., *Kolloidn. Zh*., 32, 360, 1978.

823. Fridrikhsberg, D.A., Sidorova, M.P., Shubin, V.E., and Ermakova, L.E., *Kolloidn. Zh.*, 48, 967, 1986.

824. Zukoski, C.F. and Saville, D.A., *J. Colloid Interface Sci.*, 114, 32, 1986.

825. Midmore, B.R. and Hunter, R.J., *J. Colloid Interface Sci.*, 122, 521, 1988; Midmore, B.R., Diggins, D., Hunter, R.J., *J. Colloid Interface Sci.*, 129, 153, 1989.

826. Van der Put, A.G. and Bijsterbosch, B.H., *J. Colloid Interface Sci.*, 75, 512, 1980; 92, 499, 1983.

827. Rosen, L.A. and Saville, D.A., *J. Colloid Interface Sci.*, 144, 82, 1990; *J. Colloid Interface Sci.*, 149, 2, 1992.

828. Dukhin, A.S. and van de Ven, T.G.M., *J. Colloid Interface Sci.*, 165, 9, 1994.

829. Meijer, A.E.J., van Megen, W.J., and Lyklema, J., *J. Colloid Interface Sci.*, 66, 99, 1978.

830. Russel, A.S., Scales, P.J., Mangelsdorf, C.S., and White, L.R., *Langmuir*, 11, 1553, 1995.

831. Gittings, M.R. and Saville, D.A., *Langmuir*, 11, 798, 1995.

832. Bastos-Gonzalez, D., Hidalgo-Alvarez, R., and de las Nieves, F.J., *J. Colloid Interface Sci.*, 177, 372, 1996.

833. Saville, D.A., *J. Colloid Interface Sci.*, 222, 137, 2000.

834. Alty, T., *Proc. Royal Soc.*, A106, 315, 1924.

835. Usui, S., Sasaki, H., and Matsukawa, H., *J. Colloid Interface Sci.*, 65, 36, 1978; *J. Colloid Interface Sci.*, 81, 80, 1981.

836. McShea, J.A. and Callaghan, I.C., *Colloid Polymer Sci.*, 261, 757, 1983.

837. Yoon, R.-H. and Yordan, J.L., *J. Colloid Interface Sci.*, 113, 430, 1986.

838. Graciaa, A., Morel, G., Saulnier, R., Lachaise, J., and Schechter, R.S., *J. Colloid Interface Sci.*, 172, 131, 1995.

839. Dickinson, W., *Trans. Faraday Soc.*, 37, 140, 1941.

840. Taylor, A.J. and Wood, F.W., *Trans. Faraday Soc.*, 53, 523, 1957.

841. Dunstan, D.E. and Saville, D.A., *J. Chem. Soc. Faraday Trans.*, 88, 2031, 1992; *J. Chem. Soc. Faraday Trans.*, 89, 527, 1993; *J. Colloid Interface Sci.*, 166, 472, 1994.

842. Marinova, K.G., Alargova, R.G., Denkov, N.D., Velev, O.D., Petsev, D.N., Ivanov, I.B., and Borwankar, R., *Langmuir*, 12, 2045, 1996.

843. Graciaa, A., Morel, G., Saulner, P., Lachaise, J., and Schechter, R.S., *J. Colloid Interface Sci.*, **172**, 131, 1995.

844. Exerowa, D., Zachariewa, M., Coben, R., and Platikanov, D., *Colloid & Polymer Sci.*, 257, 1089, 1979.

845. Waltermo, A., Manev, E., Pugh,, R., and Claesson, P., *J. Dispersion Sci. Technology*, 15, 273, 1994.

846. Karraker, K. A., and Radke C. J., *Adv. Colloid Interface Sci.*, 96, 231, 2002.

847. Van de Hulst, H.C., *Light Scattering by Small Particles*, Wiley, New York, 1957; 2nd ed., Dover, New York, 1981.

848. Kerker, M., *The Scattering of Light and other Electromagnetic Radiation*, Academic Press, New York, 1969.

849. Hiemenz, P.C. and Rajagopalan, R., *Principles of Colloid and Surface Chemistry*, 3rd Ed., Marcel Dekker, New York, 1997, chap. 5.

850. Lyklema, J., *Fundamentals of Interface and Colloid Science*, Vol. 1, Academic Press, New York, 1991, chap. 7.

851. McIntyre, D. and Gornick, F., Eds., *Light Scattering from Dilute Polymer Solutions*, Gordon and Breach, New York, 1964.

852. Rayleigh, L., *Phil. Mag.*, 41, 107, 1871; *Phil. Mag.*, 41, 274, 1871; *Phil. Mag.*, 41, 447, 1871.

853. Debye, P., *J. Appl. Phys.*, 15, 338, 1944.

854. O'Konski, C.T., Ed., *Molecular Electrooptics*, Marcel Dekker, New York, 1976.

855. Jennings, B. R., Ed., *Electro-opltics and Dielectrics of Macromolecules and Colloids*, Plenum Press, New York, 1979.

856. Stoilov, S.P., *Colloid Electroptics: Theory, Techniques and Applications*, Academic Press, New York, 1991.

857. Rayleigh, L., *Proc. Royal Soc.*, A84, 25, 1910; *Proc. Royal Soc.*, A90, 219, 1914; *Proc. Royal Soc.*, A94, 296, 1918.

858. Debye, P., *Ann. Phys.*, 46, 809, 1915.

859. Gans, R., *Ann. Phys.*, 65, 97, 1921; *Ann. Phys.*, 67, 353, 1923; *Ann. Phys.*, 76, 29, 1925.

860. Guinier, A., *Ann. Phys.* (France), 12, 161, 1939.

861. Yamakawa, H., *Modern Theory of Polymer Solutions*, Harper and Row, New York, 1971.

862. Shull, C.C. and Roess, L.C., *J. Appl. Phys.*, 18, 295, 1947.

863. Brenner, H., *Int. J. Multiphase Flow*, 1, 195, 1974.

864. Zero, K. and Pecora, R., in *Dynamic Light Scattering*, Pecora, R., Ed., Plenum Press, New York, 1985, chap. 3.

865. Neugebauer, T., *Ann. Phys.*, 42, 509, 1942.

866. Saito, N. and Ikeda, Y., *J. Phys. Soc. Jpn*, 6, 305, 1951.

867. Fournet, G. and Guinier, A., *J. Phys. Radium*, 11, 516, 1950.

868. Riseman, J. and Kirkwood, J.G., *J. Chem. Phys.*, 18, 512, 1950.

869. Broersma, S., *J. Chem. Phys.*, 32, 1626, 1960; *J. Chem. Phys.*, 32, 1632, 1960.

870. Kratky, O. and Porod, G., *J. Colloid Sci.*, 4, 35, 1949.

871. Becher, P., *J. Phys. Chem.*, 63, 1213, 1959.

872. Debye, P., Technical Report No 637 to Rubber Reserve Company, Washington, April 9, 1945.

873. Hearst, J.E., *J. Chem. Phys.*, 38, 1062, 1963.

874. Mie, G., *Ann. Phys.*, 25, 377, 1908.

875. Debye, P., *Ann. Phys.*, 30, 755, 1909.

876. Asano, S. and Yamamoto, G., *Appl. Opt.*, 14, 29, 1975; *Appl. Opt.*, 18, 712, 1979.

877. Glatter, O., Sieberer, J., and Schnablegger, H., *Part. Part. Syst. Charact.*, 8, 274, 1991.

878. Einstein, A., *Ann. Phys.*, 33, 1275, 1910.

879. Debye, P., *J. Phys. Colloid Chem.*, 51, 18, 1947.

880. McQuarrie, D.A., *Statistical Mechanics*, Harper and Row, New York, 1976.

881. Zimm, B.H., *J. Chem. Phys.*, 16, 1093, 1948; *J. Chem. Phys.*, 16, 1099, 1948.

882. Agterof, W.G.M., van Zomeren, J.A.J., and Vrij, A., *Chem. Phys. Lett.*, 43, 363, 1976.

883. Cazabat, A.M. and Langevin, D., *J. Chem. Phys.*, 74, 3148, 1981.

884. Brunetti, S., Roux, D., Bellocq., A.M., Fourche, G., and Bothorel, P., *J. Phys. Chem.*, 87, 1028, 1983.

885. Baker, R.C., Florence, A.T., Ottewill, R.H., and Tadros, Th.F., *J. Colloid Interface Sci.*, 100, 332, 1984.

886. Denkov, N.D., Kralchevsky, P.A., Ivanov, I.B., and Vassilieff, C.S., *J. Colloid Interface Sci.*, 143, 157, 1991.

887. Koper, G.J.M., Sager, W.F.C., Smeets, J., and Bedeaux, D., *J. Phys. Chem.*, 99, 13 291, 1995.

888. Cabannes, P., *La Diffusion Moleculaire de la Lumiere*, Presses Universitaires de France, Paris, 1929.

889. Utiyama, H., in *Light Scattering from Polymer Solutions*, Huglin, M.B., Ed., Academic Press, New York, 1972, chap. 4.

890. Eskin, B.E., *Light Scattering from Polymer Solutions*, Nauka, Leningrad, 1986, chap. 1 (in Russian).

891. Chu, B., *Laser Light Scattering: Basic Principles and Practice*, Academic Press, New York, 1974; 2nd Ed., 1991.

892. Berne, B.J. and Pecora, R., *Dynamic Light Scattering with Applications to Chemistry, Biology and Physics*, Wiley, New York, 1976.

893. Pecora, R., Ed., *Dynamic Light Scattering: Applications of Photon Correlation Spectroscopy*, Plenum Press, New York, 1985.

894. Schmitz, K.S., *An Introduction to Dynamic Light Scattering by Macromolacules*, Academic Press, New York, 1990.

895. Brown, W., Ed., *Dynamic Light Scattering: The Mehtod and Some Applications*, Clarendon Press, Oxford, 1993.

896. Brown, W., Ed., *Light Scattering: Principles and Development*, Clarendon Press, Oxford, 1996.

897. Dhont, J.K.G., *An Introduction to Dynamics of Colloids*, Elsevier, Amsterdam, 1996.

898. Jakeman, E., Oliver, C.J., and Pike, E.R., *J. Phys A*, 3, L 45, 1970.

899. Ware, B.R., *Adv. Colloid Interface Sci.*, 4, 1, 1974.

900. Durst, F., Melling, A., and Whitelaw, J. H., *Principles and Practice of Laser Doppler Anemometry*, 2nd ed., Academic Press, New York, 1981.

901. Miller, J. F., Schatzel, K., and Vincent, B., *J. Colloid Interface Sci*., 143, 532, 1991.

902. Koppel, D.E., *J. Chem. Phys.*, 57, 4814, 1972.

903. Gulari, E., Gulari, E., Tsunashima, Y., and Chu, B., *J. Chem. Phys.*, 70, 3965, 1979.

904. Provencher, S.W., *Comput. Phys. Commun.*, 27, 213, 1982.

905. Morrison, I.D., Grabowski, E.F., and Herb, C.A., *Langmuir*, 4, 496, 1985.

906. Bertero, M., Boccacci, C. De Mol, and Pike, E.R., in *Opticle Particle Sizing, Theory and Practice*, Gousbet, G. and Greban, G., Eds., Plenum Press, New York, 1988.

907. Finsy, R., de Groen, P., Deriemaeker, L., and Van Laethem, M., *J. Chem. Phys.*, 91, 7374, 1989.

908. Nicolai, T., Brown, W., Johnsen, R.M., and Stepanek, P., *Macromolecules*, 23, 1165, 1990.

909. Nicolai, T., Brown, W., Hvidt, S., and Heller, K., *Macromolecules*, 23, 5088, 1990.

910. Bryan, R.K., *Eur. Biophys. J.*, 18, 165, 1990; Landowski, J. and Bryan, R.K., *Macromolecules*, 24, 6364, 1991.

911. Schnablegger, H. and Glatter, O., *Appl. Optics*, 30, 4889, 1991.

912. Pecora, R., *J. Chem. Phys.*, 49, 1036, 1968.

913. Pusey, P.N. and Tough, R.J.A., in *Dynamic Light Scattering*, Pecora, R., Ed., Plenum Press, New York, 1985, chap. 4.

914. Batchelor, G.K., *J. Fluid Mech.*, 52, 245, 1972; 74, 1, 1976.

915. Felderhof, B.U., *Physica*, 89A, 373, 1977.

916. Felderhof, B.U., *J. Phys. A: Math. Gen.*, 11, 929, 1978.

917. Ackerson, B.J., *J. Chem. Phys.*, 64, 242, 1976; *J. Chem. Phys.*, 69, 684, 1978.

918. Hess, W. and Klein, R., *Adv. Physics*, 32, 173, 1983.

919. Schurr, J.M., *Chem. Phys.*, 111, 55, 1987.

920. Russel, W.B. and Glendinning, A.B., *J. Chem. Phys.*, 74, 948, 1981.

921. Denkov, N.D. and Petsev, D.N., *Physica A*, 183, 462, 1992.

922. Nägele, G., *Phys. Reports*, 272, 215, 1996.

923. Hirtzel, C.S. and Rajagopalan, R., in *Micellar Solutions and Microemulsions: Structure, Dynamics and Statistical Thermodynamics*, Springer-Verlag, New York, 1990, chap. 7.

924. Gaylor, K.J., Snook, I.K., van Megen, W.J., and Watts, R.O., in *Light Scattering in Liquids and Macromolecular Solutions*, Degiorgio, V., Corti, M., and Giglio, M., Eds., Plenum Press, New York, 1980.

925. Jones, R.B. and Schimtz, R., *Physica A*, 149, 373, 1988.

926. Cichocki, B. and Felderhof, B.U., *J. Chem. Phys.*, 89, 1049 and 3705, 1988.

927. Kops-Werkhoven, M.M. and Fijnaut, H.M., *J. Chem. Phys.*, 74, 1618, 1981.

928. Cichocki, B. and Felderhof, B.U., *J. Chem. Phys.*, 93, 4427, 1990; *J. Chem. Phys.*, 94, 563, 1991.

929. Petsev, D.N. and Denkov, N.D., *J. Colloid Interface Sci.*, 149, 329, 1992; Petsev, D.N., Denkov, N.D., and Nagayama, K., *Chem. Phys.*, 175, 265, 1993.

930. Corti, M. and Degiorgio, V., *J. Phys. Chem.*, 85, 711, 1981.

931. Belloni, L., Drifford, M., and Turq, P., *J. Phys. Lett.*, 46, L207, 1985; *J. Phys. Lett.*, 46, L1183, 1985.

932. Drifford, M., Belloni, L., Dalbiez, J.P., and Chattopadhyay, A.K., *J. Colloid Interface Sci.*, 105, 587, 1985.

933. Nagele, G., Mandl, B., and Klein, R., *Progress Colloid Polymer Sci*., 98, 117, 1995.

934. Ohshima, H., Healy, T.W., White, L.R., and O'Brien, R.W., *J. Chem. Soc. Faraday Trans. 2*, 80, 1299, 1984.

935. Schumacher, G.A. and van de Ven, T.G.M., *Faraday Discussions Chem. Soc.*, 83, 75, 1987; *J. Chem. Soc., Faraday Trans.*, 87, 971, 1991.

936. Bauer, D.R., *J. Phys. Chem.*, 84, 1592, 1980.

937. Cummins, P.G. and Staples, E.J., *J. Phys. E*, 14, 1171, 1981.

938. Phillies, G.D.J., *J. Chem. Phys.*, 74, 260, 1981.

939. Phillies, G.D.J., *Phys. Rev. A*, 24, 1939, 1981.

940. Dhont, J.K.G. and de Kruif, C.G., *J. Chem. Phys.*, 79, 1658, 1983.

941. Schätzel, K., *J. Modern Opt.*, 38, 1849, 1991.

942. Pusey, P.N., *Curr. Opinion Colloid Interface Sci.*, 4, 177, 1999.

943. Drewel, M., Ahrens, J., and Schatzel, K., in Proc. 2nd International Congress on Particle Sizing, Arizona University Press, 1990.

944. Segré, P.N., van Megen, W., Pusey, P.N., Schätzel, K., and Peters, W., *J. Modern Opt.*, 42, 1929, 1995.

945. Aberle, L.B., Hulstede, P., Wiegand, S., Schroer, W., and Staude, W., *Appl. Optics*, 37, 6511, 1998.

946. Tanaka, T. and Benedek, G.B., *Appl. Opt.*, 14, 189, 1975.

947. Sorensen, C.M., Mockler, R.C., and O'Sullivan, W.J., *Phys. Rev. A*, 14, 1520, 1976; *Phys. Rev. A*, 17, 2030, 1978.

948. Dhadwal, H.S. and Ross, D.A., *J. Colloid Interface Sci.*, 76, 478, 1980.

949. Auweter, H. and Horn, D., *J. Colloid Interface Sci.*, 105, 399, 1985; *J. Phys. D*, 22, 1257, 1989.

950. Thomas, J.C. and Tjin, S.C., *J. Colloid Interface Sci.*, 129, 15, 1989.

951. MacFayden, A.J. and Jennings, B.R., *Opt. Laser Technol.*, 22, 715, 1990.

952. Thomas, J.C., *Langmuir*, 5, 1350, 1989.

953. Meeren, P.V., Bogaert, H., Stastny, M., Vanderdeelen, J., and Baert, L., *J. Colloid Interface Sci.*, 160, 117, 1993.

954. Wiese, H. and Horn, D., *J. Chem. Phys.*, 94, 6429, 1991.

955. Dhadwal, H.S., Ansari, R.R., and Meyer, W.V., *Rev. Sci. Instrum.*, 62, 2963, 1991.

956. Maret, G. and Wolf, P.E., *Z. Phys. B*, 65, 409, 1987.

957. Rosenbluch, M., Hoshen, M., Freund, I., and Kaveh, M., *Phys. Rev. Lett.*, 58, 2754, 1987; *Phys. Rev. Lett.*, 60, 1130, 1988.

958. Pine, D.J., Weitz, D.A., Chaikin, P.M., and Herbolzheimer, E., *Phys. Rev. Lett.*, 60, 1134, 1988.

959. Pine, D.J., Weitz, D.A., Maret, G., Wolf, P.E., Herbolzheimer, E., and Chaikin, P.M., in *Scattering and Localization of Classical Waves in Random Media*, Sheng, P., Ed., World Scientific, Singapore, 1989.

960. Golubentsev, A.A., *Sov. Phys. JETP*, 59, 26, 1984.

961. Stephen, M.J., *Phys. Rev. B*, 37, 1, 1988.

962. Durian, D.J., Weitz, D.A., and Pine, D.J., *Science*, 252, 686, 1991.

963. Sanyal, S., Sood, A.K., Ramkumar, S., Ramaswamy, S., and Kumar, N., *Phys. Rev. Lett.*, 72, 2963, 1994.

964. Liu, A.J., Ramaswamy, S., Mason, T.G., Gang, H., and Weitz, D.A., *Phys. Rev. Lett.* 76, 3017, 1996.

965. Mason, T.G., Hu, G., and Weitz, D.A., *J. Opt. Soc. Am. A*, 14, 139, 1997.

966. Durian, D.J., *Phys. Rev. E*, 55, 1739, 1997.

967. Durian, D.J., *Curr. Opinion Colloid Interface Sci*., 2, 615, 1997.

968. Hebraud, P., Lequeux, F., Munch, J.P., Pine, D.J., *Phys. Rev. Lett.* 78, 4657, 1997.

969. Maret, G., *Curr. Opinion Colloid Interface Sci*., 2, 251, 1997.

970. Gisler, T. and Weitz, D.A., *Curr. Opinion Colloid Interface Sci*., 3, 586, 1998.

971. Debye, P., *Ann. N. Y. Acad. Sci*., 51, 575, 1949.

972. Debye, P. and Anacker, E.W., *J. Phys. Colloid Chem.*, 55, 644, 1959.

973. Mysels, K.J. and Princen, L.H., *J. Phys. Chem.*, 63, 1696, 1959.

974. Huisman, H.F., *Proc. Kon. Ned. Akad. Wet.*, B67, 367, 1964; *Proc. Kon. Ned. Akad. Wet.*, B67, 376, 1964; *Proc. Kon. Ned. Akad. Wet.*, B67, 388, 1964; *Proc. Kon. Ned. Akad. Wet.*, B67, 407, 1964.

975. Vrij, A. and Overbeek, J.Th.G., *J. Colloid Sci.*, 17, 570, 1962.

976. Becher, P., in *Nonionic Surfactants*, Schick, M. J., Ed., Marcel Dekker, New York, 1967, chap. 15.

977. Hall, D.J. and Tiddy, G.J.T., in *Anionic Surfactants: Physical Chemistry of Surfactant Action*, Lucassen-Reynders, E.H., Ed., Marcel Dekker, New York, 1981, chap. 2.

978. Eicke, H.-F., *Topics Current Chem.*, 87, 85, 1980.

979. Mukerjee, P., *J. Phys. Chem.*, 76, 565, 1972.

980. Israelachvili, J.N., Mitchell, D.J., and Ninham, B.W., *J.Chem. Soc.: Faraday Trans. 2*, 72, 1525, 1976.

981. Ruckenstain, E. and Nagarajan, R., *J. Colloid Interface Sci.*, 57, 388, 1976; *J. Colloid Interface Sci.*, 91, 500, 1983.

982. Mazer, N.A., in *Dynamic Light Scattering*, Pecora, R., Ed., Plenum Press, 1985, chap. 8.

983. Mazer, N.A., Benedek, G.B., and Carey, M.C., *J. Phys. Chem.*, 80, 1075, 1976.

984. Briggs, J., Nicoli, D.F., and Ciccolello, R., *Chem. Phys. Lett.*, 73, 149, 1980.

985. Mishic, J.R. and Fisch, M.R., *J. Chem. Phys.*, 92, 3222, 1990.

986. Schillen, K., Brown, W., and Johnsen, R.M., *Macromolecules*, 27, 4825, 1994.

987. Porte, G., Appell, J., and Poggi, Y., *J. Phys. Chem.*, 84, 3105, 1980.

988. Appell, J. and Porte, G., *J. Colloid Interface Sci.*, 81, 85, 1981.

989. Imae, T., *J. Phys. Chem.*, 94, 5953, 1990.

990. Alargova, R., Petkov, J., Petsev, D., Ivanov, I.B., Broze, G., and Mehreteab, A., *Langmuir*, 11, 1530, 1995.

991. Alargova, R.G., Danov, K.D., Kralchevsky, P.A., Broze, G., and Mehreteab, A., *Langmuir*, 14, 4036, 1998.

992. Dorshow, R., Briggs, J., Bunton, C.A., and Nicoli, D.F., *J. Phys. Chem.*, 86, 2388, 1982; *J. Phys. Chem.*, 87, 1409, 1983.

993. Missel, P.J., Mazer, N.A., Benedek, G.B., Young, C.Y., and Carey, M.C., *J. Phys. Chem.*, 84, 1044, 1980.

994. Rohde, A. and Sackman, E., *J. Colloid Interface Sci.*, 78, 330, 1980.

995. Hartland, G.V., Grieser, F., and White, L.R., *J. Chem. Soc. Faraday Trans. 1*, 83, 591, 1987; Dunstan, D.E. and White, L.R., *J. Colloid Interface Sci*., 134, 147, 1990.

996. Ortega, F., Bacaloglu, R., McKenzie, D.C., Bunton, C.A., and Nicoli, D.F., *J. Phys.Chem.*, 94, 501, 1990.

997. Corti, M. and Degiorgio, V., *Phys. Rev. Lett.*, 45, 1045, 1980; *J. Phys. Chem.*, 85, 1442, 1981.

998. Calje, A., Agterof, W., and Vrij, A., in *Micellization, Solubilization and Microemulsions*, Mittal, K., Ed., Plenum Press, New York, 1977.

999. Lemaire, B., Bothorel, P., and Roux, D., *J. Phys. Chem.*, 87, 1023, 1983.

1000. Cazabat, A.M., Langevin, D., and Pouchelon, A., *J. Colloid Interface Sci.*, 73, 1, 1980.

1001. Hou, M.J., Kim, M., and Shah, D.O., *J. Colloid Interface Sci.*, 123, 398, 1988.

1002. Auvrey, L., *J. Phys. Chem. (Paris)*, 46, 163, 1985.

1003. Fletcher, P.D.I., Howe, A.M., and Robinson, B.H., *J. Chem. Soc.: Faraday Trans. 1*, 83, 985, 1987.

1004. Fletcher, P.D.I. and Holzwarth, J.F., *J. Phys. Chem.*, 95, 2550, 1991.

1005. Lagues, M., Ober, R., and Taupin, C., *J. Phys. Lett.*, 39, 487, 1978.

1006. Lagourette, B., Peyrelasse, J., Boned, C., and Clausse, M., *Nature*, 281, 60, 1979.

1007. Eicke, H.-F., Shepherd, J.C.W., and Steineman, A., *J. Colloid Interface Sci.*, 56, 168, 1976.

1008. Guering, P. and Cazabat, A.M., *J. Phys. Lett.*, 44, 601, 1983.

1009. Guering, P., Cazabat, A.M., and Paillette, M., *Europhys. Lett.*, 2, 953, 1986.

1010. Dorshow, R.B. and Nicoli, D.F., in *Measurement of Suspended Particles by QELS*, Dahneke, B.E., Ed., Wiley, New York, 1983, p.529.

1011. Guering, P., Nilsson, P.-G., and Lindman, B., *J. Colloid Interface Sci.*, 105, 41, 1985.

1012. Kato, T., Takeuchi, H., and Seimiya, T., *J. Colloid Interface Sci.*, 140, 253, 1990.

1013. Tuzar, Z. and Kratohvil, P., in *Surface and Colloid Science*, Vol. 15, Matijevi č, E., Ed., Plenum Press, New York, 1993, chap. 1.

1014. Cogan, K.A. and Gast, A.P., *Macromolecules,* 23, 745, 1990; Chu, B., *Langmuir*, 11, 414, 1995.

1015. Satoh, N. and Tsujii, K., *J. Phys. Chem.*, 91, 6629, 1987.

1016. Thunig, C., Hoffmann, H., and Platz, G., *Progress Colloid Polymer Sci.*, 79, 297, 1989; *Progress Colloid Polymer Sci.*, 83, 167, 1990.

1017. McDonald, J. A. and Rennie, A. R., *Progress Colloid Polym. Sci.,* 98, 75, 1995.

1018. Goddard, E.D. and Ananthapadmanabhan, K.P., Eds., *The Interactions of Surfactants with Polymers and Proteins,* CRC Press, Boca Raton, FL, 1993.

1019. Bahadur, P., Dubin, P., and Rao, Y.K., *Langmuir*, 11, 1951, 1995; Li, Y., Dubin, P.L., Havel, H.A., Edwards, S.L., and Dautzenberg, H., *Macromolecules*, 28, 3098, 1995.

1020. Hayakawa, K. and Kwak, J.C.T., in *Cationic Surfactants: Physical Chemistry*, Rubingh, D.N. and Holland, P.M., Eds., Marcel Dekker, New York, 1991, chap. 5.

1021. Corti, M. and Canti, L., *Adv. Colloid Interface Sci.*, 32, 151, 1990.

1022. Bloomfield, V.A., in *Dynamic Light Svattering*, Pecora, R., Ed., Plenum Press, New York, 1985, chap. 10.

1023. Egelhaaf, S. U., Pedersen, J. S., and Schurtenberger, P., *Progress Colloid Polymer Sci*., 98, 224, 1995.

1024. Langevin, D., Ed., *Light Scattering by Liquid Surfaces and Complementary Techniques*, Marcel Dekker, New York, 1992.

1025. Earnshaw, J.C. and McCoo, E., *Langmuir*, 11, 1087, 1995.

1026. Vrij, A., Joosten, J.G.H., and Fijnaut, H.M., *Adv. Chem. Phys.*, 48, 329, 1981.

1027. Joosten, J.G.H., in *Thin Liquid Films*, Ivanov, I.B., Ed., Marcel Dekker, New York, 1988, chap. 9.

1028. Hirleman, E.D., *Part. Part. Syst. Charact.*, 4, 128, 1987.

1029. van de Hulst, H.C., *Multiple Light Scattering*, Academic Press, New York, 1980.

1030. Penders, M.G.H.M. and Vrij, A., *J. Chem. Phys.*, 93, 3704, 1990.

1031. Apfel, U., Hörner, K.D., and Ballauff, M., *Langmuir*, 11, 3401, 1995.

1032. Bryant, G. and Thomas, J.C., *Langmuir*, 11, 2480, 1995.

1033. Barber, P.W., Yeh, C., and Wang, D.-S., *Appl. Opt.*, 14, 2864, 1975; *Appl. Opt.*, 17, 797, 1978; *Appl. Opt.*, 18, 1190, 1979.

1034. Quirantes, A. and Delgado, A. V., *Progress Colloid Polymer Sci*., 98, 145, 1995.

1035. Purcell, E.M. and Pennypacker, C.R., *Astrophys. J.*, 186, 705, 1973.

1036. Buitenhuis, J., Dhont, J.K.G., and Lekkerkerker, H.N.W., *J. Colloid Interface Sci.*, 162, 19, 1994.

1037. Schaefer, D.W., *J. Chem. Phys.*, 66, 3980, 1977.

1038. Finsy, R., Moreels, E., Bottger, A., and Lekkerkerker, H., *J. Chem. Phys.*, 82, 3812, 1985.

1039. Clark, N.A., Hurd, A.J., and Ackerson, B.J., *Nature*, 281, 57, 1979.

1040. Pieranski, P., *Contemp. Phys.*, 24, 25, 1983.

1041. Pusey, P.N., *Phil. Trans. R. Soc. London*, A293, 429, 1979.

1042. van Megen, W., Pusey, P.N., and Bartlett, P., *Phase Transitions*, 21, 207, 1990.

1043. Piazza, R. and Degiorgio, V., *Physica A*, 182, 576, 1982.

1044. Degiorgio, V., Piazza, R., Corti, M., and Stavans, J., *J. Chem. Soc. Faraday Trans*, 87, 431, 1991.

1045. Dhont, J.K.G., Smits, K., and Lekkerkerker, H.N.M., *J. Colloid Interface Sci.*, 152, 386, 1992.

1046. Hiltner, P.A. and Krieger, I.M., *J. Phys. Chem.*, 73, 2386, 1969.

1047. Yoshiyama, T., Sogami, I., and Ise, N., *Phys. Rev. Lett.*, 53, 2153, 1984.

1048. Sogami, I. and Yoshiyama, T., *Phase Transitions*, 21, 171, 1990.

1049. Monovoukas, Y. and Gast, A.P., *Phase Transitions*, 21, 183, 1990.

1050. Bartsch, E., *Curr. Opinion Colloid Interface Sci.*, 3, 577, 1998.

1051. Van Megen, W., Mortenson, T.C., Müller, J., Williams, S.R., *Phys. Rev. E*, 58, 6073, 1998.

1052. D'Aguanno, B. and Klein, R., *J. Chem. Soc. Faraday Trans.*, 87, 379, 1991.

1053. Krause, R., Arauz-Lara, J.L., Nagele, G., Ruiz-Estrada, H., Medina-Noyola, M., Weber, R., and Klein, R., *Physica A*, 178, 241, 1991.

1054. Wagner, N.J., Krause, R., Rennie, A.R., D'Aguanno, B., and Goodwin, J., *J. Chem. Phys.*, 95, 494, 1991.

1055. Pusey, P.N. and van Megen, W., *Nature*, 320, 340, 1986.

1056. Härtl, W., Klemp, R., and Versmold, H., *Phase Transitions*, 21, 229, 1990.

1057. Harland, J.L. and van Megen, W., *Phys. Rev. E*, 55, 3054, 1997.

1058. Russel, W.B., Chaikin, P.M., Zhu, J., Meyer, W.V., and Rogers, R., *Langmuir*, 13, 3871, 1997.

1059. Palberg, T., *Curr. Opinion Colloid Intreface Sci.*, 2, 607, 1997.

1060. Hoffman, R.L., *J. Colloid Interface Sci*., 46, 491, 1974.

1061. Bossis, G., Brady, J.F., and Mathis, C., *J. Colloid Interface Sci*., 126, 1 and 16, 1988.

1062. Wagner, N.J. and Russel, W.B., *Phys. Fluids*, A2, 491, 1990.

1063. Ackerson, B.J. and Clark, N.A., *Physica A*, 118, 221, 1983; *Phys. Rev. A*, 30, 906, 1984.

1064. Ackerson, B.J. and Pusey, P.N., *Phys. Rev. Lett*., 61, 1033, 1988.

1065. Ackerson, B.J., *Physica A*, 174, 15, 1991.

1066. Weitz, D.A. and Oliveria, M., *Phys. Rev. Lett.*, 52, 1433, 1984.

1067. Weitz, D.A., Huang, J.S., Lin, M.Y., and Sung, J., *Phys. Rev. Lett.*, 53, 1651, 1984; *Phys. Rev. Lett.*, 54, 1416, 1985; *Phys. Rev. Lett.*, 57, 2037, 1986.

1068. Meakin, P., in *Phase Transitions*, Vol. 12, Domb, C. and Lebowitz, J.L., Eds., Academic Press, New York, 1988.

1069. Weitz, D.A., Lin, M.Y., and Huang, J.S., in *Physics of Complex and Supermolecular Fluids*, Safran, S.A., and Clark, N.A., Eds., Wiley-Interscience, New York, 1987.

1070. Kolb, M., *Phys. Rev. Lett.*, 53, 1654, 1984.

1071. Mandelbrot, B.B., *The Fractal Geometry of Nature*, Freeman, New York, 1983.

1072. Meakin, P., *Phys. Rev. Lett.*, 51, 1119, 1983.

1073. Van Dongen, G.J. and Ernst, M.H., *Phys. Rev. Lett.*, 54, 1396, 1985.

1074. Brown, W.D. and Ball, R.C., *J. Phys. A*, 18, L517, 1985.

1075. Schaeffer, D.W., Martin, J.E., Wiltzius, P., and Cannell, D.S., *Phys. Rev. Lett.*, 52, 2371, 1984.

1076. Ball, R.C., Weitz, D.A., Witten, T.A., and Leyvraz, F., *Phys. Rev. Lett.*, 58, 274, 1987.

1077. Meakin, P., Vicsek, T., and Family, F., *Phys. Rev. B*, 31, 564, 1985.

1078. Lin, M.Y., Lindsay, H.M., Weitz, D.A., Ball, R.C., Klein, R., and Meakin, P., in *Fractals in the Natural Sciences*, Fleischmann, M., Tildesley, D.J., and Ball., R.C., Eds., Princeton University Press, Princeton, 1989.

1079. Amal, R., Raper, J.A., Waite, T.D., *J. Colloid Interface Sci.*, 140, 158, 1990.

1080. Odriozola, G., Tirado-Miranda, M., Schmidt, A., Martinez Lopez, F., Callejas-Fernandez, J., Martinez-Garcia, R., and Hidalgo-Alvarez, R., *J. Colloid Interface Sci.*, 240, 90, 2001.

1081. Georgialis, Y. and Saenger, W., *Adv. Colloid Interface Sci.*, 46, 165, 1993.

1082. Georgialis, Y., Zouni, A., Eberstein, W., and Saenger, W., *J. Crystal Growth*, 126, 245, 1993.

1083. Eberstein, W., Georgialis, Y., and Saenger, W., *J. Crystal Growth*, 143, 71, 1994.

1084. Muschol, M., Rosenberger, F., *J. Chem Phys.*, 103, 10424,1995.

1085. Nikolai, T., Urban, C., and Schurtenberger, S., *J. Colloid Interface Sci.,* 240, 419, 2001.